STUDIES OF

THE SCATTERING OF FUNDAMENTAL PARTICLES

AND

THE POLARISATION OF NUCLEAR GAMMA RAYS

BY

I. S. HUGHES
DEPARTMENT OF NATURAL PHILOSOPHY,
UNIVERSITY OF GLASGOW.

Presented as a Thesis for the Degree of Ph.D.
in the University of Glasgow

APRIL 1956.

ProQuest LLC.
789 East Eisenhower Parkway
P.O. Box 1346
Ann Arbor, MI 48106 – 1346

CONTENTS.

CHAPTER /

CHAPTER /

CHAPTER /

Page

PREFACE.

The first part of the thesis describes three experiments concerned with the study of the scattering of fundamental particles by allowing the particles to pass into a nuclear emulsion and studying their scattering by the elements of the emulsion. These three experiments are described in the order in which they were performed.

In chapters I - III is described a study of the single, (large angle), Coulomb scattering of electrons and positrons of 10 Mev obtained by means of nuclear reactions performed using the Glasgow H.T. set. This work was carried out by the author in collaboration with Dr. W. Bosley.

Tracks from the plates exposed for the single scattering experiment were used independently by the author to measure the multiple Coulomb scattering of electrons and positrons of 10 Mev. The results of this work revealed an unexplained difference in the multiple scattering of electrons and positrons which is confirmed by the measurements of other workers.

The third experiment in this group was an investigation of the scattering of protons having an energy of 925 Mev by the hydrogen nuclei present in nuclear emulsions. The emulsions were exposed to the scattered-out beam of high energy protons from the Birmingham proton synchrotron by Dr. O. Lock, Dr. P. V. March, and Mr. P. J. Duke, of Birmingham University. The measurements were carried out by these members of the Birmingham group, by Dr. /

Dr. M. Gibson amd Mr. R. McKeague at Belfast University, and by Dr. H. Muirhead and the author at Glasgow University. The analysis of the elastic scattering events was also carried out jointly by all the members of the three groups. The method of analysis for the inelastic scattering events involving the production of mesons was devised by the author and this analysis was carried out initially by the author alone and later with the collaboration of Dr. P. V. March.

The results for the elastic scattering are in general agreement with those obtained by workers in the U.S.A. during the course of this experiment, using cloud chamber and counter techniques. For the inelastic scattering new evidence has been obtained which suggests that the mesons are produced by the decay of a nucleon in an excited state.

The second part of the thesis describes the development of a method, suggested by an experiment due to Dr. D. H. Wilkinson, of measuring the polarisation of gamma rays using nuclear emulsions impregnated with heavy water, and the application of the method to the measurement of the polarisation of gamma rays from three nuclear reactions. The results obtained enabled assignments of parity to be made to the ground states of ^{23}Na and ^{27}Al and to the first excited state of ^{27}Al.

The polarisation experiments were carried out by the author /

author, assisted in the later stages of the work by Mr. D. Sinclair, following a suggestion by Dr. P. J. Grant.

ACKNOWLEDGMENTS.

The author wishes to express his gratitude to Professor P. I. Dee, F.R.S., for his interest and encouragement during the course of this work and to Dr. H. Muirhead for his invaluable advice and supervision. He is also grateful to Dr. P. J. Grant for valuable discussions and advice in connection with the polarisation experiments, to Dr. W. Bosley, Mr. D. Sinclair, Dr. P. V. March and the members of the nuclear emulsion groups at Birmingham and Belfast for their co-operation in the various parts of the work described, and to the various scanners who have assisted in the examination of the emulsions. The author is grateful to the University of Glasgow for the award of a studentship during the period of this research.

PUBLICATIONS.

The Nuclear Scattering of Electrons and Positrons at 10 Mev.
W. Bosley and I. S. Hughes, 1955, Phil. Mag., 46, 1281.

Proton-Proton Elastic Scattering at 950 Mev.
P. J. Duke, W. O. Lock, P. V. March, W. M. Gibson, R. McKeague, I. S. Hughes, H. Muirhead, 1955, Phil. Mag., 46, 877.

The Polarisation of γ-Radiation from the Reactions $^{27}Al\ (p,\gamma)\ ^{28}Si$, $^{26}Mg\ (p,\gamma)\ ^{27}Al$, $^{23}Na\ (p,\gamma)\ ^{24}Mg$.
I. S. Hughes and D. Sinclair, 1956, Proc. Phys. Soc., 69, 125.

CHAPTER I

SINGLE SCATTERING OF ELECTRONS AND POSITRONS BY NUCLEI.

(i) Expressions for the differential scattering cross section.

Since electrons become highly relativistic at comparatively low energies the problem of calculating the differential cross section for the scattering of electrons or positrons by a point charge is that of solving the Dirac equation

$$[p_0 + V(r)/c - 2\pi i h(\sigma, \text{grad}) + \rho_3 m_0 c]\psi = 0$$

(where $p_0 = ih\frac{\partial}{\partial t}$ and σ and ρ are matrix operators occurring in the theory (Dirac 1928)), for the case of the coulomb potential $V(r) = Ze^2/r$. The solution has been obtained by Mott (1929, 1932) and may be written as

$$\sigma(\theta) = \left(Ze^2/hc\beta\right)^2(1-\beta^2)F^*F\cos^2\theta/2 + G^*G\sin^2\theta/2 \quad \text{I - 1}$$

The function F may be expressed in terms of an exactly known function F_0 and of F_1 an integral over an infinite series. If the series is integrated term by term an absolutely convergent series is obtained which may be evaluated numerically to any desired approximation. Similarly G may be expressed in terms of a known function G_0 and a function G_1 which may be written as a convergent series.

If /

If the expressions for F and G are inserted in I-1 we obtain for electrons

$$\sigma = \frac{Z^2e^4}{4m_0^2\beta^2c^2}(1-\beta^2)\left[\operatorname{cosec}^4\theta/2 - \beta^2\operatorname{cosec}^2\theta/2 + \pi\beta\alpha\frac{(1-\sin\theta/2)}{\sin^3\theta/2} + \text{TERMS OF ORDER}\ \alpha^2+\ldots\right] \quad \text{I-2}$$

where α has been written for $Ze^2/\hbar c = Z/137$

For positrons the cross section is obtained by substituting $-Z$ for Z in the expression I-2.

For small Z, ($\alpha \ll 1$), we may write

$$\sigma = \left(\frac{Ze^2}{2m_0\beta c}\operatorname{cosec}^2\theta/2\right)^2(1-\beta^2)(1-\beta^2\sin^2\theta/2) \quad \text{I-3}$$

and this expression has become known as Mott's simplified formula, applicable to scattering by light nuclei. If the particles are non-relativistic, $\beta \ll 1$, the expression reduces to the classical Rutherford formula

$$\sigma = \left(\frac{Ze^2}{2mv}\right)^2\operatorname{cosec}^4\theta/2 \quad \text{I-4}$$

where v is the electron velocity.

It is of interest to note that the ratio of the exact to the Rutherford cross section is almost independent of energy above about 4 Mev.

(ii) <u>Evaluation of the differential cross section.</u>

Since no closed analytical expression is available, the calculation of the differential cross section for a range of energies and atomic numbers involves lengthy computation. The earlier /

earlier calculations were made for a single element and a few values of the energy, (Bartlett and Watson, 1939; Massey, 1942), but the latest tables published by McKinley and Feshbach, (1948), and by Feshbach, (1952) enable one to obtain rather accurate values of the cross section for angles from 30° - 150° and $Z = 13$ - 80, for any energy, and for both electrons and positrons. The methods of computation have been very similar to that originally proposed by Mott. The functions F_1 and G_1 described earlier have been expanded in power series in α and β and these series are then summed numerically. More recent calculations by Curr (1955) have corrected some small errors in Feshbach's results but are in general in close agreement with them. There is also good agreement between the results of Feshbach and the calculations of Yadav (1952) for positrons. An analytical expression has been fitted empirically to the computed curves by Parzen and Wainwright (1954).

The ratios of the differential cross section, as calculated by an accurate evaluation of Mott's formula I-2, to (a) the Rutherford expression I-4, and (b) the simplified Mott formula I-3, are shown in figures I-1 and I-2. Such comparisons enable one to see how good a test of the validity of Dirac's electromagnetic theory is involved in any experiment. A parameter which is a distinctive feature of the exact /

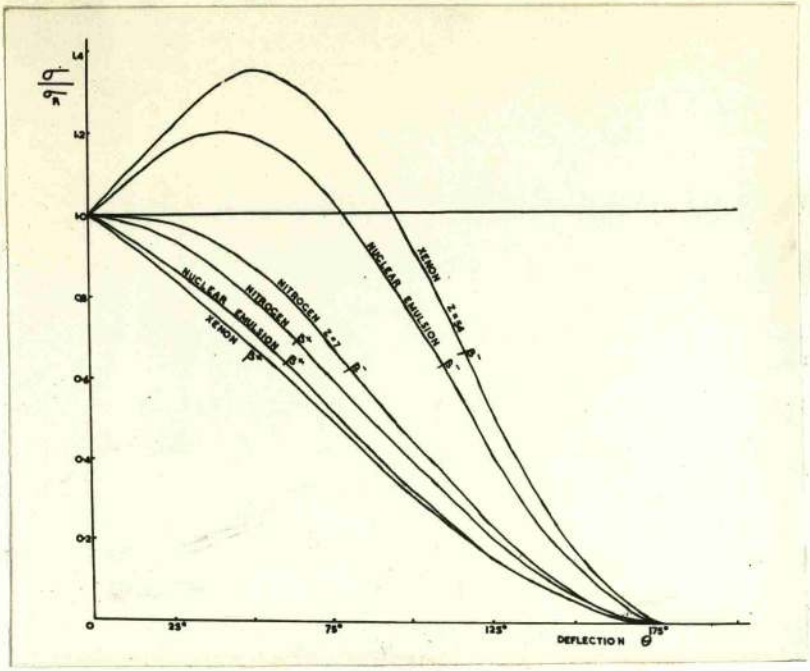

FIG. I - 1.

Ratio of the exact to the Rutherford cross section for the nuclear scattering of electrons and positrons.

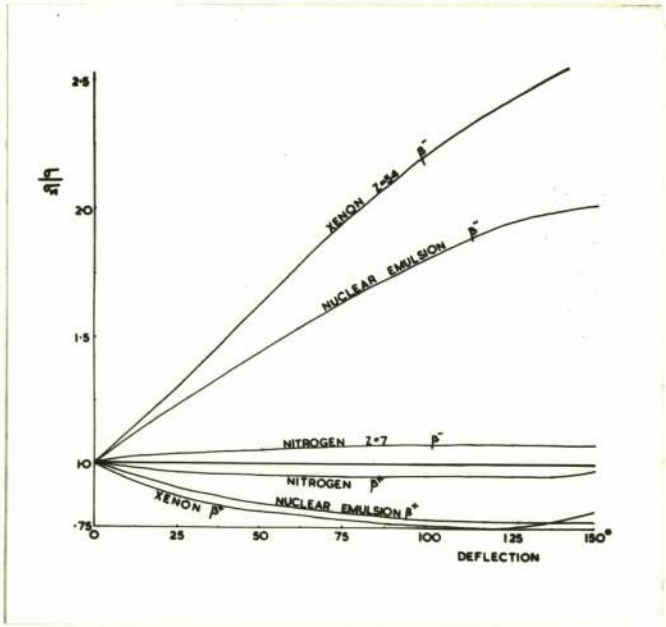

FIG. I - 2.

Ratio of the exact to Mott's simplified cross section for the nuclear scattering of electrons and positrons.

exact cross sections obtained from the Dirac equation is the difference between the scattering of electrons and positrons. The ratio of the positron and electron cross sections as a function of scattering angle is shown for various Z values in figure I-3. Since the ratio of the exact to the Rutherford cross sections is almost independent of energy at energies greater than about 4 Mev. the ratio of the scattering cross sections for electrons and positrons is also independent of energy above this value.

(iii) Modifications to the cross section for scattering by a point charge.

There are three effects which may modify the values of the scattering cross section as calculated for a point charge.

(a) The radiative correction.

(b) Effects due to the atomic electrons.

(c) The effect of finite nuclear size.

(a) The radiative correction. In the treatment so far presented it has been assumed that the incident and scattered particles have identical energies. Schwinger (1949) has however pointed out that no scattering event can be completely elastic, and has evaluated the decrease in the elastic cross section on this account. The correction decreases with decreasing energy resolution of the scattered particles and increases with increasing angle and with increasing energy. A typical /

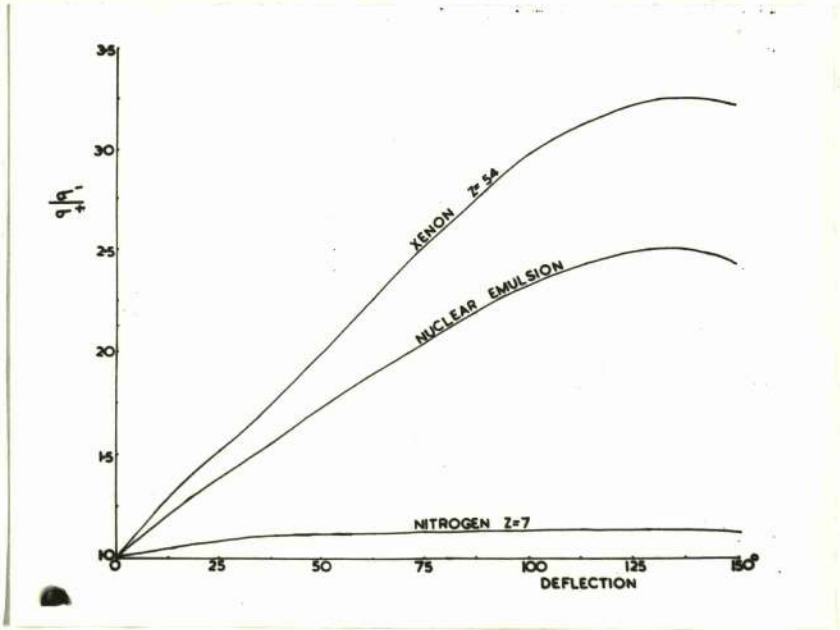

FIG. I - 3.

Ratio of the cross sections for the nuclear scattering of electrons and positrons.

typical order of magnitude for this correction is 1 - 2% for 5% resolution in the energy of the scattered particles.

(b) Effects due to the atomic electrons. The observed scattering may be affected in two ways by the atomic electrons:

(i) The atomic electrons themselves will cause scattering of the incident particles which in some types of experiment will be indistinguishable from the nuclear scattering. In such circumstances Z^2 in the scattering formula must be replaced by $Z(Z+1)$

(ii) The nuclear charge may be partially screened by the atomic electrons and the scattering is then not that due to a pure Coulomb field. Bartlett and Welton (1941) have calculated the differential cross section for the scattering of electrons of 100 Kev. and 230 Kev. by a mercury atom using a Hartree self-consistent field. The results show that the effect of screening is only noticeable at angles $\lesssim$ 60° for 100 Kev. electrons and at angles $\lesssim$ 15° for 230 Kev. electrons. Below these angles the cross section falls below that for a pure Coulomb field. Mohr and Tassie (1954) find that the effect of screening is almost negligible at energies greater than 33 Kev. for the scattering of electrons by gold and estimate an upper limit of 1 Mev. for any screening effects.

(c) Effect of finite nuclear size. In contrast to the effects of screening the effects of finite nuclear size should become /

become more important as the electron passes closer to the nucleus. Considerable deviations from pure Coulomb scattering may be expected when the electron wavelength becomes of the same order of magnitude as the nuclear dimensions.

A number of authors, (Rose 1949, Elton 1950, Acheson 1951, Feshbach 1951, Elton and Parker 1952, Schiff 1953, Smith 1954, and Yennie et al. 1954), have carried out calculations for a variety of energies and Z values, and for different assumptions concerning the distribution of the nuclear charge. The exact calculations depend on the solution of the Dirac equation both inside and outside the nuclear charge distribution, followed by fitting of the solutions at the nuclear boundary to obtain exact values of the phase shifts. Although some of the authors mentioned have used the Born approximation in their calculations, results obtained in this way can only be expected to be qualitatively true except for the light nuclei. Elton (1950) finds differences of about 100% between the exact and the Born approximation calculations for the scattering of 20 Mev. electrons through an angle of 60° by gold nuclei. The effect of the finite nuclear size is always to decrease the scattering cross section compared with that for a point charge. The decrease is greatest for large deflections and is greater for electrons than for positrons, an effect attributable to the closer approach of the electron to the nucleus for the same angles of scattering.

It /

It is possible from the foregoing discussion to distinguish three energy regions:

(a) $<$ 4 Mev. : ratio of exact to Rutherford cross section varying with energy; screening effective at lower energies; effect of finite nuclear size negligible.

(b) $\sim$ 4 - 12 Mev. : ratio of exact to Rutherford cross section independent of energy; effect of screening negligible; nuclear size effects noticeable at higher energies for intermediate and heavy nuclei.

(c) $>$ 12 Mev. : finite nuclear size effects becoming large, possibility of distinguishing shape of charge distribution.

(iv) Experimental tests of the theory of scattering.

We shall first consider briefly experiments on the scattering of particles of $\lesssim$ 3 Mev., that is falling within the first energy region mentioned above. This group comprises the vast majority of the experiments since only comparatively recently has the more general availability of accelerators made it possible to obtain particles of higher energy.

Experiments with particles of $\lesssim$ 3 Mev. have been performed by studying the scattering in the gas of an expansion chamber, in foils or plates in an expansion chamber, or in foils using /

using counters as detectors. We shall not attempt a general survey of the results of these experiments. The position may be summarised by stating that the considerable variations in the results of the early experiments, giving ratios of experimental to theoretical cross sections varying from 0.15, (Barber and Champion 1938), to ~ 20, (Skobelzyn and Stepânowa 1936), have not been confirmed by the more recent accurate counter experiments of Van de Graaf et al. (1946) and of Bayard and Yntema (1954), who find close agreement with the predicted theoretical values. It is notable also that some of the early experiments were conducted at particle energies where the effect of screening should be considered whereas the theoretical calculations with which the results were compared had not allowed for this effect.

Compared with the amount of work at energies less than 3 Mev few experiments have been performed at higher energies. Hofstadter et al. (1953, 1954) have recently carried out a series of experiments at 125 Mev and 150 Mev using magnetic analysis of both incident and scattered electron beams and detection of the particles by a Cerenkov counter. These experiments are designed to investigate the shape of the nuclear charge distribution. Experiments at 30-45 Mev have been performed by Pidd et al. (1953) using targets placed inside a synchrotron /

synchrotron donut and geiger counter detection of the scattered particles. At 15·7 Mev experiments have been carried out by Lyman, Hanson and Scott (1951) also using geiger counter detection and with magnetic analysis of the scattered particles. In these experiments a considerable finite nuclear size effect was observed for the heavy elements used, (Ag, Au), while the results for the lighter elements show fairly close agreement with the theoretical formula. The only other experiment at an energy greater than 3 Mev is due to Fowler and Oppenheimer (1938) who used particles from pair production in lead by γ -rays from the reaction $^{7}Li(p,\gamma)^{8}Be$ to study the scattering of both positive and negative electrons in a lead foil placed in a cloud chamber. In the region of pure single scattering, ($\gtrsim 14^{\circ}$ for this experiment), only 27 electron and 9 positron deflections were observed giving a ratio for the scattering cross sections for the two types of particle of $1{\cdot}6 \pm 0{\cdot}4$ compared with a theoretical prediction of $\sim 1{\cdot}5$.

When the present experiments were first undertaken only the work of Fowler and Oppenheimer had been published among the group of higher energy experiments described above. It therefore seemed desirable to make a test of the theory at as high an energy as practicable. A primary object of the experiment was a direct comparison of the scattering of electrons and /

and positrons since even at low energies there had been few experiments of such a kind, (see Lipton 1952, Howatson and Atkinson 1951).

CHAPTER II

THE SINGLE SCATTERING OF ELECTRONS AND POSITRONS OF 10 MEV IN A NUCLEAR EMULSION.

(i) Introductory.

All previous experiments on the large angle single nuclear scattering of electrons and positrons had been carried out using either counters or cloud chambers. The difficulty of collecting sufficient data to yield statistically significant results has been the principal limitation of the cloud chamber technique even for the low energy particles studied in most of the experiments. Since the scattering cross section decreases as the inverse square of the particle energy the labour involved in the successful application of this technique to higher energies becomes very considerable as is illustrated by the rather inadequate statistics of Fowler and Oppenheimer (1938). The counter method, on the other hand, involves some loss in directness of observation, rather long machine running times, good monitoring of the incident beam to obtain absolute cross sections, and, for positrons, possible difficulties due to a background of annihilation radiation.

With these considerations in mind it was decided to attempt a measurement of the differential cross section for the nuclear coulomb scattering of electrons and positrons by allowing the particles to pass into a thick nuclear emulsion and examining /

examining the deflections of the particle tracks arising from scattering by the nuclei of the constituent elements of the emulsion. In this way most of the advantages of the cloud chamber method are preserved but, since the scattering takes place in a fairly dense medium of moderately high effective atomic number, the track length required for a given number of deflections is less, even allowing for the magnification involved in the microscopic examination of the tracks in a nuclear emulsion. The emulsion method has also the advantages of simplicity in exposure to the particles and of shorter machine running times.

(ii) Experimental arrangement: exposure of the emulsions.

Ilford G5 emulsions having an unprocessed thickness of about 400μ and in the form of 3" square plates were used for the experiment. Before exposure the overall thickness of each plate was measured by placing a glass cover plate on top of the emulsion and measuring the total thickness of emulsion, glass backing, and cover plate using a micrometer screw guage. The plate was then placed in the box illustrated in figure II-1 and adjusted to make an angle of 9°.5 with the plane of this box.

Protons or deuterons were accelerated in the Glasgow H.T. set to carry out two nuclear reactions which were used to obtain the 10 Mev. particles. The positrons were all obtained by means of the reaction $^{7}Li(p,\gamma)^{8}Be$ with incident protons of about /

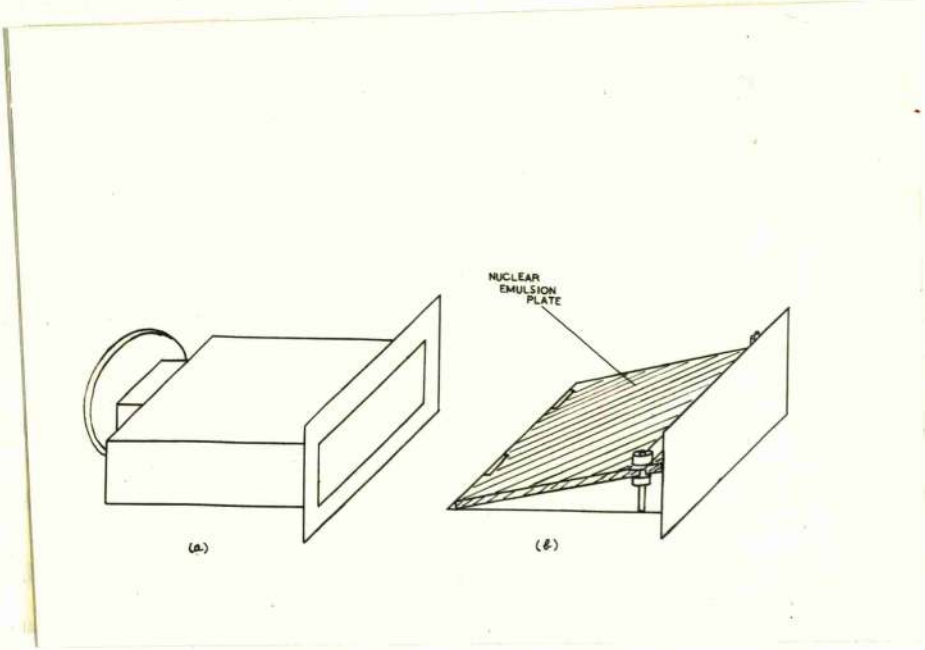

FIG. II - 1.

Container for nuclear emulsion plates in the single scattering experiment.

about 600 Kev. The 17·6 Mev γ -rays from the reaction were intercepted by a lead convector 0·8 cm. in thickness to produce pairs of electrons and positrons. The electrons were obtained by this method and also by means of the reaction $^{7}Li(\alpha,p)^{8}Li$ using deuterons of about 600 Kev. The ^{8}Li isotope decays with a half-life of 0·85 seconds and thus the reaction leads to a large yield of electrons with a maximum energy of about 12 Mev.

The experimental arrangement is illustrated in figure II-2. The protons or deuterons bent by the resolving magnet of the H.T. set fell upon a thin layer of lithium oxide on a water cooled copper backing. The lead convertor could be put in place for the $^{7}Li(p,\gamma)^{8}Be$ reaction.

Particles from the lithium target or from the lead convertor passed through collimators into the field of a 180 degree, double focussing magnetic spectrometer and to the lower end of the magnetic channel was attached the box containing the nuclear emulsion. This box was shielded from direct radiation coming from the target by 7" of lead. Both the box and the magnetic spectrometer had windows of thin aluminium foil (0·002" and 0·004" respectively) so that the box could be removed and the plate changed without breaking the vacuum in the spectrometer, which was part of the vacuum system of the H.T. set as a whole. The box containing the emulsions was thus at atmospheric pressure.

The /

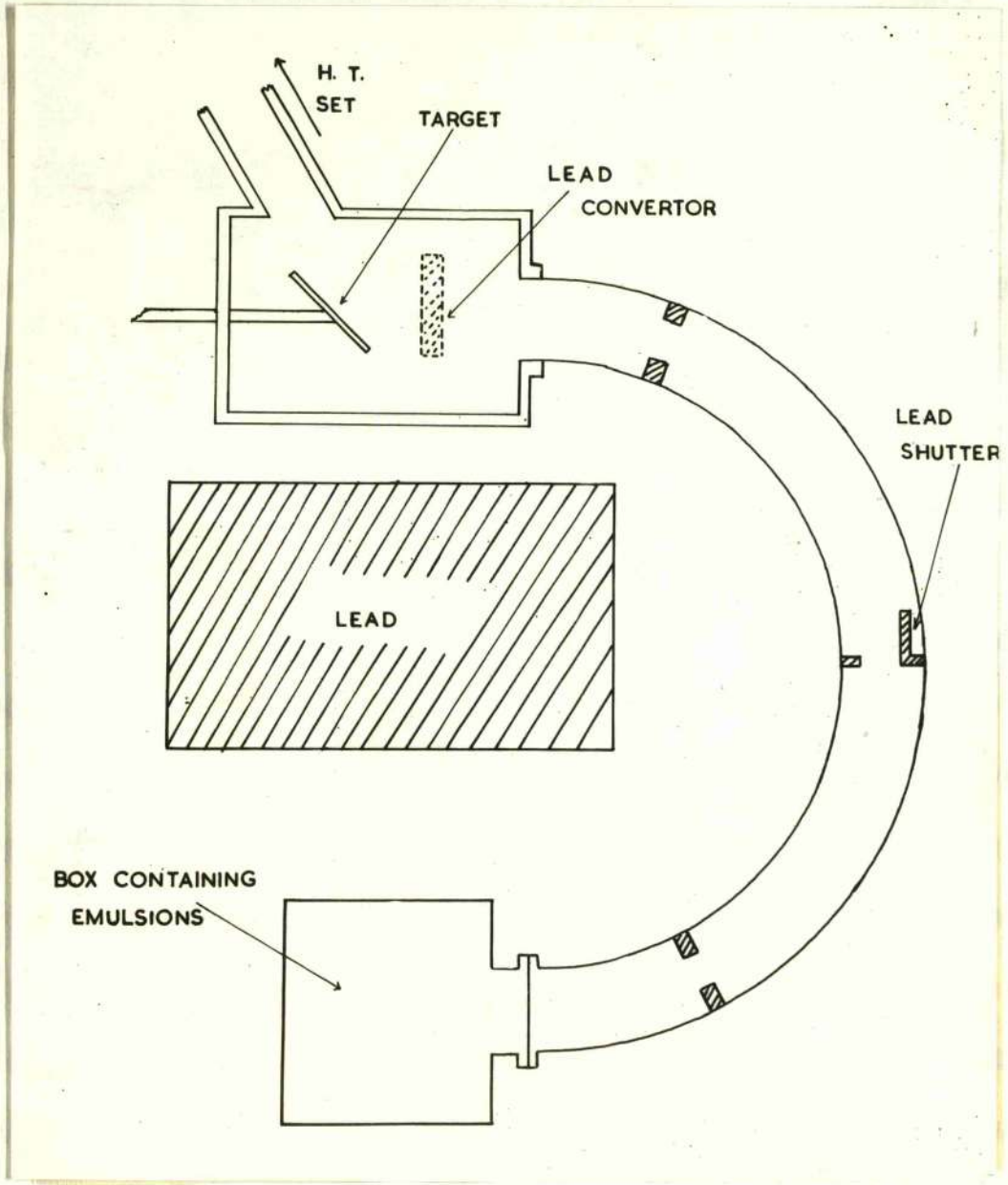

FIG. II - 2.

The experimental arrangement in the single scattering experiment.

The resolving magnet had been calibrated previously by Rutherglen et al. (private communication) using Compton electrons ejected by γ-rays of well known energy. For the present experiment the magnet current was adjusted to give particles of about 10 Mev. and field measurements to obtain the exact energy were made using a flip coil and fluxmeter. By means of the calibration curve an absolute value of the particle energy was thus obtained having a standard deviation of about $\pm$ 2·5%. The fluxmeter measurements were repeated at intervals throughout the exposure and confirmed the constancy of the magnetic field.

Before fixing into place the box containing the nuclear emulsion plate a geiger counter was put into the position to be occupied by the box. Counting rates were then measured as a function of proton or deuteron current incident on the target, (determined by means of a current integrator), (a) with the lead shutter in the spectrometer closed so that no particles passing round the magnetic channel were counted, and (b) with this shutter open. Thus was obtained a measure of the true number of 10 Mev. particles passing into the nuclear emulsion per unit of charge read on the current integrator. This method gave only rather approximate values for the necessary exposure times since it is difficult to allow for deterioration of the target during the course of a run. In the first series of exposures /

exposures four plates were exposed to electrons obtained by means of the $^{7}Li(\alpha,p)^{8}Li$ reaction. Only the plate having the shortest exposure time, eight mimutes, had a sufficiently low density of tracks, (about two tracks starting in each field of view of $2{\cdot}25\ 10^{-4}cm^2$), for satisfactory scanning conditions. Two plates were exposed, each for a time of 2·5 hours, to positrons obtained by means of pair production. These plates had a rather low density of tracks, less than one entering the surface in each field of view. In a second series plates were exposed to electrons and positrons both resulting from pair production in lead. Exposure times were ~ 2·7 hours and with rather improved proton beam current in the H.T. set, (50-60 μA resolved beam), these times gave a satisfactory density of about one track starting from the surface in each field of view.

The emulsions were developed by a conventional temperature development method, (Dainton et al. 1951), using amidol as a developing agent and a temperature of 27°C for the hot stage.

(iii) <u>Analysis of the tracks.</u>

The measurements were made on Cooke M4000 series microscopes using x 15 eyepieces and x 45 oil immersion objectives giving a field of view of about 150μ in diameter.

The particles entered the emulsion in a fairly parallel beam, ($\pm$ 12° from the mean direction), which extended across the central /

central inch of each three inch plate. Before proceeding with the single scattering measurements a check was made on the uniformity of the energy of the particles of the beam. An area was chosen 2·5 cm. square extending across the width of the beam and 0.5 cm. clear of the edge of the plate nearest the spectrometer. Thirty-six tracks in this area were selected on each plate used, such that they entered the emulsion surface at points lying on a grid pattern of 0·5 cm. spacing. Multiple scattering measurements were made on each of these tracks in order to obtain a measure of its energy. The energy of the particles on each plate was found to be uniform within the accuracy of the measurements except that particles on one edge of the beam for plates in the second exposure were found to have rather low energy values. This feature was attributed to scattering of particles from the edge of the collimators. In order to ensure particles of uniform energy only tracks from the central portion of the beam were examined.

Within this area tracks accepted for measurement had to satisfy two criteria:

(a) that they should lie within 10° of the mean beam direction.

(b) that they should have a minimum length of 500 μ for tracks entering and leaving the emulsion by the surface and of 700 μ for tracks entering the emulsion surface and leaving through the glass.

The /

The criterion (b) was introduced in order to ensure that every track accepted for measurement was sufficiently long to enable the observer to see if it was a fast electron or a background track since a small number of slow, highly scattered electrons, and of cosmic ray particles were present on most plates. The cosmic ray background had been kept to a minimum by storing the unexposed emulsions in a mine at a depth of 1400 feet until immediately prior to use. The use of the criterion (b) necessitated a correction to the results which is described in section (iv) of this chapter.

Tracks satisfying the criteria (a) and (b) were followed from their point of entry into the emulsion to a maximum length of 2000 μ or until they left the emulsion. Since the tracks suffer appreciable multiple scattering it was possible to make satisfactory length measurements only by using a calibrated eyepiece scale laid along successive sections of the track. Initially all visible sharp deflections of a track were measured, however small, but it was soon decided to impose a definite lower limit on the deflections to be measured since the measurement of very small angles is not of high accuracy and the main interest is in the large angle scattering where electron-positron differences should be greatest. An eyepiece graticule of the type illustrated in figure II-3 was made photographically. The distance between the two marks on the horizontal /

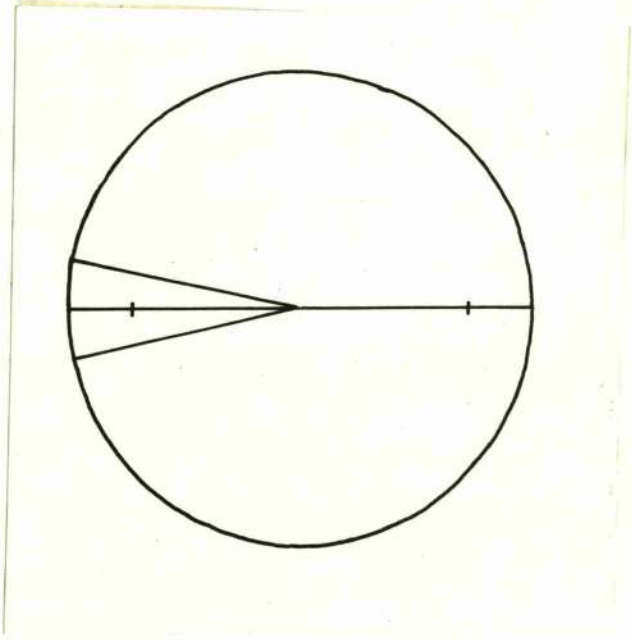

FIG. II - 3.

Graticule used in the single scattering experiment.

horizontal line corresponds to the unit of length, (95μ), and the inclined lines each make an angle of 10° with the horizontal line. Events were only accepted in which the deflected track lay on or outside the V formed by the 10° lines when the apex of the scatter was placed at the centre point and the incident track lay along the horizontal line. Thus events were only measured in which the horizontal projection of the deflection was greater than 10°. For all such events the following three measurements were made:

(a) Horizontal projection of the angle of scattering;

(b) Dip of the last 50μ of the incident track before the deflection;

(c) Dip of the 50μ of the scattered track immediately following the deflection.

(a) was measured by means of a goniometer attached to the microscope eyepiece, (b) and (c) by making measurements of the change in depth of the track over the appropriate 50μ horizontal length, by means of the microscope depth gauge, with subsequent correction for the shrinkage of the emulsion during processing. The shrinkage factor was obtained from the micrometer measurements mentioned in section (i) of this chapter combined with a measurement of the thickness of the processed emulsion, using the microscope depth guage. Measurements of the shrinkage factor by the TLC' α-particle method, (Vigneron 1949) were /

were found to be of much poorer accuracy than the direct method used unless a very great number of α-particle tracks were to be measured. The true deflection in space was obtained from (a), (b) and (c) above by using the Sigsbee diagram which affords a rapid method for such angular calculations. It should be mentioned that, except for events in which an obvious loss of energy had taken place, (as judged by a noticeable change in the multiple scattering of the track, - less than 1% of all events), tracks were not abandoned after the first deflection and occasionally more than one deflection was noted on the same track. Tracks were of course abandoned when an electron-electron scatter was observed.

In order to avoid measuring any track more than once the co-ordinates of the beginning and end of each track were noted and the start of the track was marked as a point on a map of the plate before any measurements were made.

(iv) Results.

380 cm. of electron track and 520 cm. of positron track was scanned. This total consisted of about 2500 electron tracks and 3500 positron tracks. A minimum value of 25° was chosen for the deflection in events to be used in the analysis since at such values of the angle the differential cross section is not falling so rapidly and, provided that moderately large angular intervals are used the effect of small errors in the measurement /

measurement of angles, ($\sim \pm 1{\cdot}5^{\circ}$), gives a negligible amount of 'spill over' from one interval into the next. By choosing a minimum of 25° the correction for the effect of imposing a minimum of 10° on the horizontal projection of the deflection, is also made comparatively small. The total numbers of deflections greater than 25° were 136 for electrons and 163 for positrons, and the angular distribution of these deflections is shown in table II-2 (page 25).

Before a comparison with the theoretical predictions is possible, it is necessary to apply to the measured data, corrections for the following effects:

(a) Correction for the effect of dip on the measured horizontal projections of the track lengths.

(b) Correction to the energy of the particle as obtained from the field in the magnetic spectrometer, to allow for energy losses in passing through the emulsion and the windows of aluminium foil.

(c) Correction for loss of deflections due to the minimum length acceptance criteria.

(d) Correction for loss of deflections due to the application of a minimum to the horizontal projection of the deflection.

(e) Correction for double scattering, - where two scattering events lie so close together that they are not distinguished separately.

These /

These corrections will be discussed in turn.

(a) A sample of 500 tracks was analysed to give the distribution of track lengths and the mean horizontal projection of the track length was found to be 1420μ . The vertical projection was taken to be the emulsion thickness, 400μ , for both surface to surface and surface to glass tracks. The correction factor to be applied to the measured lengths in order to obtain the true value is thus 1·04.

(b) The total energy of the electrons as obtained from measurements of the magnetic field was, for all plates 10·64 Mev. The positrons had energies of 10·64 and 10·81 Mev. Using a mean track length of 1420μ the average energy losses were calculated as:

EMULSION -	Collision loss	0·350 Mev.
	Radiation loss	0·354 Mev.
Loss in aluminium foils		0·1 Mev.
TOTAL		0·804 Mev.

Thus the mean total energies in the emulsion were 9·84 Mev for the electrons and 9·84 Mev and 10·01 for the positrons. The error introduced in the calculated value of the scattering cross section by taking a mean value of the energy rather than integrating over the energy variation is negligible. The results for all plates were normalised to an energy value of 10 Mev by multiplying the observed number of scatters by $\left(E/10\right)^2$ where E is the /

the mean total energy.

(c) The minimum lengths of 500 μ for surface to surface tracks and 700 μ for surface to glass tracks tend to bias the results against the inclusion of tracks having a large deflection in the first section of the track since such a deflection increases the probability that the track should leave the emulsion before attaining the minimum length. A calculation of the factor to be applied to correct for this effect was made by W. Bosley and was later slightly modified by the present author. The calculation consists of a geometrical analysis and subsequent numerical integrations to determine the total probability of a scattered particle leaving the emulsion with a track length less than the required minimum, as a function of the scattering angle. The results in terms of correction factors appear in table II-1, (page 24). The factors depend very slightly on the angle at which the particles enter the emulsion. This angle had been set for $9^{\circ}.5$ in the experimental arrangement and direct measurements on a sample of tracks yielded a mean value of $9^{\circ}.6$.

(d) Since no deflections were measured which had a horizontal projection of less than 10°, large angle deflections in which the scattered track dipped steeply in the emulsion but had a small horizontal projection would be missed. Thus, referring to figure II-4, tracks falling into OABC were not measured. /

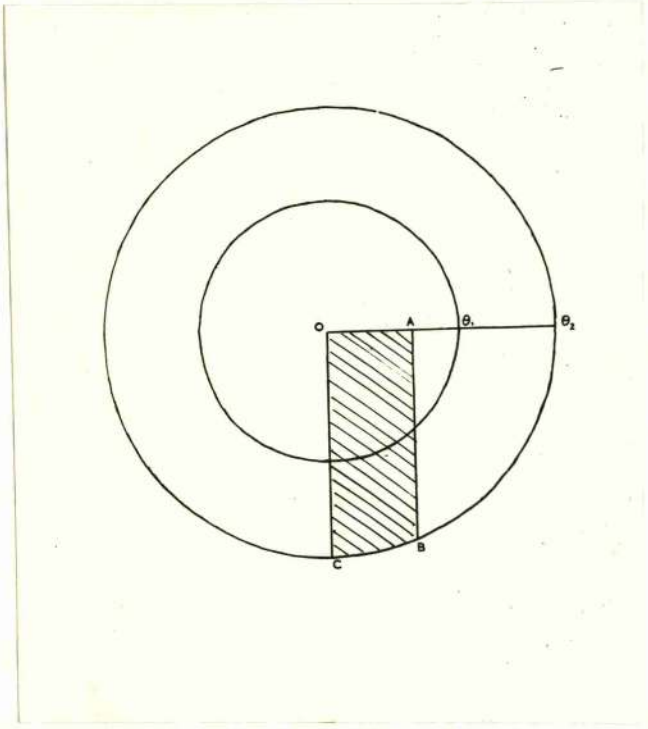

FIG. II - 4.

Illustration of the azimuthal angle correction. The incident track is normal to the paper at O. A track emerging from the paper at A has suffered a deflection of 10^{o} in the horizontal plane.

measured. If θ_1 and θ_2 are the limits of the angular interval under consideration then the correction factor is

$$\pi/2 \int_{\theta_1}^{\theta_2} \frac{\cos\theta/2 \, d\theta}{(1-\cos\theta)\cos^3\theta} \Big/ \int_{\theta_1}^{\theta_2} \frac{\cos\theta/2 \cos^{-1}\left(\frac{\tan 10^\circ}{\tan\theta}\right) d\theta}{(1-\cos\theta)\cos^3\theta}$$

where we have assumed the simple angular distribution of the Rutherford scattering law, which should be sufficiently accurate for this purpose. The integrals were evaluated numerically and yielded the correction factors for this effect given in table II-1. The measured distribution in azimuthal angle of deflections having a horizontal projection greater than 10° is shown in figure II-5 The statistical accuracy of correction factors obtained from such a plot will however be poor and the calculated value has been preferred. The values obtained from figure II-5 are $0{\cdot}75 \pm 0{\cdot}08$, $0{\cdot}83 \pm 0{\cdot}05$, and $0{\cdot}92 \pm 0{\cdot}07$, for the angular intervals $25^\circ - 35^\circ$, $35^\circ - 50^\circ$, and $50^\circ - 180^\circ$ compared with calculated values of 0·827, 0·894 and 0·991 for these intervals.

(e) Double scattering correction. It is possible that two scattering events may occur within such a short distance of each other as to appear as a single deflection. A similar problem has been treated by Wentzel (1922), and Wentzel's results were adapted to the conditions of the present experiment by W. Bosley. The author was mainly responsible for carrying out an independent analysis and rather laborious calculations /

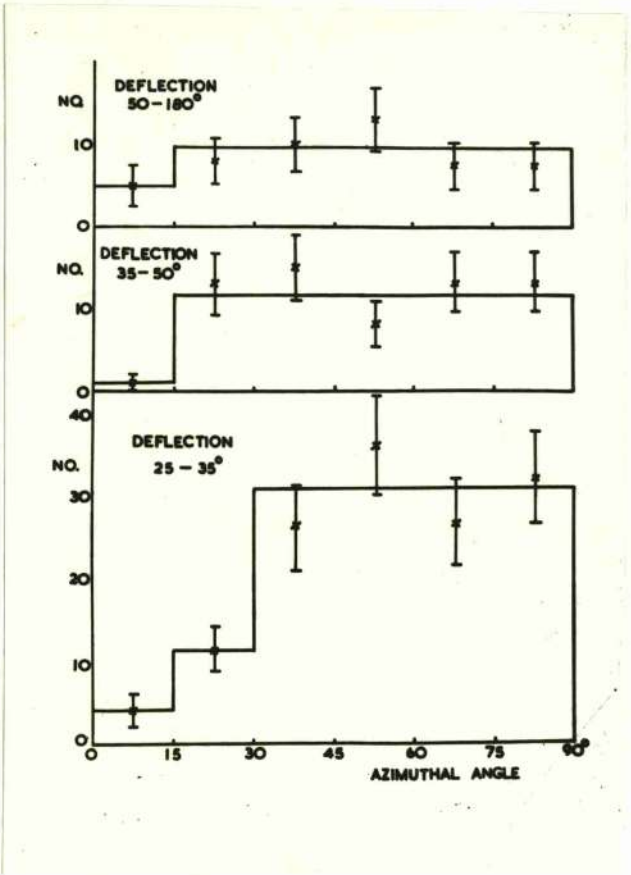

FIG. II - 5.

Distribution in azimuthal angle of deflections greater than 25°. The continuous lines represent estimated means for the distributions.

calculations for the correction factor to be applied to the number of deflections in the angular interval $10^{\circ} - 15^{\circ}$ yielded a value of 0·986. Since this correction will certainly decrease with increasing angle of scattering, it has been neglected. W. Bosley has arrived at a similar result using the Wentzel method.

The correction factors to be applied to the measured mean free paths are presented in table II-1. The measured data and the corrected results for both electrons and positrons are presented in table II-2 in terms of the mean free path for scattering through angles in the intervals stated.

TABLE II - 1.

CORRECTION FACTORS
TO BE APPLIED TO THE MEASURED MEAN FREE PATHS.

ANGULAR INTERVAL	$25^{\circ} - 35^{\circ}$	$35^{\circ} - 50^{\circ}$	$50^{\circ} - 180^{\circ}$
CORRECTION FOR ESCAPE	0·918	0·918	0·827
AZIMUTHAL ANGLE CORRECTION	0·827	0·894	0·991
TOTAL CORRECTION FACTOR	0·760	0·820	0·819

TABLE II - 2 /

TABLE II - 2.

EXPERIMENTAL VALUES OF THE MEAN FREE PATH.

A. Positrons: 517 cm. Track Length (Corrected).

ANGULAR INTERVAL	25° - 35°	35° - 50°	50° - 180°
NUMBER OF SCATTERS: EXPOSURE I	71	45	22
NORMALISED TO 10 MeV. (x 0·97)	68·8	43·6	21·3
EXPOSURE II	15	5	6
NORMALISED TO 10 MeV. (x 1·00)	15	5	6
TOTAL NUMBER (NORMALISED TO 10 MeV.)	83·8	48·6	27·3
MEAN FREE PATH (CM.)	6·17	10·62	18·94
CORRECTED MEAN FREE PATH (CM.)	4·69 ± 0·52	8·72 ± 1·49	15·51 ± 3·38

B. /

B. Electrons: 381 cm. Track Length (Corrected).

ANGULAR INTERVAL	25° - 35°	35° - 50°	50° - 180°
NUMBER OF SCATTERS: EXPOSURE I	62	29	19
EXPOSURE II	18	9	15
TOTAL	80	38	34
NORMALISED TO 10 MeV. (x 0·97)	77·6	36·8	33
MEAN FREE PATH (CM.)	4·91	10·33	11·53
CORRECTED MEAN FREE PATH (CM.)	3·73 ± 0·44	8·46 ± 1·39	9·46 ± 1·59

THE ERRORS SHOWN ARE ALL STANDARD DEVIATIONS.

TABLE III - 1.

COMPOSITION OF ILFORD G5 NUCLEAR EMULSIONS.

ELEMENT	ATOMS /C.C. (x 10^{22})
HYDROGEN	2·93
CARBON	1·51
NITROGEN	0·31
OXYGEN	0·75
SULPHUR	0·02
BROMINE	1·15
SILVER	1·17
IODINE	0·03

CHAPTER III

COMPARISON OF THE EXPERIMENTAL RESULTS WITH THEORY

(i) Evaluation of the theoretical values for the differential cross section for scattering by a point charge.

When the present experiment was first undertaken the best calculations available for the scattering from a point charge were those of Yadav (1952) for positrons and an evaluation made by Lyman, Hanson and Scott (1951) based on the work of Bartlett and Watson (1939) and of McKinley and Feshbach (1948), for electrons. The results obtained by these authors were checked against the later calculations of Feshbach (1952) for both electrons and positrons and found to be in excellent agreement.

For the purpose of the present experiment it was necessary to obtain values of the scattering cross section for a medium consisting of a mixture of the elements contained in the nuclear emulsion. The emulsion composition as given by Ilford Ltd., is reproduced in table III-1. The simplified Mott cross section and the Rutherford cross section were first evaluated for a series of values of the atomic number Z covering all the elements contained in the nuclear emulsion and for a range of angles from 5° - 180°.

The /

The simplified Mott cross section for a mixture of elements and integrated over an angular interval ($\theta_1 - \theta_2$) may be written

$$\sigma_M = \frac{\pi e^4}{p^2 v^2} \sum_i N_i Z_i^2 \left(\cot^2 \theta_1/2 - \cot^2 \theta_2/2 - 2\beta^2 \log_e \frac{\sin \theta_1/2}{\sin \theta_2/2} \right)$$

where N_i is the number of atoms of the i^{th} element having atomic number Z_i, present per c.c. of the emulsion. We may re-write this expression in the form

$$\sigma_M = \frac{\pi e^4}{p^2 v^2} \sum_i N_i Z_i^2 f(\theta)$$

(P is the particle momentum). Similarly we may write the Rutherford cross section as

$$\sigma_R = \frac{\pi e^4}{p^2 v^2} \sum_i N_i Z_i^2 F(\theta)$$

We may now write the exact point charge cross section as

$$\sigma_c = \frac{\pi e^4}{p^2 v^2} \sum_i N_i Z_i^2 f(\theta) G(Z_i, \theta)$$

where for a single element and a particular angle $G(Z_i, \theta)$ is the ratio of the exact to the simplified Mott cross section. A similar relation may be written linking the exact and the Rutherford cross sections.

The values of $G(Z_i, \theta)$ and the Rutherford cross section equivalent, for each element in the emulsion and at a series /

series of angles, were obtained by interpolation in the results of Lyman, Hanson and Scott and of Yadav (loc. cit.) who have presented their results in terms of the ratio of the exact to the Mott simplified cross section and to the Rutherford cross section respectively. Thus for each angular interval σ_c was found by summing the cross sections for the individual elements. It is clear from the dependence of the cross section on $N_i Z_i^2$ that the scattering is mainly, (~ 97%), by the silver and bromine nuclei. The calculated mean free paths for the angular intervals used are given in table III-1 (page 32).

(ii) <u>The effect of the finite nuclear size.</u>

Of the three subsidiary effects considered in chapter I, (page 4), only the finite nuclear size need be considered in the present experiment. The conditions were such that the small deviations from truly elastic scattering which are involved in the radiative correction would certainly not be detected, the energy of the particles is such that the effect of screening is completely unimportant, and scattering through angles greater than 25° by an atomic electron will always produce a distinctive two pronged event which is discarded.

For the calculation of the effect of the finite nuclear size the results of Acheson (1951) for <u>electrons</u> have been slightly extrapolated to the required energy of 10 Mev. Acheson gives ratios of the scattering cross section for a point nucleus /

nucleus to that for a finite distribution of charge of radius $1{\cdot}45.10^{-13}A^{-\frac{1}{3}}$, (a) of uniform density and (b) in the form of a shell. Using these results the point charge cross sections for the individual elements were corrected in each angular interval and the summation and integration repeated as before. Calculations of the size effect for positrons have only been made for the particular case of the scattering of 20 Mev particles by gold (Elton and Parker 1953). These authors have calculated the ratio of the cross section for scattering by a finite nucleus to that for scattering by a point charge, as a function of the scattering angle, for both positrons and electrons. In the absence of exact calculations applying to the conditions of the present experiment it has been assumed that the following ratio R is not very dependent on either the particle energy or the atomic number:

$$R = \frac{1 - \sigma_F^+/\sigma_c^+}{1 - \sigma_F^-/\sigma_c^-}$$

where $\sigma_c^{\pm}$ are the cross sections for the scattering of positrons and electrons by a point nucleus and $\sigma^{\pm}$ are the cross sections for scattering by a finite nucleus. This ratio obtained from the results of Elton and Parker for gold at 20 Mev was used in conjunction with the results of Acheson for 10 Mev particles and the requisite Z values, and with the known values of σ_c^+, to obtain σ_F^+ for the conditions of the present /

present experiment. Although the assumption used can only be expected to be approximately correct the errors introduced in this way will produce a negligible effect on the final result since the correction for the effect of the finite size is small.

The final correction factors to be applied to the point charge cross sections to allow for the effect of the finite nuclear size are shown in table III-1.

TABLE III - 1.

THEORETICAL VALUES OF THE MEAN FREE PATH.

ANGULAR INTERVAL	25° - 35°	35° - 50°	50° - 180°
THEORETICAL MEAN FREE PATH IN CM. (POINT NUCLEUS).			
ELECTRONS	3·52	6·46	9·06
POSITRONS	4·98	10·62	18·90
FINITE SIZE CORRECTION FACTOR.			
ELECTRONS:			
UNIFORM DISTRIBUTION	1·02	1·03	1·08
SHELL DISTRIBUTION	1·03	1·05	1·12
POSITRONS:			
UNIFORM DISTRIBUTION	1·01	1·01	1·02
SHELL DISTRIBUTION	1·01	1·01	1·02
CORRECTED MEAN FREE PATHS. (UNIFORM CHARGE DISTRIBUTION).			
ELECTRONS	3·59	6·65	9·81
POSITRONS	4·93	10·51	18·51

(iii) /

(iii) Comparison of theoretical and experimental results: conclusions.

The theoretical and experimental results are compared in table III-2 and figure III-1. Table III-2 also contains the values of the mean free path predicted by the Mott simplified expression and by the Rutherford formula, (equations (3) and (4) of chapter I). The exact theoretical results have been calculated assuming a uniform charge distribution in the nucleus.

TABLE III - 2.

COMPARISON OF THEORETICAL AND EXPERIMENTAL RESULTS FOR THE VALUE OF THE MEAN FREE PATH FOR SCATTERING.

ANGULAR INTERVAL		25° - 35°	35° - 50°	50° - 180°
ELECTRONS	MEASURED	3·70 ± 0·44	8·45 ± 1·39	9·45 ± 1·59
	THEORETICAL	3·59	6·65	9·81
POSITRONS	MEASURED	4·70 ± 0·52	8·70 ± 1·49	15·50 ± 3·38
	THEORETICAL	4·93	10·51	18·51
MOTT'S SIMPLIFIED FORMULA		4·31	8·78	14·40
RUTHERFORD FORMULA		4·01	7·33	9·00

The following conclusions may be drawn from the results:

(a) /

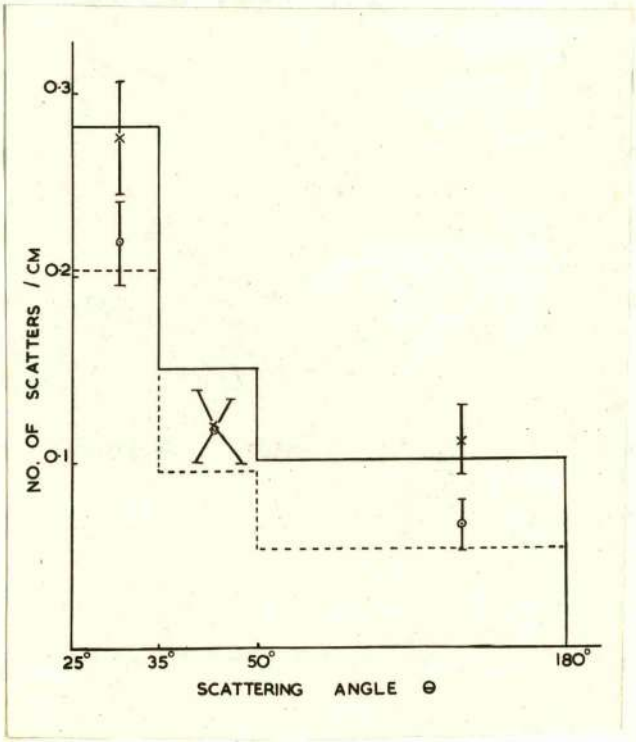

FIG. III - 1.

Theoretical and experimental values for the number of scatters per cm. of track length as a function of the scattering angle θ, for 10 Mev electrons and positrons in a nuclear emulsion.

(a) The results appear to confirm the theoretical prediction of a difference between the nuclear scattering of electrons and positrons at 10 MeV due to the difference in the spin-orbital forces on the two types of particle. The results also show that the theories of single coulomb scattering based on the Dirac equation predict cross sections of the correct magnitude at this energy.

(b) The statistical errors associated with the experimental data are too large to allow a detailed examination to be made of the differences in the scattering probabilities for electrons and positrons as a function of scattering angle. The difficulty of improving the statistical accuracy using this technique is such that for work requiring such accuracy at energies greater than 10 MeV it is clear that counter techniques provide the only possible method.

CHAPTER IV

MULTIPLE COULOMB SCATTERING OF ELECTRONS AND POSITRONS.

(i) Introductory.

The theory of the multiple scattering of particles involves (a) the operative single scattering law, especially as it applies to scattering through small angles, and (b) the statistical combination of the individual scattering events to give the resultant deflection over a finite scattering thickness. Studies of multiple scattering would thus seem not to be of such direct theoretical interest as those on single scattering. Multiple scattering experiments are of importance however in studying the outer regions of the scattering potential, and also, since multiple scattering, particularly using the nuclear emulsion technique, has come to be an important adjunct to the measurement of particle masses and momenta.

The review which follows is not intended to give a derivation of the theoretical results but rather as an appraisal of the influence on the scattering of the various parameters involved, with particular regard to any factors which might lead to a difference between the scattering of electrons and positrons.

(ii) Theory of multiple scattering.

We shall first present a description of the multiple scattering process which although simplified illustrates the main /

main features of the theory.

The mean square angle of scattering for particles passing through an infinitesimal layer of scatterer of thickness dx is

$$\langle\theta^2\rangle_{AV,dx} = dx \int_{\theta_{MIN}}^{\theta_{MAX}} \theta^2 \xi(\theta) 2\pi\theta\, d\theta$$

where $\xi(\theta)$ is the probability of a deflection θ, and θ min. and θ max. are the minimum and maximum deflections and will be discussed later. For small angles we may write

$$\xi(\theta)\, d\omega = 4N Z^2/A \; \frac{m_0 e^2}{p^2\beta^2c^2} \; \frac{d\omega}{\theta^4}$$

where the symbols have the usual meanings. Then

$$\langle\theta^2\rangle_{AV,dx} = dx\, K \log \frac{\theta_{MAX}}{\theta_{MIN}}$$

where we have written K for $8\pi \frac{NZ^2}{A} \frac{m_0 e^2}{p^2\beta^2c^2}$ and the mean square value of θ for a scatterer of thickness t can be obtained by integration of this equation to give

$$\langle\theta^2\rangle_{AV,t} = t K \log \frac{\theta_{MAX}}{\theta_{MIN}}$$

The distribution function for θ may be obtained by the integration of a simple first order diffusion equation, (Rossi and Griesen 1941), and may be written

$$F(t,\theta) = \frac{1}{2\sqrt{\pi}} \; \frac{\sigma}{t^{1/2}} \; e^{-1/4\,\sigma^2\theta^2/t}$$

where $\sigma^2 = 2/K \log \frac{\theta_{MAX}}{\theta_{MIN}}$ Thus the distribution of the scattering angle is gaussian.

In /

In most experiments it is most convenient to measure the projection of the multiple scattering angles on a plane at right angles to the line of vision. If this angle is denoted by ϕ it may be shown that for a gaussian distribution of θ the distribution of ϕ is also gaussian.

Several features of the treatment outlined above require further consideration.

(a) A simple Rutherford scattering law has been used.

(b) The treatment leading to a gaussian distribution function contains approximations which limit the result to small angles.

(c) θ max. and θ min. remain to be defined in terms of known quantities.

Despite these limitations the formula obtained above for $\langle\theta^2\rangle_{AV,C}$ illustrates the principal features of the multiple scattering process: dependence of the scattering on the inverse of the particle momentum, approximate independence of the particle mass, and proportionality to Nz^2, since the logarithmic term can only be a slowly varying function of these parameters.

We may now discuss the limitations (a), (b) and (c) above, as they are treated by published theories of multiple scattering.

Theory of E. J. Williams (1939).

(a) Scattering law. Williams discusses the magnitude of the deviations to be expected from the scattering as calculated from /

from the Rutherford single scattering law if the exact Dirac equation is used and finds such deviations to be very small.

(b) Distribution function. An angle θ_1 is defined such that, on the average, a particle will suffer one deflection greater than θ_1 in traversing the scattering thickness. The distribution of the resultant deflections due to individual scattering events with angles less than θ_1 is taken to be gaussian. The influence on the distribution function and on the mean value of the scattering angle, of individual deflections greater than θ_1 is calculated separately and added to the original. A second angle θ_2 is defined such that beyond this angle single scattering is greater than multiple scattering as calculated using the gaussian distribution. The scattering beyond θ_2 is taken to be single only and the junction between the single and multiple scattering curves is smoothed to produce a composite distribution for all angles.

(c) θ max. and θ min. Except for energies such that the small angle scattering is influenced by the finite nuclear size θ max. is the same as Williams' θ_1. θ min. depends on the screening of the nucleus by the orbital electrons. For exponential shielding the potential is $V = ze^2/r \cdot e^{-r/a}$ where 'a' is the Thomas-Fermi radius, and in the Born approximation one obtains θ min. $\sim \lambda\!\!\!^{-}/a$ where $\lambda\!\!\!^{-}$ is the particle wavelength. For a more accurate treatment it is possible to use /

use a potential given by a better calculation of the atomic field. This was in fact done by Williams who obtains θ min = $1{\cdot}75\,\pi/a$. Williams has used the Born approximation in obtaining this result and the use of this approximation may lead to errors in the scattering distribution around $\theta = \pi/a$. Williams also gives a treatment for the purely classical case.

Theory of G. Molière (1947, 1948).

Molière's theory is more exact but mathematically more involved than the treatment given by Williams.

(a) and (c): Scattering law and θ min. In Molière's theory the exact form of the scattering law only enters through the parameter θ min. Whereas Williams treats only the classical and Born approximation extreme cases Molière (1947) has given a treatment which is accurate for the complete range. Using a Thomas-Fermi potential Molière obtains

$$\theta_{MIN} = \pi/a\,(1{\cdot}13 + 3{\cdot}76\alpha^2)^{1/2}$$

where $\alpha = Z/137\beta$ (Born approximation $\alpha \ll 1$, classical case $\alpha \gg 1$), and the α^2 term represents the deviation from the Born approximation.

(b) Distribution function. Molière obtains the distribution function in terms of a series of Bessel functions by a method equivalent to solution of the standard diffusion equation. This leads to the definition of the parameter B which is the greater solution of the equation $B - \ln B = \ln \Omega_b - 0{\cdot}115$

where /

where $\Omega_b = 2\pi e^2 (Nz^2)^{1/2} z t^{1/2} / p v \theta^2_{MIN}$ and is a measure of the average number of collisions suffered by the particle in traversing the thickness t. In terms of the projected angle ϕ the distribution function may be written

$$F(\phi)d\phi = \left[\frac{2}{\pi^{1/2}} \cdot e^{-\varphi^2} + f_1(\phi) B^{-1} + f_2(\phi) B^{-2} + \cdots \right] \quad \text{IV - 1.}$$

The first term of this expression gives the gaussian distribution, the second leads at large angles to the single scattering distribution and the subsequent terms are corrections of rapidly decreasing importance. $f_1(\phi)$ and $f_2(\phi)$ are tabulated by Molière and, more extensively, by Bethe (1953).

Other theories have been published by Snyder and Scott (1949) and by Goudsmit and Saunderson (1940). These theories are equivalent to that of Molière in the general mathematical treatment and yield results in close agreement with those obtained by him.

(iii) <u>Differences between the multiple scattering of electrons and positrons.</u>

Differences between the multiple scattering of electrons and positrons might be expected to arise from the following causes:

(a) Differences in the nuclear scattering of the two types of particle.

(b) Differences in the scattering of the two types of particle by the atomic electrons.

(c) /

(c) Differences in energy loss by the two types of particle in passing through the scattering medium, with consequent differences in the effective energies of the particles.

(a) The spin orbital effect operative in single scattering will give rise to a small difference between the multiple scattering of electrons and positrons. The finite nuclear size will have no effect on the scattering at such small angles, (Williams 1939, Elton and Parker 1952), but the effects of screening may be important. Calculations of the difference to be expected have been performed by Mohr and Tassie (1954) using the second Born approximation and assuming that the fractional error in the value given for the electron-positron difference by the second Born approximation is the same for the screened field as for the unscreened coulomb field. Since the fractional error involved can be ~ 50% for heavy nuclei this assumption may not be completely valid. Mohr's results are reproduced in figure IV-1.

(b) The scattering of the particles by the atomic electrons will contribute a fraction $\sim \Sigma N_i Z_i / \Sigma N_i Z_i^2$ (2·7% in a nuclear emulsion), of the nuclear scattering, (the effect of the different values of θ min. for nuclei and electrons has been discussed by Fàno (1954). For the conditions of the present experiment the effect is negligible). The ratio of the scattering cross sections for electrons by electrons and for positrons by electrons is then obtained by taking the ratio of the Møller (1931, 1932) and Bhabha (1936) /

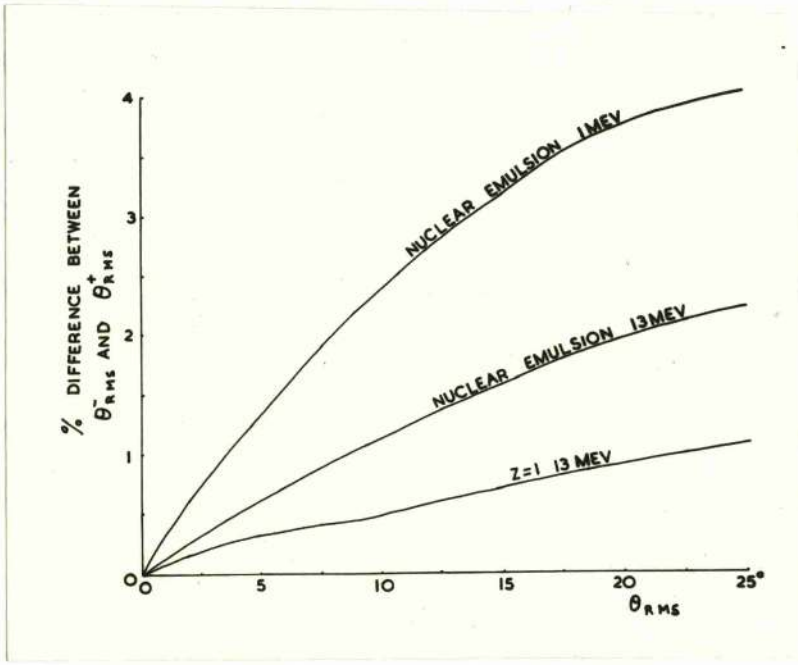

FIG. IV - 1.

Percentage difference between the root mean square angles of scattering for electrons and positrons as calculated by Mohr and Tassie (1954).

(1936) cross sections for small angles. The difference in the total cross section due to this source is obtained by multiplying this ratio by $\Sigma N_i Z_i / \Sigma N_i Z_i^2$

(c) Since the particles will lose different amounts of energy in passing through the scattering material the effective energy will be different for electrons and positrons. Rohrlich and Carlson (1954) have integrated the Møller and Bhabha cross sections to obtain the energy losses due to collision processes and for 10 Mev particles passing through a nuclear emulsion the difference between the losses of electrons and positrons is 1·8% of the mean ionisation loss and this fraction varies only slowly with both energy and atomic number. Neither the results of Bethe and Heitler (1934) nor of Maximon, Davies and Bethe (1952) predict any difference in electron and positron bremsstrahlung. One might however expect some small difference due to the closer approach of the electron to the nucleus. The upper part of the bremsstrahlung spectra due to electrons and positrons has been examined by Fisher (1953) who finds for particles ~247 Mev mean energy a ratio of positron to electron radiative cross sections of 0·973 ± 0·017 for losses greater than 6 Mev. This evidence together with the theoretical predictions leads us to put an upper limit ~2% on the difference in radiative loss even for low energy quanta.

Although all the effects mentioned reduce the scattering /

scattering of positrons compared with electrons the total magnitude of the predicted difference in cross sections is small ($\lesssim 1\%$) in all cases so far studied experimentally.

(iv) The measurement of multiple scattering.

The experimental data obtained from any multiple scattering measurement is the angular distribution of the scattered particles. It is possible to take as a measure of the scattering any quantity which is determined by the width of the distribution such as the root mean square angle, the half width at half maximum, or the arithmetic mean of the scattering angles.

In the simple treatment

$$\bar{\theta} = \left[\frac{2\langle\theta^2\rangle_{AV}}{\pi}\right]^{1/2} = \left[\frac{2K}{\pi}\log\frac{\theta_{MAX}}{\theta_{MIN}}\right]^{1/2}\cdot t^{1/2}$$

and it is easily shown that a similar relation holds for the angles projected on a plane normal to the direction of observation. Williams obtains for the mean projected angle

$$\bar{\phi}_W = \left\{0.80\left[\log\frac{Z^{4/3}Nt\hbar^2}{(1.45)^2 2\pi m_0^2\beta^2c^2}\right]^{1/2} + 1.45\right\}\cdot\delta$$

where we have written δ for the unit of angle $\delta = \left(\frac{4NtZ^2e^4}{p^2\beta^2c^2}\right)^{1/2}$

Molière obtains a mean projected angle

$$\bar{\phi}_M = B^{1/2}\left[1 + {}^{0.982}/_{B} - {}^{0.114}/_{B^2}\right]\cdot\delta$$

where B has been defined earlier. Thus in each case we may write

$$\bar{\phi} = K_1\, {}^{t^{1/2}}/_{pv} \qquad \text{IV - 2.}$$

where /

where K_1 is known as the scattering constant for the medium and is independent of $p\nu$ and only a slowly varying function of t. K_1 for the various theories is obtainable from the above expressions in terms of known properties of the scattering medium. It is clear that, especially if the statistical accuracy of the measurements is not high, the presence or absence of a few large values of the scattering angle in the tail of the distribution may have a considerable effect on its mean. To avoid this difficulty a 'cut' value of the mean angle and a corresponding cut value of the scattering constant are frequently employed, in which all angles greater than four times the mean value are excluded.

(v) Experiments on multiple scattering.

The experiments which have been performed on multiple scattering fall into two classes: (a) scattering by thin foils and (b) scattering in the gas of a cloud chamber or in a nuclear emulsion. Cloud chambers and nuclear emulsions are particularly suited to these measurements since the individual particle may, using these techniques, be followed inside the scattering medium and it is thus possible to measure the scattering for a very large range of values of t in a single experiment. It should also be emphasised that, in contrast with experiments on single scattering, multiple scattering measurements using nuclear emulsions may be carried out in a comparatively /

comparatively short time with moderately high statistical accuracy.

We shall not present here a detailed survey of previous experiments on multiple scattering. The results for the scattering of electrons and positrons in nuclear emulsions are summarised in table 4 of chapter V and at the time when the present experiments were undertaken the state of knowledge concerning multiple scattering could be summarised as follows:-

(a) Experiments with foils confirmed the z-dependence of Molière's theory for low and intermediate z-values.

(b) Experiments with foils and with nuclear emulsions confirmed the momentum dependence of the theory except at very low values of momentum (Hisdal 1952).

(c) Experiments with foils and with emulsions confirmed the theoretical predictions for the dependence on cell size, (scattering thickness), for large cell sizes, (greater than 100μ for emulsions).

(d) The general form predicted by Molière for the distribution function had been confirmed by nearly all the experiments within the limits of experimental error.

(e) The absolute values of the mean scattering angle were in some cases, (particularly for lead), lower than those predicted and complete agreement, (within 15%), had not been attained concerning the scattering in nuclear emulsions.

(f) /

(f) The dependence on cell size had been found to be anomalous for small cell sizes, (Bosley and Muirhead 1952) and the anomaly indicated a divergence between experiment and theory concerning the tail of the scattering distribution.

(g) The experiments of Groetzinger et al. (1950) on the scattering of 1·5 - 2·5 Mev. electrons and positrons in argon in a cloud chamber and of Corson (1951) on the scattering of 196 Mev. electrons and positrons in a nuclear emulsion indicated a difference $\sim$ 10% in the multiple scattering of the two types of particle.* Cusack and Stott (1955) obtain values of (93 $\pm$ 5)% of the theoretical value for the scattering of positrons in nitrogen, (101 $\pm$ 5)% for electrons in nitrogen and (92 $\pm$ 5)% and (91 $\pm$ 5)% of the theoretical value for the scattering of positrons and electrons respectively in argon.

* Corson (1951) does not explicitly remark on this difference.

CHAPTER V

THE MULTIPLE SCATTERING OF ELECTRONS AND POSITRONS OF 10 MEV IN A NUCLEAR EMULSION.

(i) Introductory.

The purpose of the present experiment was to investigate the last two anomalous features presented in the summary at the end of chapter IV.

It is clear from the results of Bosley and Muirhead (1952) that for small cell sizes the scattering of electrons is considerably greater than that predicted, theoretically, (fig. V-1a). If the experimental scattering distribution is cut off at four times the mean value then the scattering constants calculated for this cut distribution are in good agreement with theory, (fig. V-1b) and thus the anomaly is a feature of the tail of the scattering distribution. Since this anomalous behaviour had not been noted prior to the work of Bosley and Muirhead it was of interest to check this result.

The results of Groetzinger, Humphrey and Ribe (1952) and of Corson (1951) indicate a difference in the multiple scattering of positrons and electrons of the same energy. Possible reasons for such a difference have been mentioned in chapter IV but, (see page 54), an evaluation of the anticipated magnitude of the difference gives values $< 1\%$ whereas differences $\sim 10\%$ are observed experimentally. In view of the theoretical interest and possible practical

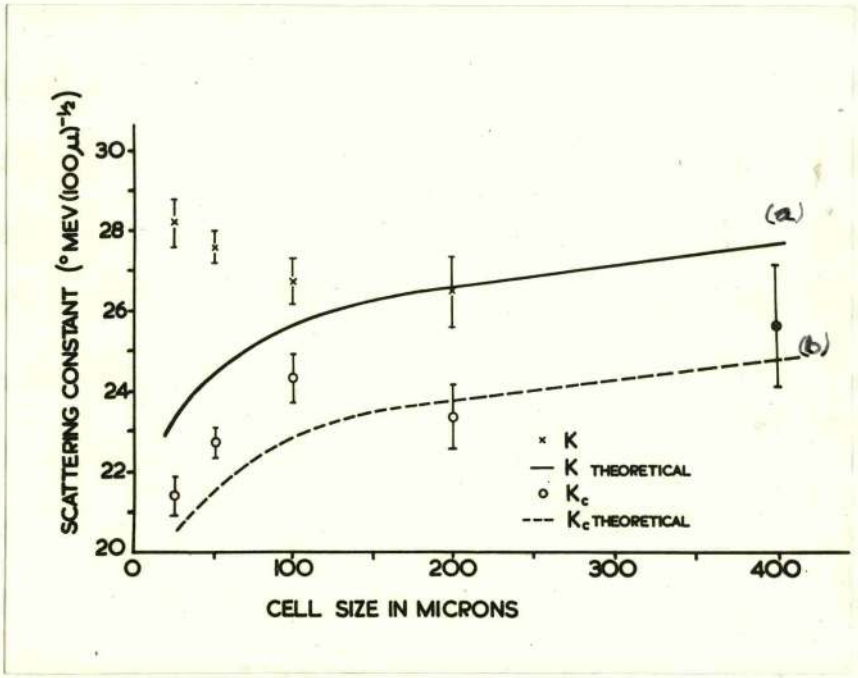

FIG. V - 1.

Scattering constants as measured by Bosley and Muirhead (1952) for electrons.

importance of such a difference it was thought desirable to investigate this feature using the nuclear emulsions exposed to electrons and positrons, under almost identical conditions, for the single scattering experiment described earlier.

(ii) Measurements.

The emulsions used were the Ilford G 5 400μ plates exposed for the single scattering experiment described in chapter II. Only tracks from the central portion of the beam were used for measurement and the same length and angle of entry criteria were employed as in the earlier experiment. The plates were fixed to the stage of M4000 Cooke, Troughton and Simm's microscopes so that the mean beam direction made only a small angle with the x - movement. The measurement of the scattering was made using a x 45 oil immersion objective and x 15 eyepieces one of which contained a graticule having a graduated scale. This scale had 60 divisions and with the magnification and interocular distance employed was found by direct calibration to have a length of 100μ. The method used for measuring the scattering was the co-ordinate technique devised by P. H. Fowler (1950) and the eyepiece scale was set so as to lie exactly in the direction of the y - movement of the microscope.

Tracks satisfying the acceptance criteria were chosen at random over the central area of each plate. It was customary /

customary to take the first reading on the eyepiece scale about 100 μ from the beginning of a track in order to avoid the rather heavier deposit of grains on the emulsion surface. Readings of the position at which the track crossed the vertical eyepiece scale were then taken at intervals of 25 μ on the x - movement to a maximum length of 2000 μ. The eyepiece scale was read to 0·1 units, (equivalent to 0·1665 μ), with a probable error of $\pm$ 0·1 units. If these readings of the eyepiece scale are denoted $y_1, y_2, \ldots y_n \ldots$ then first and second differences, $(y_1 - y_2)$, $(y_2 - y_3) \ldots (y_n - y_{n+1})$ and $(y_1 - 2y_2 + y_3) \ldots (y_n - 2y_{n+1} + y_{n+2}) \ldots$ were obtained, the differences always being treated algebraically. Thus the data obtained from a track of maximum allowed length consisted of 78 second differences each with + or - sign.

(iii) Results.

A frequency distribution of the second differences, such as those shown in figure V-8, was constructed for each plate. The arithmetic mean of the second differences was then obtained by evaluating $\sum_i n_i x_i / \sum_i n_i$. With the co-ordinate technique it is easy to obtain the angle between chords having a length which is any integral multiple of the measured chord length. Thus frequency distributions and average values of the scattering angle were obtained for each plate for cell sizes, (chord lengths), of 25 μ, 50 μ, 100 μ, 200 μ and 400 μ. The average values for electrons and for positrons /

positrons, with and without cut off, appear in table V-1.

TABLE V - 1.

AVERAGE ANGLES BETWEEN SUCCESSIVE CHORDS. (DEGREES).

	AVERAGE ANGLE BETWEEN CHORDS. (UNCUT).					AVERAGE ANGLE BETWEEN CHORDS. (CUT).				
CELL SIZE (μ)	25	50	100	200	400	25	50	100	200	400
ELECTRONS	1·743	2·146	2·975	4·25	6·01	1·443	1·878	2·760	3·925	5·79
POSITRONS	1·622	1·981	2·553	3·606	5·16	1·241	1·698	2·293	3·36	4·85

(iv) Corrections.

The averages of the measured scattering angles require corrections for the following effects:

(a) Spurious scattering, ('noise'), due to uneven movements of the microscope stage and to inaccuracies of measurement.

(b) Inclination of the tracks to the x - axis.

(c) Distortion of the tracks during the processing of the emulsion.

(a) Noise: The noise may be conveniently determined by performing scattering measurements on the track of a very fast cosmic ray particle passing through the emulsion at a small angle. Such a track may be assumed to have negligible true scattering /

scattering and the measured values are solely due to noise. This procedure was carried out for each of the two microscopes used. The corrected value of the scattering was then obtained from the relation $\alpha_{COR} = (\alpha_M^2 - \alpha_N^2)^{1/2}$ where α_N is the average spurious scattering angle, α_M the average measured angle and α_{COR} the corrected value.

(b) Inclination of the tracks to the x - axis: An inclination of the track at an angle θ can be seen by a simple geometrical consideration to lead to an increase in the measured value of the scattering angle by a factor $\sec^2\theta$ and an increase in the cell size by a factor $\sec\theta$. Thus for scattering constants

$$K_{TRUE} = K_{MEASURED} \times (\cos\theta)^{5/2}$$

θ was determined in the present experiment from a sample of tracks by noting the difference Δy in the y co-ordinates of the beginning and end of the track for tracks with a continuous variation in y and over the separate sections of tracks which showed both increases and decreases. The length l of each track or section of track was also noted and θ_{AV} for each track was taken as the mean over the sections of the track of angles θ obtained from $\sin\theta = \Delta y/l$. A mean value of θ_{AV} was obtained for each plate from samples of thirty tracks. The mean values obtained were $5{\cdot}6^\circ$, $5{\cdot}7^\circ$ and $7{\cdot}0^\circ$ yielding values of $(\cos\theta)^{5/2}$ of 0·987, 0·987 and 0·982 respectively.

(c) Distortion: Distortion during the processing or the subsequent drying of the emulsion will in general produce a curvature /

curvature in otherwise straight tracks which becomes apparent if one examines the frequency distribution of the second differences taking the algebraic signs into account. Undistorted tracks should give a distribution symmetrical about zero whereas a distorted track may be expected to give an asymmetrical distribution. The amount by which the central peak of the distribution is displaced from zero is a measure of the distortion and the distortion may be expected to increase approximately as the square of the cell size.

The 100μ and 400μ cell size second difference distributions were plotted with regard to sign for each of the three plates used. The distributions for 100μ cell size are reproduced in fig. V - 2. It is clear that only plate II2 from the second set of exposures shows evidence of distortion. This conclusion is completely confirmed by the distributions for 400μ cell size. For plate II2 the distributions were examined for each cell size and the distortion was corrected by displacing the zero so that $\Sigma N^{+} = \Sigma N^{-}$. The effect of the correction is illustrated in table V-2. The correction for plate II2 is $\sim 3\%$ for the 100μ cell and $\sim 15\%$ for the 400μ cell. The variation of distortion with cell size for this plate is illustrated in fig. V-3.

(v) Discussion.

The corrections to the uncut values of the average scattering angle are presented in table V-2; the corrections

to /

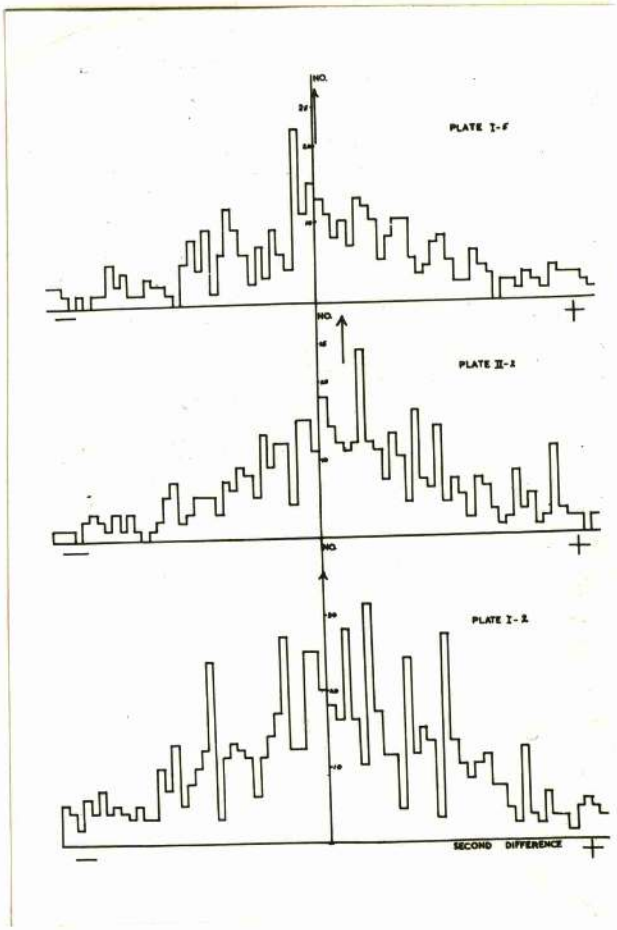

FIG. V - 2.

Frequency distributions of the second differences obtained from measurements on electron and positron tracks for the three plates used, at a cell size of 100μ. The medians for each plate are indicated by arrows.

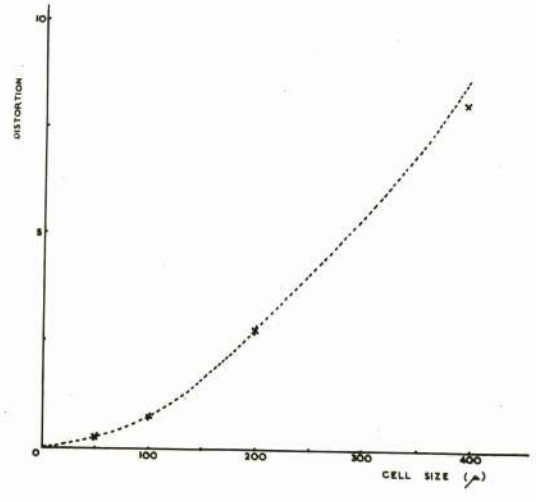

FIG. V - 3.

Variation with cell size, of the deviation from zero of the mean of the second differences for plate II - 2. The dotted curve represents a variation of the distortion as the square of the cell size.

TABLE V - 2.

CORRECTIONS TO THE AVERAGE, (UNCUT) SCATTERING ANGLES.

	POSITRONS					ELECTRONS				
CELL SIZE (μ)	25	50	100	200	400	25	50	100	200	400
MEASURED VALUES	1·622°	1·981°	2·553°	3·606°	5·16°	1·743°	2·146°	2·975°	4·25°	6·01°
CORRECTED FOR DISTORTION	1·622	1·962	2·519	3·51	4·75	1·743	2·146	2·975	4·25	6·01
CORRECTED FOR 'NOISE'	1·517	1·931	2·512	3·51	4·75	1·61	2·113	2·951	4·25	6·01
CORRECTED FOR INCLINATION	1·492	1·901	2·468	3·45	4·67	1·59	2·085	2·908	4·19	5·92
OVERALL CORRECTION	8%	4%	3%	4%	9%	9%	3%	2%	1%	1%

to the cut values are almost identical. The corrected results, in terms of the scattering constant are presented and compared with the values obtained by other workers in table V-4, and are shown in figure V-4.

We may discuss the results under two headings: (a) the difference in the multiple scattering of electrons and positrons and (b) the absolute values of the scattering constant.

(a) The positron-electron difference: The ratios of the scattering constants for electrons and positrons are shown in table V-3 below. The values of this ratio calculated taking into account the three effects discussed in chapter IV are also shown and these effects are seen to be inadequate to account for the experimental results if their theoretical treatment is correct. The ratios obtained by other workers who have measured the scattering of both types of particle under the same conditions are also included and appear to be in approximate agreement with the present work despite the great differences in energy. The corrections applied to the results are small for the 50μ , 100μ and 200μ cell sizes, and the results for these sizes must be considered most reliable. These results

TABLE V - 3. /

TABLE V - 3.

THE RATIO OF THE SCATTERING CONSTANTS FOR ELECTRONS AND POSITRONS.

	K^-/K^+ (UNCUT)					K^-/K^+ (CUT)				
CELL SIZE (μ)	25	50	100	200	400	25	50	100	200	400
PRESENT WORK 10 MeV.	1·04 ±·02	1·06 ±·03	1·15 ±0·03	1·18 ±·04	1·21 ±·07	1·01 ±·02	1·13 ±·02	1·20 ±·03	1·16 ±·04	1·25 ±·07
CALCULATED FOR PRESENT EXPERIMENT	1·004	1·004	1·006	1·007	1·009	1·003	1·004	1·005	1·007	1·009
CORSON (1951) 196 MeV.	-	-	1·09 ±·05	-	-	-	-	-	-	-
HEYMAN AND WILLIAMS (1955) 2·5 MeV.	-	1·17 ±·02	-	-	-	-	1·14 ±·02	-	-	-

THE ERRORS SHOWN ARE STANDARD DEVIATIONS.

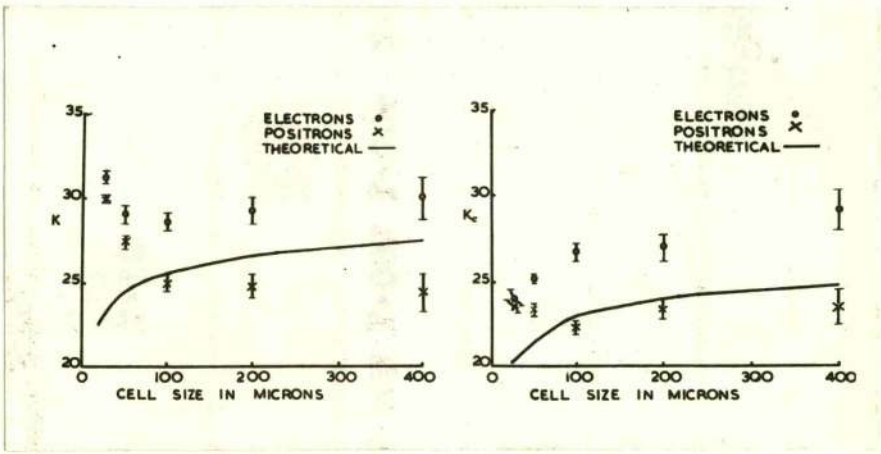

FIG. V - 4.

Measured values of the scattering constant, (after correction), for electrons and positrons. The lines correspond to the theoretical predictions of Moliere (1948).

TABLE V - 4.

(a) COMPARISON OF UNCUT SCATTERING CONSTANTS.

AUTHOR	PARTICLE AND ENERGY	K_u (UNCUT) CELL SIZE (μ) 25	50	100	200	400
PRESENT WORK	10 MEV ELECTRONS	$31{\cdot}2 \pm 0{\cdot}5$	$29{\cdot}0 \pm 0{\cdot}5$	$28{\cdot}6 \pm 0{\cdot}5$	$29{\cdot}2 \pm 0{\cdot}8$	$29{\cdot}9 \pm 1{\cdot}3$
	POSITRONS	$29{\cdot}9 \pm 0{\cdot}3$	$27{\cdot}3 \pm 0{\cdot}5$	$24{\cdot}9 \pm 0{\cdot}5$	$24{\cdot}7 \pm 0{\cdot}7$	$24{\cdot}4 \pm 1{\cdot}1$
BOSLEY AND MUIRHEAD (1952)	9-19 MEV ELECTRONS	$28{\cdot}2 \pm 0{\cdot}6$	$27{\cdot}1 \pm 0{\cdot}8$	$26{\cdot}5 \pm 1{\cdot}2$	$25{\cdot}8 \pm 1{\cdot}7$	$25{\cdot}3 \pm 2{\cdot}6$
HEYMAN AND WILLIAMS (1956)	2·5 MEV ELECTRONS	-	$25{\cdot}9 \pm 0{\cdot}5$	-	-	-
	POSITRONS	-	$22{\cdot}2 \pm 0{\cdot}5$	-	-	-
GOTTSTEIN ET. AL. (1951)	105 and 185 MEV POSITRONS	-	-	-	$26{\cdot}7 \pm 0{\cdot}6$	$24{\cdot}9 \pm 0{\cdot}8$
CORSON (1951)	196 MEV ELECTRONS	-	-	$27{\cdot}3 \pm 0{\cdot}8$		
	POSITRONS	-	-	$25{\cdot}0 \pm 0{\cdot}8$		
MACDIARMID (1951)	PAIRS FROM 70 MEV RAYS	-	-	24·4		
THEORETICAL MOLIÈRE (1948)	ELECTRONS AND POSITRONS ALL ENERGIES	23·1	24·5	25·5	26·6	27·4

ERRORS SHOWN ARE ALL STANDARD DEVIATIONS.

TABLE V - 4.

(b) COMPARISON OF CUT SCATTERING CONSTANTS.

AUTHOR	PARTICLE AND ENERGY	K_c (CUT) CELL SIZE (μ) 25	50	100	200	400
PRESENT WORK	10 MEV ELECTRONS	$23{\cdot}9 \pm 0{\cdot}4$	$25{\cdot}2 \pm 0{\cdot}3$	$26{\cdot}7 \pm 0{\cdot}5$	$26{\cdot}9 \pm 0{\cdot}8$	$29{\cdot}1 \pm 1{\cdot}2$
	POSITRONS	$23{\cdot}5 \pm 0{\cdot}3$	$23{\cdot}3 \pm 0{\cdot}3$	$22{\cdot}2 \pm 0{\cdot}4$	$23{\cdot}2 \pm 0{\cdot}6$	$23{\cdot}3 \pm 1{\cdot}0$
BOSLEY AND MUIRHEAD (1952)	9 - 19 MEV ELECTRONS	$21{\cdot}4 \pm 0{\cdot}5$	$21{\cdot}9 \pm 0{\cdot}7$	$23{\cdot}5 \pm 0{\cdot}9$	$24{\cdot}5 \pm 1{\cdot}7$	$25{\cdot}3 \pm 2{\cdot}6$
HEYMAN AND WILLIAMS (1956)	2·5 MEV ELECTRONS	-	$24{\cdot}7 \pm 0{\cdot}5$	-	-	-
	POSITRONS	-	$21{\cdot}6 \pm 0{\cdot}5$	-	-	-
GOTTSTEIN ET. AL. (1951)	105 and 185 MEV POSITRONS	-	-	-	$26{\cdot}2 \pm 0{\cdot}6$	$24{\cdot}0 \pm 0{\cdot}8$
MACDIARMID (1951)	PAIRS FROM 70 MEV RAYS	-	-	22·6	-	-
VOYVODIC AND PICKUP (1952)	PAIRS FROM 16·7 MEV RAYS	-	$21{\cdot}2 \pm 0{\cdot}7$	-	-	-
THEORETICAL MOLIÈRE (1948)	ELECTRONS AND POSITRONS ALL ENERGIES	20·2	21·4	22·8	23·6	24·7

ERRORS SHOWN ARE ALL STANDARD DEVIATIONS.

suggest a ratio of about 1·14, although if taken in conjunction with the smaller and larger cells there is some evidence for an increase of the ratio with cell size. It is of interest to note that the ratios for K_u and K_a are of the same order indicating that the difference is not a feature of the 'tail' of the scattering distribution.

No satisfactory explanation of the observed difference has been found.

(b) Absolute values of the scattering constant: The measured values of the scattering constant after correction, are shown in figure V-4 and in table V-4 where they may be compared with earlier results and with theory. It is difficult to summarise a comparison of the results of so many workers but the present work may be said to be in fairly good agreement with previous results except for the values of the uncut scattering constant at very small cell sizes. In this region the present results lie above those of Bosley and Muirhead (1952).

A comparison with the theory confirms the anomalous rise in the uncut constant at small cell sizes detected by Bosley and Muirhead. Figure V-4 shows that, apart from this anomaly the values of the measured scattering constant for electrons are greater and those for positrons smaller than the theoretical values of Molière (1948).

CHAPTER VI

PROTON-PROTON SCATTERING AT VERY HIGH ENERGIES

(1) Introduction.

At energies below the threshold for meson production, (290 Mev), experiments on the scattering of protons by protons yield values of the total and differential scattering cross sections, while recently measurements have been made of the polarisation of the scattered particles and also using polarised incident beams. Above the threshold for meson production it is also possible to measure the distributions in angle and momentum of all the particles emerging from the collision. It has become customary to call reactions in which no mesons are produced 'elastic' and those from which one or more mesons emerge 'inelastic'.

A complete theoretical treatment of all features of proton-proton scattering would start from meson-nucleon and nucleon-nucleon interactions based on a satisfactory meson theory. Such a complete solution is not available and in its absence attempts have been made to explain the low energy, (less than 10 Mev), and intermediate energy, (up to about 350 Mev), results by means of static potentials with a possible spin dependence. This approach compares the phase shifts calculated for certain assumed potentials with those obtained from the measurements, in an endeavour /

endeavour to find a potential which will give a satisfactory fit to the measurements for a large range of energies.

The lack of a satisfactory fundamental theory has also, for the inelastic processes, given rise to phenomenological treatments such as those of Rosenfeld (1954), and of Gell-Mann and Watson (1954), for energies near the meson production threshold, and to the statistical type of theory and its modifications, (Fermi, 1950, 1953; Heisenberg, 1949; Landau, 1953; Kovacs, 1956), for the very high energy region.

(2) Extension of the theoretical treatments applied at low energies.

(a) Elastic scattering. Thaler and Bengston (1954), Garren (1953), and other workers, have made phase shift analyses for the results of nucleon-nucleon scattering experiments at energies up to about 300 Mev. At the higher energies studied it is difficult to obtain unambiguous assignments of phase shifts even when a number of simplifying assumptions are made, such as the neglect of possible mixing of ^3S and ^3D waves. The phase shifts calculated by Thaler and Bengston (loc. cit.) have not been confirmed by the more recent polarisation experiments, (Chamberlain et al., 1954; Fried, 1954; Fischer and Baldwin, 1955).

Attempts have been made to find an interaction which will give the correct magnitude for the total cross section at low and intermediate /

intermediate energies, will reproduce the isotropic angular distribution of the scattered particles, and will also explain the n - p scattering results while preserving charge independence, (Jastrow, 1951; Case and Pais, 1950; Christian and Noyes, 1950). Only the Christian and Noyes tensor interaction has been found to give even approximate agreement with experiment when compared with the polarisation measurements.

At an energy of 925 Mev for the primary proton it seems possible that particles having angular momenta as high as 5ħ may contribute to the scattering. In view of the difficulty of making unambiguous phase shift analyses at energies ~ 300 Mev it would seem unlikely that such an analysis would yield significant results at 925 Mev where the number of contributing phase shifts may be greater, and where the statistical accuracy of the measurements is poorer, than at lower energies. Even were such an analysis made, it would be improbable that the results could be interpreted in terms of a static potential. At such an energy also, the neglect of relativistic effects would introduce serious errors into a calculated result.

(b) Inelastic scattering. Rosenfeld, and Gell-Mann and Watson, (loc. cit.), have analysed the cross sections for all possible two nucleon events in terms of the three total cross sections for the charges $1 \rightarrow 0$, $0 \rightarrow 1$, and $1 \rightarrow 1$ in the isotopic /

isotopic spin of the two nucleons during the reaction. By assuming, (i) that the meson is in an S or a P state with respect to the two nucleon system, (ii) that only the S-wave nucleon-nucleon interaction is important, and (iii) that the effect of the meson on the nuclear force can be neglected, it is then possible to obtain the angular distributions of the product particles from reactions corresponding to the basic cross sections described above. The variation of the cross sections as a function of the maximum momentum of the meson may also be obtained. The expressions calculated for the angular and momentum distributions contain undetermined parameters which can only be expected to remain independent of energy near the threshold for meson production. The neglect of all but the S-wave interaction between the nucleons becomes a bad approximation at energies greater than about 20 Mev and since other features of the theory limit its use to energies near the meson production threshold it would be unprofitable to attempt to apply this treatment at energies as high as 925 Mev.

(3) Theories applicable at very high energies.

Since the difficulties of extending the range of applicability of the theories used at low energies are so considerable there remain the statistical type of theory such as that of Fermi (loc. cit.) and the optical model treatment, (Fernbach, Serber, and Taylor 1948, Serber and Rarita 1955), while the /

the consequences of the excited nucleon model due to Peaslee (1954) and others must also be considered.

(a) Statistical theory. Fermi has proposed a model in which, when the two nucleons collide, a great quantity of energy is released in a small volume around the two particles. Since the interactions of the meson field are strong the energy is rapidly distributed among the various degrees of freedom available, according to statistical laws.

The only adjustable parameter in the theory is Ω , the volume in which the energy of the colliding particles is released. If the Lorentz contraction is neglected Ω is taken to be a sphere of radius R, where R is of the order of the range of nuclear forces; $R \sim \frac{\hbar}{\mu c} = 1{\cdot}4.10^{-13}$ cm., (μ is the meson mass). If the Lorentz contraction is taken into account Ω is an ellipsoid of volume

$$4/3\ \pi R^3\ \frac{2Mc^2}{W}$$

where W is the total energy of the nucleons in the centre of momentum system and M is the rest mass of the nucleon. The total cross section is approximately geometrical = πR^2.

The probability of forming a final state of any given kind is then given by an expression of the type

$$|m|^2\ \frac{dN}{dE}$$

where the square of the matrix element is taken to be proportional only to the probability that, for the state in question, /

question, all the particles are contained at the same time in the volume Ω. Thus, for a state involving n' independent particles

$$|m|^2 \propto \left(\frac{\Omega}{V}\right)^{n'}$$

where V is the customary large normalisation volume. Substituting expressions for the density of available states dN/dE, Fermi obtains for the probability of producing n mesons, the expression

$$f(n) \propto \frac{\left[\frac{251}{\omega}(\omega-2)^3\right]^n}{\left(\frac{3}{2}\cdot\frac{5}{2}\cdot\ldots\cdot\frac{6n+1}{2}\right).n!} \qquad \text{- VI - 1.}$$

where ω has been written for W/Mc^2 and where the nucleons have been treated as non-relativistic, and the mesons as extremely relativistic.

The conservation of momentum has been taken into account in an approximate way in the analysis leading to equation VI - 1 by assuming that the momentum carried off by the mesons is very small compared with that taken by the nucleons and thus that only one nucleon but all the mesons may be treated as independent. The conservation of charge and of isotopic spin may also be taken into account to divide the probability for producing a given number of mesons into the probabilities for the various possible charge combinations. Fermi (1953) has made this extension to the theory by writing $P(n)$ as the number of possible charge combinations /

combinations for particles having a total isotopic spin T = 1. Then the probability of obtaining n mesons becomes

$$f'(n) = \frac{P(n) f(n)}{\sum_n P(n) f(n)}$$

We need not consider the possibility of a total isotopic spin T = 0 for collisions between protons. When one meson is produced in a p - p collision the possible charge combinations are (P N π^+) and (P P π^o). The relative probabilities of these combinations may be shown to be $3/4$ and $1/4$ respectively. Thus since $P(n) = 2$ the probabilities of obtaining the combinations (P N π^+) and (P P π^o) are $f(1) \times 2 \times 3/4 = 3/2 f(1)$ and $f(1) \times 2 \times 1/4 = 1/2 f(1)$ respectively. The relative probabilities of obtaining all the various possible combinations of nucleons and mesons when the energy of the primary proton is 925 Mev have been calculated using this treatment and are given in table VIII - 3 (page 96).

Fermi (1951) has calculated the angular distribution of the outgoing particles when the primary nucleon is of such an energy that a thermodynamic model is appropriate (~ 50 Bev). The conservation of angular momentum entails a forward peaking of the angular distribution in the centre of momentum system, which is very considerable at the energies for which the calculation has been performed. At lower energies the prediction of the angular distribution is difficult and no results are available.

By evaluating the density of available states in terms of

the /

the momentum of the meson it is also possible to predict the momentum distribution of this particle on the assumption that the nucleons may be treated as non-relativistic.

A less extremely statistical model than that of Fermi has been proposed by Heisenberg (1949) and elaborations of the Fermi theory which attempt to take into account the interactions of the particles in emerging from the reaction, have been proposed by Landau (1953) and Kovacs (1956).

(b) Optical Model. The optical model was suggested by Fernbach, Serber, and Taylor, (1949), for the scattering of neutrons by nuclei. When applied to the scattering of protons by protons, (Serber and Rarita, 1955), the model considers the diffraction and absorption of the wave representing each nucleon by a black sphere representing the other. The total cross section is thus $2\pi R^2$ where R is the proton radius, and the angular distribution of the elastically scattered particles is proportional to

$$\frac{J_1^2(kR\sin\theta)}{\sin^2\theta}$$

where J_1 is the first order Bessel function. R is determined from the total cross section and since k is known from the energy of the incident particle, the shape of the distribution is uniquely determined. It is doubtful whether the optical model can be applied in a situation where the wavelength of the incident /

incident particle is of the same order of magnitude as the radius R of the obstacle while another unsatisfactory feature of this model is the apparent assymetry in the treatment of the two particles involved.

(c) Nucleon Isobar. The $T = 3/2$, $J = 3/2$ resonance in the scattering of positive π mesons by protons has been interpreted as an excited state, or isobar, of the proton having an energy of excitation $\sim$ 160 Mev and a breadth $\sim$ 100 Mev, (see for instance Aitken et al., 1954; Peaslee, 1954). Applied to the scattering of nucleons by nucleons this model postulates a two-stage process in which either one or both the nucleons are first excited to the energy level at about 160 Mev and then decay to the ground state by emission of a π meson. Peaslee (loc. cit.), has used this model to calculate the yields of π^+, π^0, and π^- mesons from p - p and n - p collisions in terms of two parameters which are the cross sections for the excitation of one or both the nucleons involved. Peaslee assumes that mesons are only produced from the decay of the excited nucleons which must be in a state of total isotopic spin $T = 3/2$. With these assumptions it is found that the fractional weights for decay of only one nucleon in proton-proton scattering are $5/6$ for decay by π^+ meson emission and $1/6$ by emission of π^0 mesons.

(4) Experimental results on the scattering of protons by protons at high energies.

During the course of the present work results have been published /

published giving values of the total and elastic cross sections for the scattering of protons by protons at a series of energies up to 5·3 Bev and results have also been given for the differential cross section for a number of energies up to 4·4 Bev., (Wright et al., 1955; Cork and Wenzel, 1955; Cester et al., 1955; Smith et al., 1955; Morris et al., 1955; Shapiro et al., 1954). The measurements of the total cross section show a rise from the nearly constant value of 25 mb. over the range of proton energies 150-400 Mev to about 48 mb. at 900 Mev . Above about 1 Bev the cross section appears to fall slowly and the measurements of Wright et al. (loc. cit.) give a value of $29{\cdot}5 \pm 5{\cdot}5$ mb. for the total cross section at 5·3 Bev. The elastic cross section appears to fall slowly from 25 mb. at 400 Mev to 15 - 20 mb. at 1 Bev. The differential cross section for elastic scattering shows that, in contrast with the isotropic distribution observed at energies up to 400 Mev , (Hartzler and Siegel, 1954) the differential cross section becomes rapidly more peaked in the forward direction with increasing energy, (Smith et al., loc. cit.).

Direct measurements concerning the inelastic scattering have been made by Morris et al. (private communication), at an energy of 900 Mev and by Cester et al., (1955), at 3 Bev Yuan and Lindenbaum, (1954), have measured the distribution in momentum of π^+ mesons emitted at an angle of 32° to beams of 1 Bev and 2·3 Bev /

Bev protons striking targets of beryllium. These results are discussed and compared with those obtained in the present experiment, in chapter VIII.

CHAPTER VII

THE SCATTERING OF PROTONS BY PROTONS AT 925 Mev.

(1) Description of the measurements.

The method used to study proton-proton scattering was to allow the primary proton beam to pass into nuclear emulsions and to examine the interactions of the primary particles with the hydrogen nuclei normally present in the emulsion. This technique was first used by Goldhaber, (1952, 1953), and has recently been employed by Kao and Clark (1954) to study proton-proton scattering at 420 Mev.

Ilford G 5 nuclear emulsions having an unprocessed thickness of about 400μ were used in the present experiment. The emulsions were exposed to a single pulse of the scattered-out proton beam of the Birmingham synchrotron, (Moon, Riddiford, and Symonds, 1955), by members of the nuclear emulsion group in the Department of Physics at Birmingham University. The plates were placed so that the protons entered the emulsion at grazing incidence parallel to the edge of the plate. The energy of the scattered-out proton beam has been calculated from the accurately known energy of the circulating beam on the assumption that the scattered beam is produced almost entirely by a process of diffraction scattering at the inflector guide plate. When allowance /

allowance has been made for energy loss by the particles in passing out through the window in the vacuum chamber the energy is found to be 925 ± 30 Mev.

The plates were fixed to the stages of Cooke series M4000 microscopes so that the mean direction of the proton tracks lay along the x-movement of the microscope stage. On an area of the plate clear of the edges, tracks were followed which were of minimum grain density and made an angle of not more than $2\frac{1}{2}^{\circ}$ with the mean direction of the beam. Tracks were followed for a maximum length of 2·6 cm, or until they passed out of the emulsion or produced an event. The length followed on each track was read directly on the x movement of the microscope stage. A rather low beam intensity of 2×10^4 protons per cm^2 was used in order to reduce the chance of an observer changing from one track to another and missing events.

All events found were noted, including scatterings of the primary track. For all two prong stars free from a short recoil track or a β -decay electron, the following measurements were carried out:

(a) The horizontal projections θ , of the angles between the secondary tracks and the track of the primary proton, were measured using an eyepiece goniometer.

(b) The dips β_0 and β_1, β_2 , of the primary and secondary tracks were measured by observing the change in depth of the tracks over successive 100μ or 50μ intervals.

(c) /

(c) Grain counts were made on the primary and secondary tracks over a length of 300 - 500 μ .

(d) The emulsion thickness at a marked spot near the centre of the plate was measured using the microscope depth guage.

(2) Identification of elastic proton-proton collisions.

An elastic proton-proton collision appears in the emulsion as a star with two secondary particles, (2 P event). It is necessary to distinguish 2 P events corresponding to elastic scattering from a background of events occurring in complex nuclei and from events involving the production of mesons.

2 P events could be discarded as not elastic without further measurement if:-

(a) the angle between the tracks was greater than 90°,

(b) either track made an angle of more than 90° with the primary,

(c) either track could be identified as due to an α-particle or heavier fragment.

For 2 P events satisfying the preliminary criteria the angles in space, α , between the primary and secondary tracks were obtained from the relation

$$\cos\alpha = \cos\beta_0 \cos\beta - \sin\beta_0 \sin\beta \cos\theta$$

where /

where β_0 and β are the dip angles of the primary and secondary tracks respectively and θ is the horizontal projection of the angle between them. In order to determine the dip angles it is necessary to know the shrinkage factor of the emulsion. Accurate values of this factor were obtained by measuring the thickness of the emulsion and glass backing at a fixed point, before and after processing, with a comparator. The microscope depth guage was then used to measure the emulsion thickness at the same spot each time an event was examined, (Duke, Lock, March, and Munir, 1955). The shrinkage factor measured in this way is believed to have a probable error $\sim \pm 1\%$.

The laws of conservation of energy and momentum give, for the collision of a moving proton with a proton at rest in the emulsion, the relation

$$\tan\alpha_1 \tan\alpha_2 = {}^2/_E \qquad \text{——————} (1)$$

where E is the total energy of the two particle system measured in units of the proton rest mass and α_1 and α_2 are the angles between the primary and the secondary particles. For a primary energy of 925 ± 30 Mev $\tan\alpha_1 \tan\alpha_2 = 0{\cdot}670 \pm 0{\cdot}01$.

An elastic scattering event must also be coplanar and this condition may be expressed in the form $\varphi = 0$, where φ is the angle which the primary track makes with the plane containing the two secondary tracks. φ is given in terms of the measured quantities /

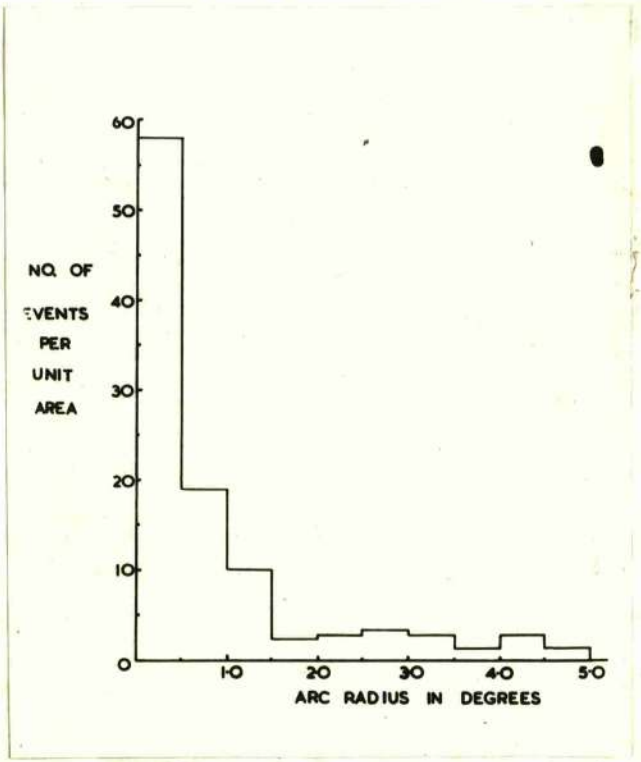

FIG. VII - 2.

Density of points on the φ - $\Delta\alpha$ plot as a function of the radial distance from the origin.

quantities by the expression

$$\sin\varphi = \frac{\cos\beta_0 \cos\beta_1 \cos\beta_2}{\sin \textcircled{H}} \left[\tan\beta_2 \sin\theta_1 - \tan\beta_1 \sin\theta_2 + \tan\beta_0 \sin(\theta_2 - \theta_1) \right] \qquad (2)$$

where the β_s are the dip angles and the θ_s the horizontal projections of the angles as before, and where $\textcircled{H}$ is the true angle between the two secondary tracks. For an elastic collision between free protons $\textcircled{H} = \alpha_1 + \alpha_2$ and lies between 78° and 90° for the bombarding energy used in the present experiment.

In order to separate elastic scattering events from those of other types the amount by which the measured quantities failed to satisfy exactly the condition (1) and the coplanarity condition was measured as follows:

(i) The larger of the two values of the angles α was substituted into equation (1) and the value of the other could then be calculated since E was known. The difference between this calculated value and that <u>measured</u> for the smaller angle is called $\Delta\alpha$ and is a measure of the failure of the measured quantities to satisfy the condition (1).

(ii) φ was calculated for each event using equation (2). φ is a measure of the deviation from coplanarity.

For each event in which $\varphi \leq 5°$, $|\Delta\alpha| \leq 5°$, and $70° \leq \textcircled{H} \leq 90°$ a point was plotted on a graph of φ against $\Delta\alpha$, (fig. VII - 1). On this graph all true elastic scattering events /

events should be represented by points within distances of the origin equivalent to the experimental errors involved in the measured quantities. Repeated measurements and a consideration of the effects of the errors in typical cases lead to the values below:

QUANTITY	PROBABLE ERROR
Horizontal angle, θ	$\pm 15'$
Dip angle, β	$\pm 45'$
True angle, α	$\pm 50'$
Coplanarity, φ	$\pm 1^{\circ} 10'$
Correlation, $\Delta\alpha$	$\pm 1^{\circ} 20'$

If it is assumed that φ and $\Delta\alpha$ are independent, (the effect of making the contrary assumption has been found to be small), then all true elastic scattering events will correspond to points lying within a semi-circle centred on the origin and having a radius $\sim 1{\cdot}5^{\circ}$.

It is clear from figure VII - 1 that there is a definite grouping of the points about the origin. This feature is illustrated in figure VII-2 where the number of events per unit area in successive semi-circular rings centred on the origin is plotted against the radius of the ring. The distribution in this figure is fitted by a Gaussian curve with a long tail of background events. The form of this distribution is consistent /

consistent with the choice of 1·5° as the limit within which points in figure VII-1 may be taken to represent elastic scattering events.

(3) Results for the elastic proton-proton scattering.

The number of events falling within the semi-circle in figure VII - 1 is 65, while 56 background events lie outside the semi-circle and within the 5° x 5° area of the figure. This background density implies that 4 such events will fall within the 1·5° semi-circle giving a corrected number of 61 cases of elastic scattering. Certain other corrections to this figure may be necessary and are considered below.

(a) Correction for scanning loss.

The distribution of the azimuthal angles of all events lying within the 1·5° semi-circle is shown in figure VII - 3(a) and this distribution is divided into events for which the smaller of the angles α is $< 12°$, and for which this angle is $> 12°$, in figures VII - 3(b) and (c). From these figures it would appear that events may be missed in which the plane of the secondary tracks lies at a large angle with respect to the plane of the emulsion and that this loss is serious for events in which one of the secondary tracks makes a small angle with the primary. It is difficult to understand the reason for such an effect since any deviation of the primary track is most carefully examined as are also the few cases in which the primary stops without secondary prongs.

Three /

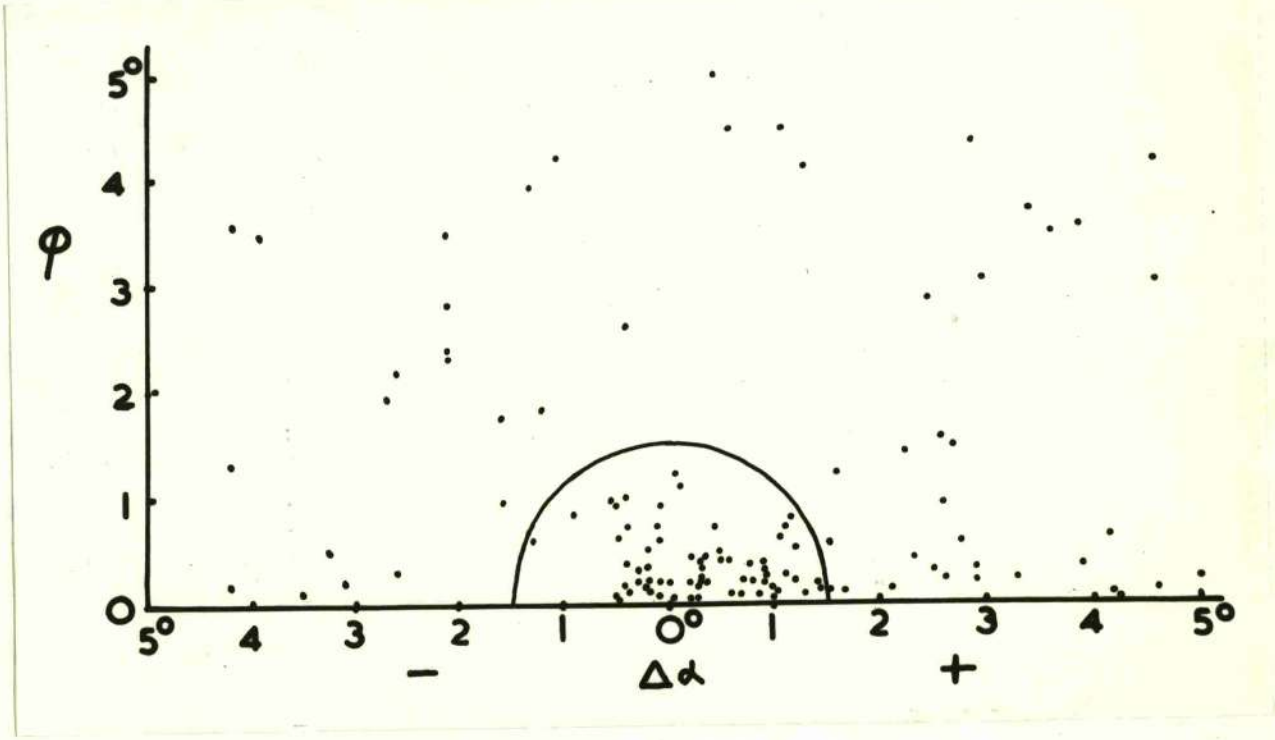

FIG. VII - 1.

φ - Δα plot showing the 1·5° semicircle inside which true elastic scattering events were taken to lie.

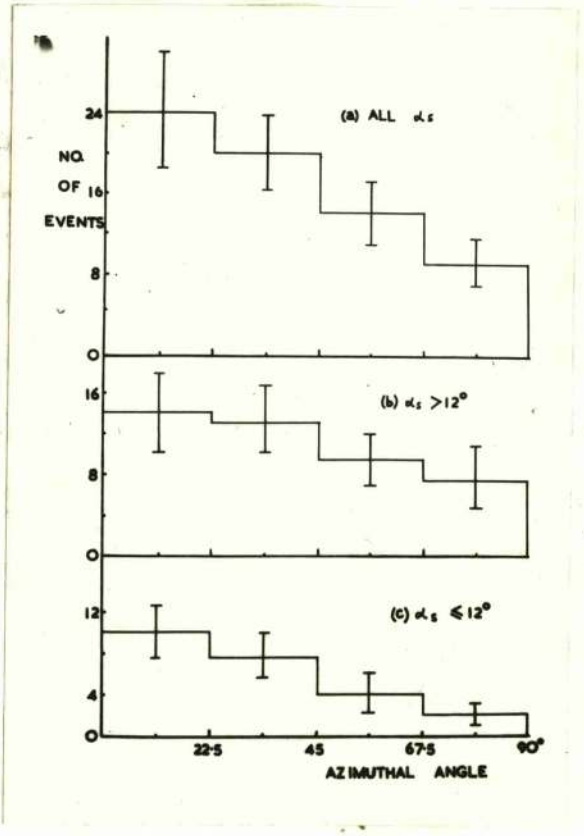

FIG. VII - 3.

Distribution of the azimuthal angles of protons from elastic p - p scattering. (b) and (c) refer to events in which the smaller of the angles between a secondary track and the primary is respectively greater or less than 12°.

Three methods of correction for the apparent loss of events have been attempted. (i) The distribution of figure VII - 3(a) may be squared to produce isotropy. (ii) A correction may be determined from separate data concerning single scattering events. 800 events were measured in which the primary proton is scattered by a heavy nucleus. Thus the statistical accuracy of the distribution of the azimuthal angles of these events is good. For the single scattering events evidence of loss was only found for deflections of $< 12^{\circ}$. Thus the azimuthal angular distribution of elastic $2p$ events having the smaller space angle $< 12^{\circ}$ may be corrected using factors derived from the single scattering results. (iii) If there is no loss of events for values of the smaller space angle $> 12^{\circ}$ we may assume that the apparent loss of figure VII - 3(b) is due to statistical fluctuations and correct only the distribution of VII - 3(c) to give isotropy. Using the three methods of correction the measured number of 65 events inside the $1{\cdot}5^{\circ}$ semi-circle becomes 89·6, 71·7, and 77·5 for (i), (ii), and (iii) respectively.

(b) Assymetry of the points in the $\varphi - \Delta\alpha$ plot.

There is an excess of points having positive values of $\Delta\alpha$ on the $\varphi - \Delta\alpha$ plot, and such an excess might be taken to imply the evidence of a low energy tail in the incident proton beam. Apart from the lack of any apparent source of such a low energy contamination,/

contamination, checks of the energy of samples of the primary protons by several methods do not support this hypothesis. Measurements made by the Birmingham group have shown that almost all the protons enter the emulsion within 1° of the mean beam direction. Since protons of different energies produced at the target must follow different trajectories in order to reach the emulsion the small angular spread of the beam is evidence that the spread in energy is also small. Multiple scattering measurements although seldom giving an energy measurement of high accuracy were consistent with a primary energy of 925 Mev. In the course of the scanning examples were found of events in which one of the secondary tracks stopped in the emulsion. The energy of such a proton can be accurately determined by a measurement of its range, and can be used in conjunction with measurements of the angles of one or other of the secondary particles to obtain a value for the energy of the primary. Eight out of nine events of this type gave primary energies consistent with 925 Mev, but in most cases the value of energy obtained was somewhat greater than that found by evaluating the expression $E = \frac{2}{\tan\alpha_1 \tan\alpha_2}$ indicating a systematic effect tending to displace $\Delta\alpha$ towards positive values.

The reason for this assymetry is not understood, but it can have little effect on the value of the cross section in view of the strong grouping indicated in figure VII - 2. The checks

on /

on the primary energy described above all lead to the conclusion that any low energy contamination of the beam must be less than ~ 5%.

The total length of track followed in the search for elastic scattering events was 1539 metres. If no correction for loss of events is made the mean free path is thus $^{1539}/_{61}$ = 25·2 ± 1·7 metres. The free hydrogen content of the emulsion corresponding to the humidity at which the plates were exposed is (3·17 ± 0·06) x 10^{22} atoms per c.c., (Waller, private communication). The cross section for elastic scattering, uncorrected for loss, is then 12·5 ± 2 mb. The cross sections obtained when the azimuthal angular distribution is corrected by the factors obtained from the single scattering data, by levelling the azimuthal angular distribution for events with one angle less than 12°, and by levelling the azimuthal distribution for all events are 13·8 ± 2·0 mb, 15 ± 2·0 mb., and 17·5 ± 2·0 mb. respectively where the errors indicated are standard deviations. The last value is almost certainly an over-correction and the values of 13·8 and 15 mb. must be taken to be most reliable.

The angles of the secondary tracks with respect to the primary, in the centre of momentum system, (c-system), were calculated from the formula

$$\tan \alpha = (1 - \beta_c^2)^{1/2} \tan \alpha^*/2$$

where β_c is the velocity of the c-system and α^* is the angle of the /

the particle in this system. For protons of 925 Mev

$$\tan\frac{\alpha^*}{2} = 1.226 \tan\alpha$$

The angular distribution in the c-system for the 65 events inside the 1.5° semi-circle is shown in figure VIII - 8. (page 102).

(4) Identification of events in which π-mesons are produced.

The thresholds for the production of one, two, and three, mesons occur at proton energies of 290, 600, and 940 Mev. Thus both single and double meson production are possible in the present experiment whereas triple meson production has a threshold on or above the maximum proton energy available.

Events in which a single meson is produced may be of three kinds:

$$p + p \longrightarrow \pi^+ + D \qquad \text{(a)}$$

$$\longrightarrow \pi^+ + p + n \qquad \text{(b)}$$

$$\longrightarrow \pi^0 + p + p \qquad \text{(c)}$$

We shall consider the identification of each kind of event in turn.

(a) $p + p \longrightarrow \pi^+ + D$: In this reaction since there are only two secondary particles both of which are observed it is easy to apply criteria for distinguishing the event which are similar to those required for the elastic collisions. The primary and secondary particles must be coplanar and a unique relationship exists between the angles of emission of the two particles. A feature of this reaction is that the deuteron

cannot /

cannot make an angle of more than 17° with the primary proton at the bombarding energy of 925 Mev. The relationships between the energies and angles of the secondary particles were also determined. No event was found which satisfied all the acceptance criteria.

(b) $p + p \longrightarrow \pi^+ + p + n$: The identification of this type of event is more difficult than that of elastic scattering or of the production of a meson and a deuteron since there are three secondary particles and since one of these particles is neutral and unobserved. These features of the reaction make it impossible to apply acceptance criteria dependent on the angles of the particles alone, and it becomes necessary to measure in addition, the energies of the secondary proton and π meson. It is seldom possible to determine these energies with a precision comparable with that of the angular measurements, since the energy determinations normally depend on grain counts or multiple scattering measurements on a limited length of track.

Apart from events identified as cases of elastic scattering, all 2 P stars without a recoil, a β -decay electron, or an α -particle track, were compared with the curves illustrated in figure VII - 4 which give the minimum grain density or maximum energy of the proton or meson as a function of the angle of emission of the particle. The maximum angle of emission for protons from this reaction is 57°.

Events /

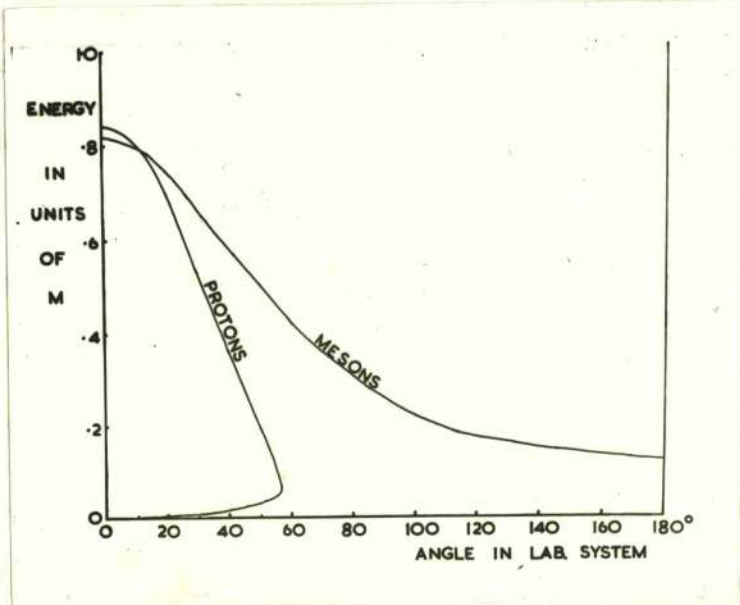

FIG. VII - 4.

Relationship between the energies and angles in the laboratory system for protons and mesons from the reaction $p + p \longrightarrow \pi^+ + p + n$. Possible values lie to the left of the plotted curves.

Events satisfying these preliminary criteria were subjected to an identification procedure based on a comparison of the two energies of the neutron as calculated separately from the principles of conservation of momentum and of energy. The measured values of the angles between the primary particle and the secondary proton and meson were assumed to be correct and energies were calculated for these particles such that energy and momentum are simultaneously conserved in the reaction. The probability that the proton and meson should have these requisite energies was determined from a knowledge of the measured values of these quantities and their standard deviations. This probability is described by a ratio R. For R = 0 the measured values of the energies give identical values for the energy of the neutron as calculated from the principles of conservation of energy and momentum. The calculated distribution of R for true events of the type $p + p \longrightarrow \pi^{+} + p + n$ is superimposed on the measured distribution in figure VII - 5. The details of the method of discrimination, the definition of R and the calculation of its frequency distribution are described in appendix II.

The observed distribution of R shown in figure VII - 5 is somewhat broader than the calculated curve. This feature is due to the fact that the calculated curve does not allow for any inaccuracy in the computation of R which will tend to broaden the observed distribution. It is important to compare the observed distribution /

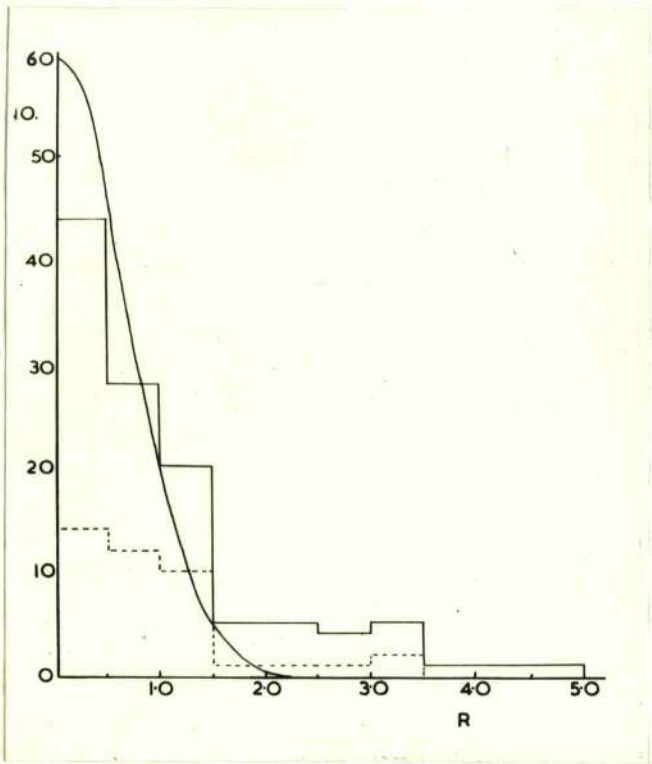

FIG. VII - 5.

Frequency distribution of the ratio R for the reaction $p + p \longrightarrow \pi^+ + p + n$. The continuous line represents the calculated distribution. The dotted histogram refers to events in which the π meson was positively identified.

distribution with one for events definitely known not to correspond to the assumed reaction. This has been done in two ways. (a) A distribution of R calculated for a sample of events consisting of some identified as elastic proton-proton scattering and some rejected by the preliminary criteria is flat. (b) For all events in which a sufficient length of track was available an attempt was made to achieve a definite identification, by grain counting and scattering measurements, of tracks postulated to be π mesons. In this way it was found that for a number of events for which the value of R was small the track which had been postulated to be a meson was in fact a proton. Thus this type of background appears to give a distribution of R which is peaked at zero. The existence of such a background was suspected from an assymetry about 90° of the angular distributions of the particles in the c-system. When events had been discarded in which incorrect identifications had been detected the angular distributions in the c-system became symmetrical about 90° within the statistical errors.

Of 92 events accepted as corresponding to the reaction $p+p \longrightarrow \pi^{+}+p+n$ only 36 had secondary tracks sufficiently long to make a positive identification of the π meson possible. The cases in which positive identification is not possible are usually those where a track of low grain density makes a fairly large /

large angle with the primary track, since tracks of high grain density are usually identifiable even when the track length available is small. Such low grain density, large angle tracks are rather unlikely to be protons since a complicated mechanism, such as double scattering of the primary particle in a heavy nucleus, must be postulated to explain such events. These considerations, combined with the symmetry of the angular distributions and the agreement of the value obtained for the total cross section with that measured using counters, (Shapiro et al. 1954: see page 92), have led to the decision to include as genuine cases events in which it was not possible to identify the π meson but in which if one track was postulated to be a π meson energy and momentum could be conserved. Almost no events were found in which it was possible to postulate either secondary track to be a π meson and for which it was possible to balance energy and momentum with high probability for both cases. If the unidentified mesons are divided in the ratio of the number of postulated mesons positively identified as mesons to the number of those shown to be protons then the number of accepted events would in fact be reduced by a factor of 0·7. The azimuthal angular distributions for the particles from this reaction are shown in fig. VII - 6 and show no evidence of scanning loss. 453 2-P events were found in the course of the scanning 65 of which were identified as examples of the elastic scattering /

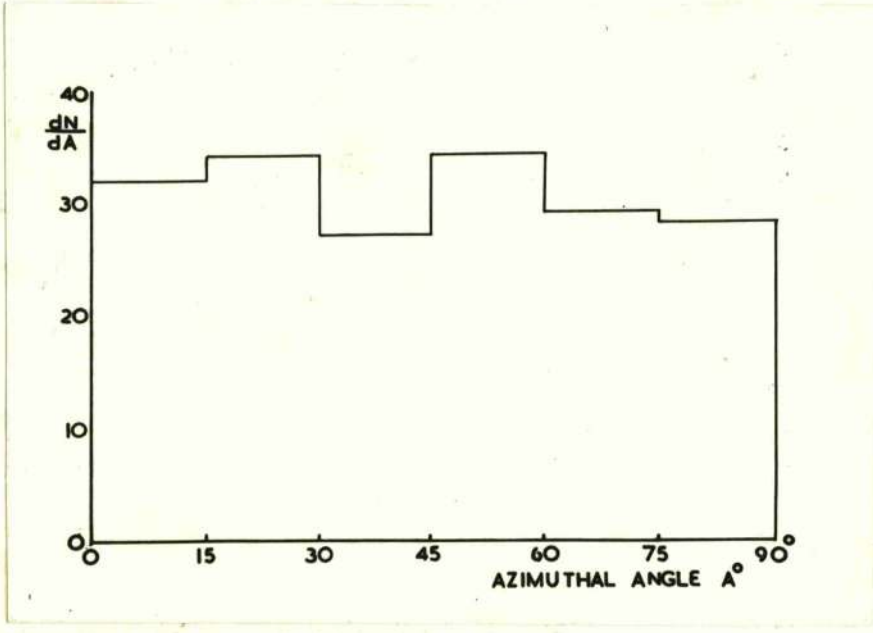

FIG. VII - 6.

Distribution in azimuthal angle of protons and mesons from the reaction $p + p \longrightarrow \pi^+ + p + n$.

scattering of protons by protons. 150 of the remaining 2 P events were rejected as not corresponding to inelastic scattering by means of the preliminary criteria. 238 events were subjected to the procedure for the balance of energy and of momentum and of these 114 appear in figure VII - 5 with a value of R less than 6.

Consideration of the distribution of R in figure VII - 5, of the distribution for events in which mesons were definitely identified, and of the theoretical distribution, lead to a limit of $R < 1{\cdot}5$ for acceptable events. Within this range there are 92 events in 36 of which the meson has been positively identified. From the region $R > 1{\cdot}5$ it is clear that there is present a small continuous background. There will on the other hand be a small number of true events for which $R > 1{\cdot}5$. Since the corrections for both these effects are rather difficult to estimate but will certainly be small and tend to cancel each other no correction for either has been made. The track length used in this experiment was 1076 metres giving a mean free path for the reaction of $11{\cdot}7 \pm 1{\cdot}4$ metres and a cross section of 27 ± 3 mb. Qualitative considerations indicate that the contribution to this cross section by events occurring in a complex nucleus, which have failed to be distinguished from those with free hydrogen, must be very small.

For the events accepted the angular and momentum distributions of the particles in the c-system are presented in tables /

Angular distributions in the C - system, of particles from the reaction

$$p + p \longrightarrow \pi^+ + p + n$$

TABLE VII - 1.

ANGULAR INTERVAL	0-15	15-30	30-45	45-60	60-75	75-90	90-105	105-120	120-135	135-150	150-165	165-180°
NO. OF PROTONS, MEASURED	0	6(4)	8(2)	10(1)	10(4)	8(3)	24(10)	8(2)	10(3)	5(0)	7(4)	3(1)
NO. OF PROTONS, CONSISTENCY	0	6(4)	7(4)	9(0)	12(3)	5(2)	22(12)	5(2)	10(3)	5(1)	7(3)	4(2)
NO. OF NEUTRONS, MEASURED	3(1)	8(2)	8(2)	4(1)	7(2)	10(2)	18(5)	12(7)	12(2)	11(7)	2(1)	3(2)
NO. OF NEUTRONS, CONSISTENCY	2(1)	6(0)	4(2)	10(4)	6(2)	12(3)	10(4)	11(4)	10(4)	14(9)	5(1)	2(2)
NO. OF MESONS, MEASURED	2(2)	5(2)	9(7)	15(8)	5(2)	6(1)	17(4)	12(4)	15(1)	11(4)	1(0)	0
NO. OF MESONS, CONSISTENCY	2(2)	6(2)	8(6)	14(10)	4(1)	4(2)	17(4)	11(3)	14(2)	9(2)	2(2)	1(0)

The 'measured' numbers are those obtained in the C-system by using the measured momenta of the particles in the laboratory frame. The 'consistency' values are those in the C-system for which energy and momentum balance exactly. The numbers in brackets refer to events in which the π^+meson has been definitely identified by grain counting and scattering. The excess of events in the interval 90°-105° is due to allocating to this interval the rather large number of events with an angle of 90°. The consistency distributions folded about 90° and expressed in terms of numbers per unit solid angle are shown in figure VIII - 1, (page 97).

Angular correlations in the C - system, between particles from the reaction $p + p \longrightarrow \pi^+ + p + n$

TABLE VII - 2.

ANGULAR INTERVAL	0–15	15–30	30–45	45–60	60–75	75–90	90–105	105–120	120–135	135–150	150–165	165–180°
PROTON-MESON ANGLE NUMBER, MEASURED	1(0)	2(1)	1(1)	4(0)	7(2)	5(2)	12(5)	11(4)	15(7)	11(6)	15(4)	13(3)
PROTON-MESON ANGLE NUMBER, CONSISTENCY	1(0)	3(2)	0	5(0)	5(2)	4(1)	14(6)	10(5)	11(4)	13(8)	15(6)	11(2)
NEUTRON-MESON ANGLE NUMBER, MEASURED	7(0)	10(5)	6(0)	9(3)	10(5)	9(5)	6(2)	10(2)	12(5)	7(3)	7(4)	5(1)
NEUTRON-MESON ANGLE NUMBER, CONSISTENCY	2(0)	11(5)	7(1)	5(2)	9(6)	8(2)	8(2)	7(2)	11(3)	11(5)	8(6)	5(2)

The numbers in brackets refer to events in which the π^+ meson has been definitely identified.

The consistency distributions expressed in terms of numbers per unit solid angle are shown in figure VIII - 2, (page 98).

Momentum distributions in the C - system, of particles from the reaction

$$p + p \longrightarrow \pi^+ + p + n$$

TABLE VII - 3.

MOMENTUM: UNITS OF 1/C (PROTON MASS)	0-·1	·1-·2	·2-·3	·3-·4	·4-·5	·5-·6	·6-·7	·7-·8	·8-·9
NO. OF PROTONS, MEASURED	1(0)	13(5)	18(6)	15(7)	17(6)	21(6)	5(3)	5(1)	3(1)
NO. OF PROTONS, CONSISTENCY	2(0)	9(5)	14(7)	12(4)	16(5)	39(15)	0	0	0
NO. OF NEUTRONS, MEASURED	3(0)	6(1)	17(9)	20(11)	26(7)	13(4)	11(2)	2(1)	0
NO. OF NEUTRONS, CONSISTENCY	0	1(0)	8(4)	19(8)	44(19)	20(5)	0	0	0
NO. OF MESONS, MEASURED	21(6)	38(16)	22(13)	1(0)	1(0)	1(1)	2(0)	1(0)	0
NO. OF MESONS, CONSISTENCY	11(3)	24(13)	26(15)	11(5)	0	0	0	0	0

The numbers in brackets refer to events in which the π^+ meson has been definitely identified.

The consistency distributions are plotted in terms of Mev/c in figure VIII - 3,4, (page 99).

tables VII - 1, 2 and 3. The c system data for these distributions are immediately available from the analysis used to distinguish the π meson events and described in appendix II. Two sets of distributions are presented: (a) the c - system quantities corresponding to the measured values of angles and energies and (b) the values of the quantities for which energy and momentum can be balanced exactly. Only for the momentum distributions of the neutron and proton are the plots (a) and (b) significantly different.

(c) $p+p \longrightarrow \pi^{o}+p+p$ For this reaction the preliminary acceptance criteria are similar to those for the proton in π^{+} meson production. In addition it is however impossible for both tracks to make angles of more than 37° with the primary proton in the laboratory system. A relationship between the grain densities of the two tracks for true events may also be found but is of little assistance in rejecting reactions of other types. The detailed analysis applied for this reaction was similar to that described in appendix II for π^{+} meson production. 58 events were subjected to detailed analysis and the distribution of R for events with R less than 6 is shown in figure VII - 7. 22 events with $R < 1{\cdot}5$ were accepted as examples of π^{o} production yielding a mean free path of 49 ± 9 metres and a cross section of $6{\cdot}5 \pm 2$ mb. Although for this reaction the contribution of protons bound in nuclei may be greater /

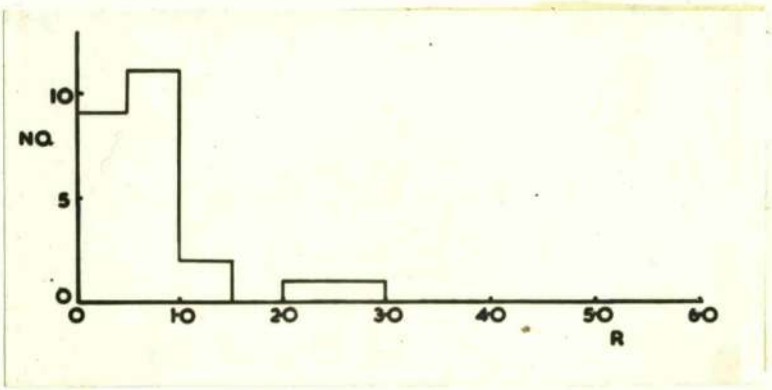

FIG. VII - 7.

Frequency distribution of the ratio R for the reaction
$p + p \longrightarrow \pi^0 + p + p$.

Angular distributions in the C - system of particles from the reaction

$p + p \longrightarrow \pi^0 + p + p$

TABLE VII - 4.

ANGULAR INTERVAL	0-30	30-60	60-90	90-120	120-150	150-180°
NO. OF PROTONS, MEASURED	3	11	4	12	8	6
NO. OF PROTONS, CONSISTENCY	4	11	5	10	8	6
NO. OF MESONS, MEASURED	5	3	4	2	4	4
NO. OF MESONS, CONSISTENCY	3	3	5	5	3	3

The consistency distributions folded about 90° and expressed in terms of numbers per unit solid angle, are shown in figure VIII- 6, (page 101).

Momentum distributions in the C - system of particles from the reaction

$p + p \longrightarrow \pi^0 + p + p$

TABLE VII - 5.

MOMENTUM: UNITS OF 1/C (PROTON MASS)	0-0·1	0·1-0·2	0·2-0·3	0·3-0·4	0·4-0·5	0·5-0·6	0·6-0·7	0·7-0·8	0·8-0·9
NO. OF PROTONS, MEASURED	2	4	8	13	9	3	2	2	1
NO. OF PROTONS, CONSISTENCY	2	3	9	11	11	6	2	0	0
NO. OF MESONS, MEASURED	0	5	3	12	1	1	0	0	0
NO. OF MESONS, CONSISTENCY	2	3	7	10	0	0	0	0	0

The consistency distributions are plotted in terms of Mev/c in figure VIII-7, (page 101).

greater than in π^+ meson production the energy and momentum balance criterion appears to be more stringent.

The angular and momentum distributions for this reaction are shown in tables VII - 4 and 5.

(d) $p + p \longrightarrow p + p + \pi^+ + \pi^-$ Of the four reactions

$$p + p \longrightarrow p + p + \pi^+ + \pi^-$$
$$\longrightarrow p + n + \pi^+ + \pi^0$$
$$\longrightarrow n + n + \pi^+ + \pi^+$$
$$\longrightarrow p + p + \pi^0 + \pi^0$$

involving the production of two mesons, we can only hope to identify the first which will appear as a four prong star. In such an event no proton can emerge at an angle of more than 36° to the primary particle. Using this criterion and applying the principle of momentum conservation it was possible to reject all the four prong events as not being examples of double meson production. Since no events of this type were found in a track length of 1539 metres an upper limit of 0·2 mb may be assigned to the cross section for this reaction.

All the results obtained are summarised and discussed in the following chapter.

CHAPTER VIII

DISCUSSION OF THE RESULTS OF THE PRESENT EXPERIMENT

(1) Cross-sections.

The cross sections for the elastic scattering of protons by protons at various energies are summarised in table VIII - 1 which also includes the present result.

TABLE VIII - 1.

ENERGY (MeV)	ELASTIC SCATTERING CROSS SECTION mb.	REFERENCE
437	23·8 ± 1·2	Sutton et al. (1955)
440	24 ± 2	Smith et al. (1955)
460	22	Mescheryakov (1954)
590	25 ± 2	Smith et al. (1955)
660	23 ± 2	Bogachev and Vzorov (1954)
800	21 ± 2	Smith et al. (1955)
900	21 ± 2·5	Morris et al. (1955
925	14 ± 2	Present work.
1000	19 ± 3	Smith et al. (1955)

These results indicate that the cross section, which is approximately /

approximately constant from 200 to 600 Mev , thereafter decreases slowly with increasing energy. The errors in the value of the cross section obtained from the present work just overlap with those of the value obtained by Smith et al., (1955), at 1000 Mev using counters but lie definitely below the cross section obtained by Morris et al. (1955) at 900 Mev, using a diffusion cloud chamber. The values of the cross section obtained by means of counter measurements always rely on an extrapolation of the differential cross section in the c - system from about 30° to 0° and it is possible that this procedure may lead to an error not present in measurements using cloud chambers or nuclear emulsions. In the present experiment the minimum angle which could be measured was about $2{\cdot}5^{\circ}$ in the c - system, although considerable corrections are applied to the results obtained for small angles. Even if the possible systematic errors discussed in chapter VII are assumed to have their maximum value it seems unlikely that agreement can be achieved with the result of Morris et al., but since only preliminary results of the cloud chamber experiment have so far been published it is difficult to assess satisfactorily any possible reasons for the discrepancy.

It is possible that destructive interference between the Coulomb scattering and the scattering due to nuclear forces may produce /

produce a decrease in the cross section at small angles. At an energy of 925 Mev however the Coulomb scattering is negligible at angles greater than 5° in the c - system. Due to the small solid angle available in this angular region the effect of such interference on the value of the total cross section must be very small.

The total scattering cross section for protons by protons has been measured by Shapiro et al. (1954), at a series of energies, using counters. Shapiro et al. find values of 49 ± 2 mb. at proton energies of 830 and 1075 Mev. Morris, Garrison, and Fowler, (1955 loc. cit., and private communication), have briefly reported on measurements using a diffusion cloud chamber and give a value of 38 ± 6 mb. for the total cross section at 900 Mev divided into 17 mb. for inelastic and 21 mb. for elastic, scattering. The total cross section obtained in the present experiment is 47 ± 4 mb., in good agreement with the counter measurements. The division of this cross section into 33 ± 4 mb. for inelastic, and 14 ± 2 mb. for elastic, scattering, is however in marked disagreement with the results of Morris et al., (loc. cit.). It is possible that the value of the cross section for inelastic scattering obtained in the present experiment includes a contribution due to events in complex nuclei, but, as mentioned earlier, this contribution is expected to be small and could scarcely account for the differences between the results /

results quoted above. In the results of Morris et al. no correction has been made for possible scanning loss although the angular distribution for the elastic scattering events indicates that such a correction may be necessary. An increase in the total cross section due to such a correction would achieve better agreement with that obtained from other measurements but the consequent increase in the elastic cross section would increase the discrepancy in the values obtained for this quantity.

The statistical theory of Fermi, (1953, loc. cit.), predicts the relative probabilities of obtaining any combination of nucleons and mesons from the interaction at a given energy for the primary particle. Assuming a total cross section of 48 mb. a value of $13.0.10^{-39}$ cm^3 is obtained for Fermi's interaction volume Ω and the cross section for the various possible events are given in the second column of table VIII - 3, (page 96).

Peaslee (1954) has assumed that meson production is due solely to the decay of nucleons in an excited state of total isotopic spin $T = {}^3/_2$. For excitation of only one of the nucleons involved Peaslee finds a ratio of 5: 1 for the cross sections for the production of positive and neutral π mesons but does not relate these cross sections to that for elastic scattering.

It is possible to incorporate the hypothesis of the excited nucleon into the statistical theory by postulating an alternative /

alternative mode of decay for the compound system of this theory, into a normal nucleon and an excited nucleon in a state having total isotopic spin $T = {}^3/_2$. When the energy available in the centre of momentum system is sufficiently high compared with the excitation energy of the $T = {}^3/_2$ resonance state we might expect that this state would be formed with a probability equal to that for elastic scattering except that the resonant state will be favoured by a weight factor of two due to the non-identity of the two product particles. If we now assume with Peaslee that all meson production proceeds by way of the excited nucleon we may obtain values for the cross sections for the possible reactions.

A state of $T = {}^3/_2$ decomposes into states having Z components of the total isotopic spin $T_z = {}^3/_2$ and $T_z = {}^1/_2$ with fractional weights ${}^3/_4$ and ${}^1/_4$ respectively. The $T_z = {}^3/_2$ state can decay only into a π^+ meson and a proton but the $T_z = {}^1/_2$ state has fractional weights of ${}^1/_3$ and ${}^2/_3$ for decay into a π^+ meson and a neutron and into a π^0 meson and a proton respectively. Thus the weights for decay of the excited nucleon are

PRODUCTS	WEIGHT	
π^+, P	${}^3/_4 \times 1 = {}^3/_4$	TOTAL $\pi^+ = {}^5/_6$
π^+, N	${}^1/_4 \times {}^1/_3 = {}^1/_{12}$	
π^0, P	${}^1/_4 \times {}^2/_3 = {}^1/_6$	

It would appear that at the present energy, excitation of both nucleons /

nucleons is not possible and this process has been disregarded.

The probabilities of the possible events calculated using this modified theory are shown in table VIII - 2.

TABLE VIII - 2.

REACTION	RELATIVE PROBABILITY
$p+p \longrightarrow p+p$	1
$\longrightarrow p^* + n \longrightarrow \pi^+ p n$	$2 \times {}^3/_4 = 1{\cdot}5$ } TOTAL $\pi^+ = 1{\cdot}667$
$\longrightarrow p + n^* \longrightarrow \pi^+ p n$	$2 \times {}^1/_{12} = {\cdot}167$ }
$\longrightarrow p + n^* \longrightarrow \pi^0 p p$	$2 \times {}^1/_6 = {\cdot}33$
$\longrightarrow p p \pi^+ \pi^-$	0

Normalising to a total cross section of 48 mb. the cross sections for the various processes calculated from the statistical theory and from the theory including the excited nucleon hypothesis are shown in table VIII - 3 in which are also given the measured cross sections.

TABLE /

TABLE VIII - 3.

REACTION	CROSS SECTIONS. mb.		
	STATISTICAL THEORY	MODIFIED THEORY	MEASURED VALUES
$p+p \longrightarrow p+p$	24	16	14 ± 2
$\longrightarrow \pi^{+}+D$	--	--	< 0.2
$\longrightarrow \pi^{+}+p+n$	17.5	26.7	27 ± 3
$\longrightarrow \pi^{0}+p+p$	6	5.3	6 ± 2
$\longrightarrow \pi^{-}+\pi^{+}+p+p$	.3	0	< 0.2

The measured cross sections are seen to be in good agreement with the modified theory though not with the original statistical theory. A quantity independent of the slightly arbitrary relative weight of two assigned to production of excited nucleons compared with elastic scattering, is the ratio of the cross sections for the production of positive and neutral mesons. For the statistical theory the ratio is 3 and for the modified theory 5, (cf. Peaslee, loc. cit.), whereas the measured ratio is $92/22 = 4.2 \pm 1.0$. Morris et al. (loc. cit.) state that in their experiment the ratio of positive to neutral mesons may be as high as 23:1.

(2) Angular and momentum distributions of particles from inelastic scattering reactions.

From the statistical theory in which the conservation of angular /

angular momentum is not considered, the angular distribution in the c - system is predicted as isotropic as also is the distribution of the angle between the meson and either of the nucleons. The conservation of angular momentum entails some forward peaking of the distribution but no quantitative calculations of the effect are available for energies near that used in the present experiment. It is however easily possible to calculate the momentum distribution of the π mesons from inelastic scattering using purely statistical considerations, if it is assumed that the nucleons may be considered as non-relativistic particles.

The results for the production of positive and neutral mesons are considered in turn.

(a) $p + p \longrightarrow \pi^+ + p + n$: The angular distributions of the secondary particles in the c - system are shown, folded about 90°, in figure VIII - 1. In these and the following figures are plotted the distributions of 'consistency values', (see chapter VII, page 87), of the quantities. As pointed out earlier these distributions usually differ only slightly from those for the measured values. The distributions of figure VIII - 1 are isotropic within the statistical errors although the errors are not small enough to exclude a small anisotropic component. Although the results of Morris et al., (loc. cit.), appear /

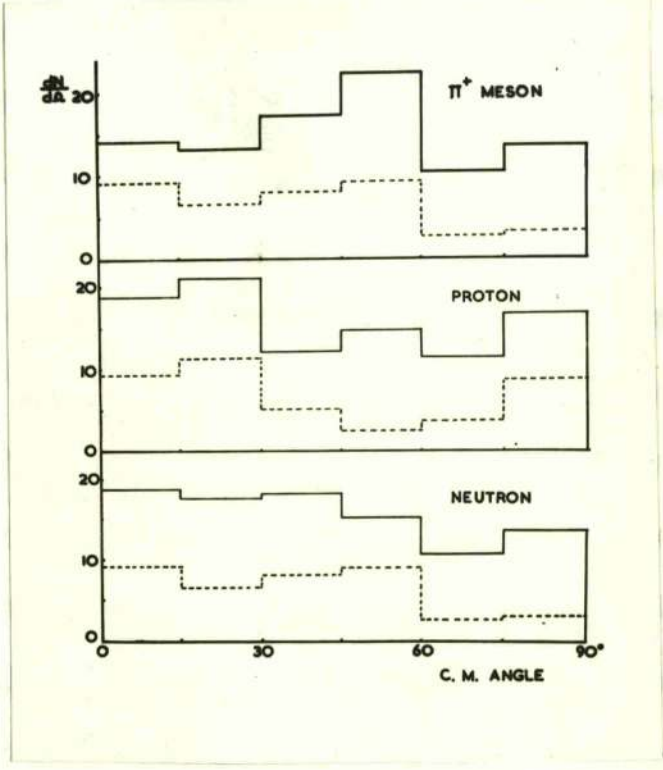

FIG. VIII - 1.

Angular distributions per unit solid angle of particles from the reaction $p + p \longrightarrow \pi^+ + p + n$. The distributions have been folded about 90°. The dotted histograms in this and the following figures refer to events in which the π meson was positively identified.

appear to show some peaking of the distributions for the proton and the π^+ meson at small angles, the statistical accuracy of their measurements is poorer than that of the measurements made in the present experiment and the effect cannot be considered significant.

An important feature of the present results is the strong angular correlation between the proton and the π^- meson. The distribution of the angle between these two particles in the c - system is shown in figure VIII - 2(a). The distribution of the angle between the π^+ meson and the neutron is shown in figure VIII - 2(b) which gives little evidence of correlation. These features of the reaction are in good agreement with the results to be expected on the excited nucleon hypothesis. On this theory $^8/_9$ of the π^+ mesons are produced by the decay of the excited particle into a proton and a π^+ meson while $^1/_9$ are produced by decay into a neutron and π^+ meson. In the c - system of the excited particle the angle between the products is 180° but since this system is moving relative to that for which the angles have been calculated we should expect that the angle would in fact be less than this value as is found in the measurements. The small rise towards 180° in the distribution of the angle between the meson and the neutron is to be expected since $^1/_9$ of the reactions pass through the excited neutron state. The slight evidence of a rise in this distribution at small angles is also not /

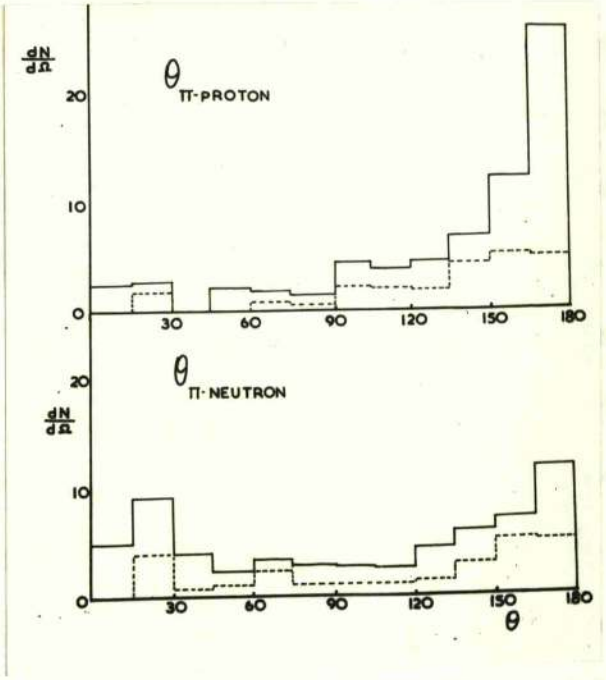

FIG. VIII - 2.

Angular correlations per unit solid angle between the proton and the π^+ meson and between the neutron and the π^+ meson from the reaction $p + p \longrightarrow \pi^+ + p + n$.

not unexpected since the tendency of the nucleons to emerge in opposite directions in order to conserve momentum, combined with the strong meson-proton correlation, may be expected to produce such an effect.

The momentum distribution for the π^+ meson in the c - system is shown in figure VIII - 3, in which is also drawn the distribution to be expected from simple statistical considerations of the density of the available momentum states. The measured distribution tends to lower momenta than the calculated curve, having a maximum at an energy of about 70 Mev. Yuan and Lindenbaum (1954, 1955) have measured the distribution of momentum of π^+ mesons emitted at 32° to a proton beam of energy equal to 1 Bev incident on a target of beryllium and this distribution shows a maximum at 90 Mev. Morris et al. (loc. cit.) state only that no mesons were observed with momentum less than 50 Mev/c in agreement with the present results. For the proton and the neutron from the reaction the momentum distributions are shown in figures VIII - 4(a) and (b). These distributions are notably different although from the statistical theory with charge independence they must be expected to be identical. For the neutron the distribution shows a broad peak having a maximum at a momentum equivalent to an energy of about 105 Mev in the c - system. Such a peak is to be expected if the reaction passes through an intermediate stage /

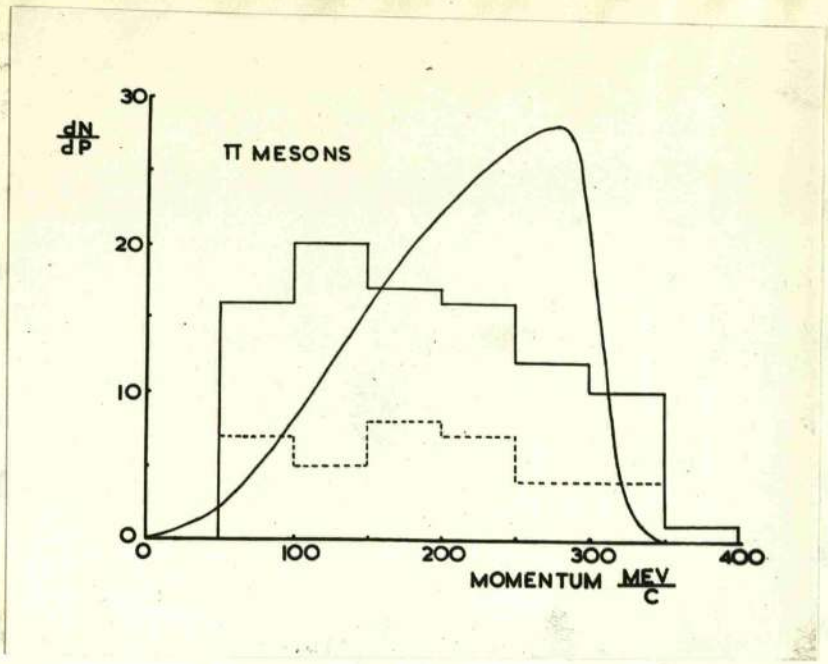

FIG. VIII - 3.

Momentum distribution of the π^+ meson from the reaction $p + p \longrightarrow \pi^+ + p + n$. The line represents the distribution calculated purely from momentum space considerations.

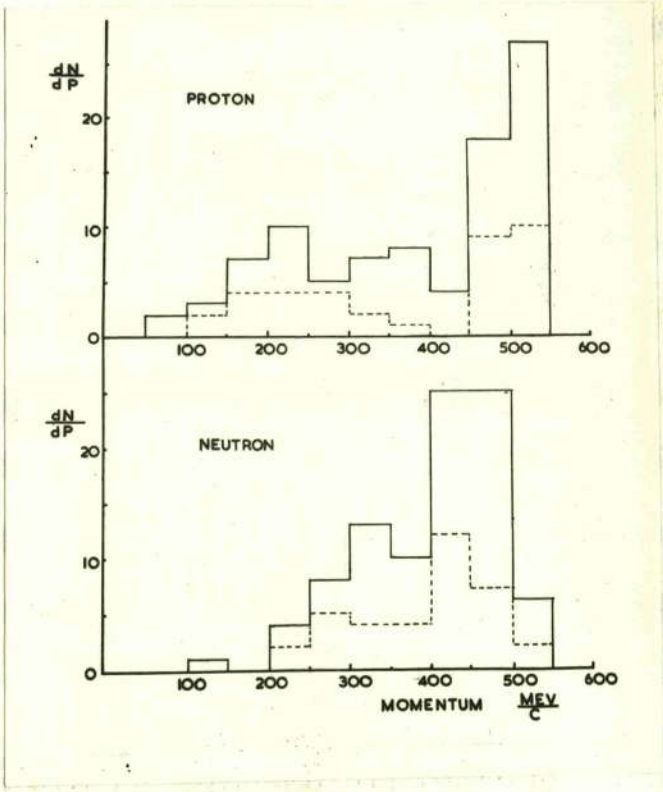

FIG. VIII - 4.

Momentum distributions of the proton and neutron from the reaction $p + p \longrightarrow \pi^+ + p + n$.

stage in which only two particles emerge one of which is in an excited state of considerable breadth. The protons tend to take the maximum momentum allowed by the kinematics of the reaction.

It is possible that the high values of the proton momentum and the low values of that for the π^+ meson, may be explained in terms of the angular distribution of the scattering of π^+ mesons by protons at energies near the $T = {}^3/_2$, $J = {}^3/_2$, resonance. This angular distribution is peaked at 0° and 180° but the peak in the backward direction is almost three times as intense as that at 0°. Thus one might expect that the mesons should be emitted predominantly backwards and the protons predominantly forwards in the c - system of the excited particle. Such a distribution in angle in this system would lead to the observed trends for the momentum distributions in the c - system for which they have been calculated. The angular distributions in the c - system of the excited particle are to be calculated.

If it is assumed that the proton and the π^+ meson result from the disintegration of an excited nucleon it is possible to calculate the Q value for this disintegration from the energies and momenta of the product particles and the angle between them. Q values calculated for the 92 events corresponding to the production of π^+ mesons are shown in figure /

figure VIII - 5. The distribution shows a maximum at ~ 100 Mev and has a median value of 115 Mev. The discrepancy between the position of the maximum at 100 Mev for this distribution and the energy of 160 Mev for the peak of the resonance in the scattering of π^+ mesons by protons, is not fully understood.

(b) $p+p \longrightarrow \pi^0+p+p$: Since only 22 examples of this reaction have been observed the angular and momentum distributions are of poor statistical weight. The distributions are shown in figures VIII - 6, 7 . Since it is not possible to determine which of the secondary protons is the result of the decay of the excited nucleon any possible angular correlations will be very weak. The angular distributions of the particles in the c - system (fig. VIII - 6) are rather similar to those for π^+ meson production. The distribution in momentum of the protons in the c system might be expected to correspond to the sum of the distributions of the neutron and the proton in production. In fact however there seems to be less tendency for the protons to take the maximum possible momentum and the mesons show the equivalent trend to take higher momenta than the π^+ mesons. Thus the data from this reaction although completely consistent with the decay of an excited nucleon afford no positive evidence in support of such a hypothesis.

(3) <u>Angular distribution of protons from elastic scattering.</u>

The angular distribution of the elastically scattered protons /

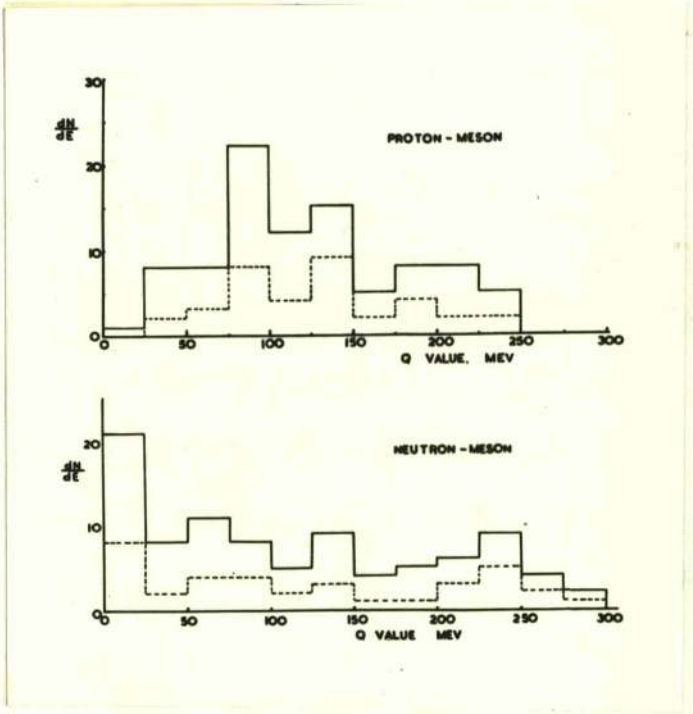

FIG. VIII - 5.

Q values calculated for the decay of a compound particle consisting of π^+ meson and proton and π^+ meson and neutron.

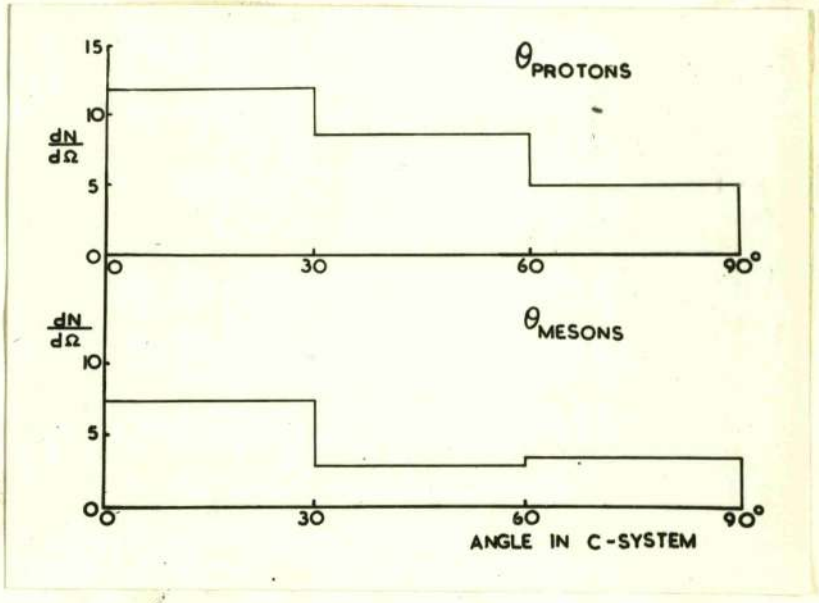

FIG. VIII - 6.

Angular distributions per unit solid angle, of particles from the reaction $p + p \longrightarrow \pi^0 + p + p$.

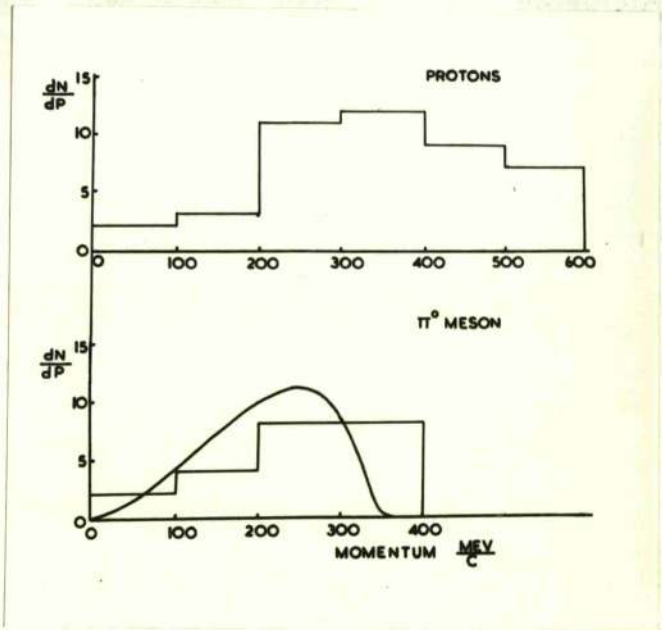

FIG. VIII - 7.

Momentum distributions of particles from the reaction $p + p \longrightarrow \pi^{\circ} + p + p$. The line in the distribution for the π° meson represents the distribution calculated purely from considerations of momentum space.

protons in the c - system is shown in figure VIII - 8. In this distribution the points for the smallest angular intervals employed have been corrected for loss as described in chapter VII. The dot line in figure VIII-8 represents the results of Smith et al. (1955) while the present results are compared with those of Morris et al. (1955) for 70 events in table VIII - 4.

TABLE VIII - 4.

ANGULAR RANGE IN C-SYSTEM	CORRECTED NO. OF EVENTS: PRESENT EXP.	NO. OF EVENTS MORRIS ET AL. (UNCORRECTED)	$\frac{d\sigma}{d\Omega}$ mb/ster. PRESENT EXP.
$2\frac{1}{2}$ - 10	5·3 ± 1·5	1	11·4 ± 3·0
10 - 20	12·4 ± 3·0	13	8·9 ± 2·2
20 - 30	13 ± 3·6	17	5·8 ± 1·6
30 - 40	12 ± 3·5	11	3·9 ± 1·2
40 - 50	17 ± 4·1	7	4·5 ± 1·1
50 - 60	4 ± 2·0	6	0·9 ± 0·5
60 - 70	4 ± 2·0	7	0·8 ± 0·4
70 - 80	2 ± 1·4	4	0·4 ± 0·3
80 - 90	2 ± 1·4	4	0·4 ± 0·3

The shape of the distribution obtained in the present experiment is in good agreement with those of Smith et al. and Morris et al. (loc. cit.).

Although /

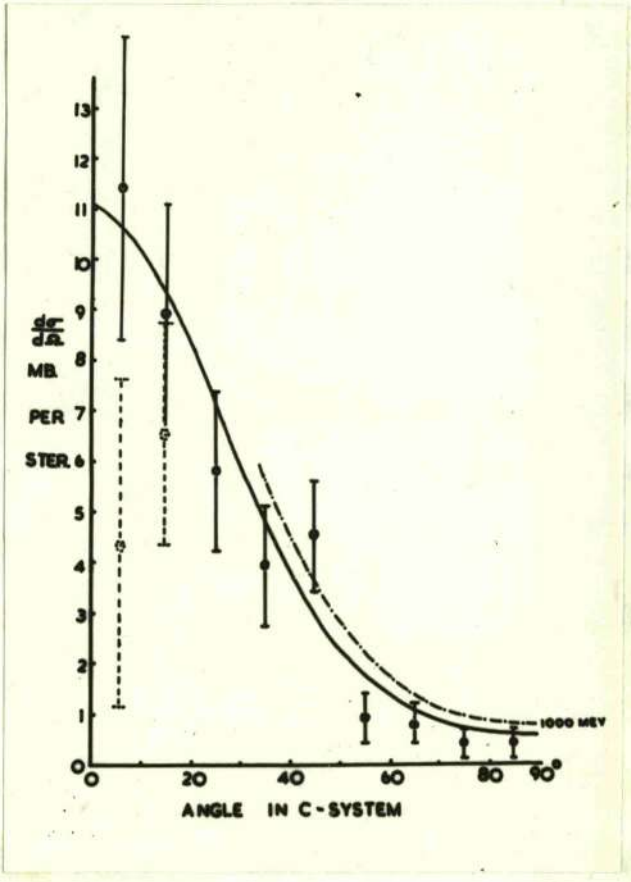

FIG. VIII - 8.

Differential cross section for the elastic scattering of protons by protons at 925 Mev. The cross sections for the two lowest angular intervals have been corrected for loss. The uncorrected values are indicated by the dotted points. The continuous line represents the distribution calculated using an optical model, and the dotted line the results of Smith, McReynolds, and Snow, (1955).

Although the conservation of angular momentum will produce a forward peak in the distribution, if allowed for in the statistical theory, it is difficult to imagine that the effect could be as strong as that observed when the energy available for each nucleon in the c - system is only ~ 220 Mev. No quantitative calculations are however available.

As described in chapter VII, (page 64), the optical model has been used by Serber and Rarita (1955) to calculate the angular distribution for the elastic scattering. No details of the work of Serber and Rarita are at present available but the angular distribution for the present experiment has been calculated on the same basis as that of these authors. The total cross section for scattering , $2\pi R^2$, is taken as 48 mb. yielding a value of $R = 8{\cdot}4.\ 10^{-14}$ cm. The angular distribution is then given by

$$W(\theta) = \frac{J_1^2(kR\sin\theta)}{\sin^2\theta}$$

where J_1 is the first order Bessel function and k is the wave number of the proton. This distribution is superimposed on the experimental results in figure VIII - 8, (continuous line), where the curves have been normalised to the experimental value of the elastic cross section. The agreement between the calculated and measured distributions normalised in this way is good. The assumption of scattering by a classical black sphere however appears /

appears to entail equal cross sections of 24 mb. for the elastic and inelastic scattering in disagreement with the present results.

(4) Conclusions.

The cross sections obtained for elastic and inelastic scattering at 925 Mev are in general agreement with those measured at similar energies by Shapiro et al. (1954) and Smith et al. (1955) using counters, although the value obtained for the cross section for elastic scattering is lower than that obtained by these methods.

The angular correlations and momentum distributions observed for particles from the reaction $p+p \longrightarrow \pi^{+}+p+n$ are satisfactorily explained if it is assumed that this reaction proceeds by means of an intermediate state in which an excited nucleon having total isotopic spin $T = {}^{3}/_{2}$ is produced, which thereafter decays into a π^{+} meson and a normal nucleon. The excitation energy of the nucleon shows some discrepancy with that expected from the scattering of π^{+} mesons by protons. The results for the reaction $p+p \longrightarrow \pi^{0}+p+p$ are also consistent with such an interpretation.

The relative cross sections for the production of π^{+} and π^{0} mesons are found to have a ratio of $4{\cdot}2 \pm 1{\cdot}0$ compared with a ratio of 5 predicted on the excited nucleon hypothesis and about 23 as reported from preliminary measurements by Morris et /

et al. (loc. cit.) at a similar energy. If it is assumed that the elastic scattering process and the formation of the excited nucleon are alternative modes of decay of the compound state described in Fermi's statistical theory, having relative probabilities 1; 2, then close agreement is found between the calculated and measured cross sections.

The differential cross section for elastic scattering as measured in the present experiment is found to be strongly peaked in the forward direction and is in satisfactory agreement with that measured by Smith et al. and Morris et al. (loc. cit.). The shape of the distribution is fitted by a curve calculated by means of an optical model with a proton radius $R = 0.84.10^{-13}$ cm. The optical model however gives relative cross sections for elastic and inelastic scattering which are not in agreement with the measurements and the validity of its application to a situation where the particle wavelength and the radius of the obstacle are nearly equal in magnitude is open to question.

CHAPTER IX

THE POLARISATION OF NUCLEAR γ-RAYS.

(i) The relation between the polarisation of the γ-rays and the properties of the nuclear states involved in the γ-ray transition.

Both the classical theory involving the solution of Maxwell's equations, and the correct quantum mechanical treatment, give for the angular dependence of the fields due to a distribution of charges, currents and magnetic material, expressions

$$\left.\begin{aligned} \underset{\sim}{E} &\propto \underset{\sim}{X}_{\ell m}(\theta,\varphi) \\ \underset{\sim}{H} &\propto \underset{\sim}{\nabla} \times [k \underset{\sim}{X}_{\ell m}(\theta,\varphi)] \end{aligned}\right\} \text{IX-1} \qquad \left.\begin{aligned} \underset{\sim}{E} &\propto \underset{\sim}{\nabla} \times [k \underset{\sim}{X}_{\ell m}(\theta,\varphi)] \\ \underset{\sim}{H} &\propto \underset{\sim}{X}_{\ell m}(\theta,\varphi) \end{aligned}\right\} \text{IX - 2}$$

for pure multipole radiation. $\underset{\sim}{E}$ and $\underset{\sim}{H}$ are the electric and magnetic fields respectively, k is a constant, and $\underset{\sim}{X}_{\ell,m}$ are the vector spherical harmonics of order ℓ, m (see for instance Blatt and Weisskopf, 1952). The indices ℓ and m may be shown to correspond to the angular momentum quantum numbers ℓ and m for a particle. In the most general case more than one set of values of ℓ and m are involved and the fields involve summations over these indices.

The angular distribution of the radiation is given by the angular dependence of the Poynting vector $S = \frac{c}{4\pi} \underset{\sim}{E} \times \underset{\sim}{H}$. The polarisation is described by the angular distribution of $\underset{\sim}{E}$ or $\underset{\sim}{H}$ alone. The pairs of expressions IX-1 and IX-2 above correspond /

correspond to the two possible types of radiation, magnetic and electric, respectively. The two types differ in the parity of their fields.

It is convenient in polarisation problems to express $\underset{\sim}{E}$ or $\underset{\sim}{H}$ as the vector sum of $\underset{\sim}{E}_{\theta_0}$ and $\underset{\sim}{E}_{\varphi_0}$, ($\underset{\sim}{H}_{\theta_0}$ and H_{φ_0}), where $\underset{\sim}{\theta}_0$ and $\underset{\sim}{\varphi}_0$ are unit vectors as shown in figure IX-1. If $\underset{\sim}{E}_{\theta_0}$ is not equal to $\underset{\sim}{E}_{\varphi_0}$ the polarisation will have the general elliptical form. By writing the $\underset{\sim}{X}_{\ell,m}$ in terms of $\underset{\sim}{\theta}_0$, $\underset{\sim}{\varphi}_0$ and the ordinary spherical harmonics $Y_{\ell m}(\theta, \varphi)$ we obtain

$$\left.\begin{aligned} \left[\underset{\sim}{E}_{\theta_0}\right]_{MAG} = \left[\underset{\sim}{E}_{\varphi_0}\right]_{EL} &\propto \frac{1}{\sin\theta}\frac{\partial}{\partial\varphi}\left[Y_{\ell,m}(\theta,\varphi)\right] \\ \left[\underset{\sim}{E}_{\varphi_0}\right]_{MAG} = \left[\underset{\sim}{E}_{\theta_0}\right]_{EL} &\propto \frac{\partial}{\partial\theta}\left[Y_{\ell,m}(\theta,\varphi)\right] \end{aligned}\right\} \quad \text{IX - 3}$$

so that the polarisations of electric and magnetic radiation of the same multipole order differ everywhere by $\pi/2$. Thus the information obtained from a measurement of the polarisation is the electric or magnetic nature of the radiation and, in turn, whether or not the transition involves a change of parity.

So far we have implied the existence of a fixed direction with respect to which measurements of the polarisation may be made, such as the direction of the magnetic field in the Zeeman effect for which the equations IX-3 give the polarisations at once. In fact even if we have a defined direction the radiation from nuclei will be isotropic and unpolarised as long as /

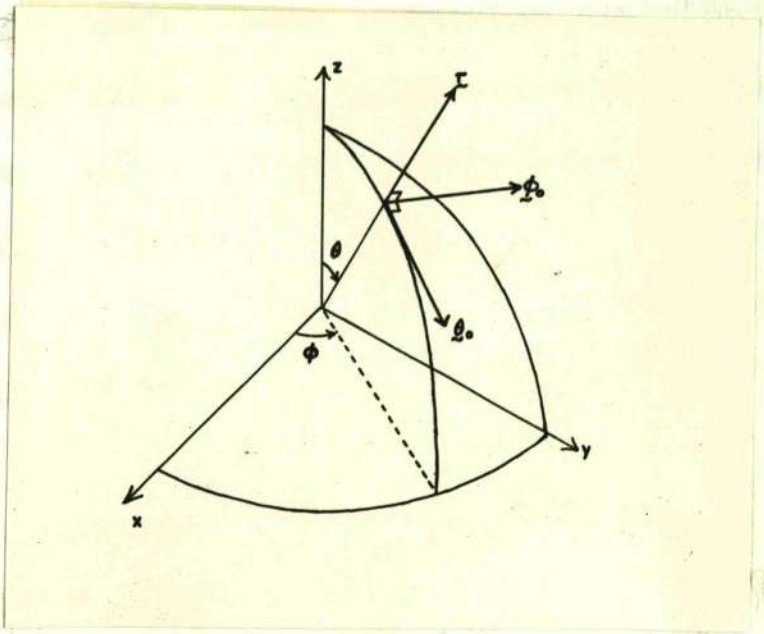

FIG. IX - 1.

Illustration of the vectors $\underline{\theta}_o$ and $\underline{\varphi}_o$.

as the sublevels of the initial state, corresponding to all possible values of the quantum number m, are equally populated, since the radiations which have different m values always add to give isotropy. If however the nucleus is excited to an initial state in such a way that the populations of the states having different m values are different then the radiation is unlikely to be isotropic and unpolarised. Such an excitation may be achieved either through a nuclear reaction to give an 'angular distribution' or by a γ-ray cascade to give an 'angular correlation' between the two γ-rays. The polarisation of the γ-ray from the reaction may then be measured with respect to the plane of the incident particle and the γ-ray direction or, for a correlation, with respect to the plane of the two γ-rays. Angular distributions are measured with respect to the direction of the incident particle in a nuclear reaction, angular correlations with respect to the direction of the first γ-ray.

Such correlations and distributions may always be written in the form

$$W(\theta) = \sum_i a_{2i} \cos^{2i}\theta$$

for pure multipole radiation. This form is easily obtained for particular cases by adding incoherently the contributions of transitions involving all the possible m values for any pure multipole transition. The coefficients a_i are functions of /

of the spins of the initial, intermediate, and final states, the spin of the particles involved and the orbital angular momenta of particles and γ-rays. Yang (1948) has derived this result in a general manner by group theoretical methods. $W(\theta)$ is of course the same for electric and magnetic radiation of the same multipolarity.

Since the polarisation and angular distribution of radiation are closely related it is convenient to express the polarisation in terms of the coefficients occurring in the angular distribution. Such a treatment has been given by Hamilton (1948). The polarisation is taken to be elliptical and, if the transitions are randomly phased, is completely specified by stating the linear intensities J_θ and J_φ in the directions $\underset{\sim}{\theta}_0$ and φ_0. In general the complete transition consists of the sum of transitions between the sublevels of the states taking part. We let $\beta_{|\Delta m|}$ be the relative numbers of transitions for different m changes for dipole radiation and $f_{\Delta m,\theta}$, $f_{\Delta m,\varphi}$ represent the intensities of radiation corresponding to a change Δm and polarised in the θ and φ directions. Then for dipole radiation

$$W(\theta) = \beta_0 f_0 + 2\beta_1 f_1 \quad \text{-- IX -- 4}$$

where $f_0 = f_{0\varphi} + f_{0\theta}$

$f_1 = f_{1\varphi} + f_{1\theta}$

$$[J_\varphi]_{EL} = [J_\theta]_{MAG} = \beta_0 f_{0\varphi} + 2\beta_1 f_{1\varphi}$$

$$[J_\theta]_{EL} = [J_\varphi]_{MAG} = \beta_0 f_{0\theta} + 2\beta_1 f_{1\theta}$$

The /

The f_s are easily calculated as a function of θ from equations IX-3 and for electric dipole radiation

$$f_{0\varphi} = 0, \quad f_{1\varphi} \propto 1, \quad f_{1\theta} \propto \cos^2\theta, \quad f_{0\theta} \propto 1 - \cos^2\theta$$

Also $W(\theta) = 1 + a_2 \cos^2\theta$ for dipole radiation. If we normalise so that

$$\int W(\theta) d\Omega = \int (J_\theta + J_\varphi) d\Omega = 8\pi$$

and equate coefficients of the powers of $\cos\theta$ in equation IX-4 we obtain

$$\beta_0 = \frac{3(1-a_2)}{3+a_2} \quad \text{and} \quad \beta_1 = \frac{3(1+a_2)}{3+a_2}$$

Thus $\left[J_\theta / J_\varphi\right]_{EL} = \dfrac{1 + a_2 \cos 2\theta}{1 + a_2}$ and the inverse expression holds for magnetic radiation. An exactly similar treatment yields for quadrupole radiation

$$\left[J_\theta / J_\varphi\right]_{EL} = \frac{(1 + a_2 + a_4) - \frac{1}{2} a_4 \sin^2 2\theta}{1 + (a_2 + a_4)\cos 2\theta}$$

A measurement of the polarisation, that is of the ratio J_θ / J_φ at any polar angle θ should thus give both the electric or magnetic nature of the radiation and also the coefficients $a_2, a_4 \ldots\ldots$ In practice direct measurements of angular distributions may be made with a much greater statistical accuracy than that obtained in measurements of polarisation. Thus the principal function of polarisation measurements is to determine /

determine the electric or magnetic nature of the radiation.

(ii) Parity assignments and the shell model.

The evidence for a shell structure in nuclei and the features of the nuclear models which have been postulated to account for the experimental observations are well known, (see, for instance, Pryce 1954). In the one particle model it is implicit that the paired-off nucleon core is in a state of even parity and the parity of the nucleus as a whole is determined by that of the state of motion of the odd nucleon. Since the shell model can predict the order of the one nucleon levels for any assumed potential it is nearly always possible to predict the angular momentum state of the odd nucleon and thus the parity of the ground state of even-odd nuclei. Thus for the first shell holding two nucleons we have an S state of even parity, the next shell, nucleon numbers 3-8, consists of p - states of odd parity, the third shell 9-20, of d and s states again of even parity, and so on.

Two cases of disagreement between the measured spin value and that predicted by the shell model, are well known. ^{23}Na, $(Z=11)$, has spin $3/2$ instead of the predicted value of $5/2$, and ^{55}Mn, $(Z = 25)$, has spin $5/2$ instead of the predicted value $7/2$. Talmi (1951, 1952) calculates that for no reasonable central potential is $I = 3/2$ the lowest level in a configuration $(d_{5/2})^3$ nor $I = 5/2$ in $(f_{7/2})^3$ though they may come close to the ground level. /

level. These calculations are confirmed by Edmonds and Flowers (1952) and some additional effect must be postulated to account for the anomaly.

In view of the importance of the shell model in low energy nuclear physics it is of value to make checks on the parities of the ground states of nuclei.

(iii) <u>The measurement of the polarisation of γ -rays.</u>

The polarisation of γ-rays produces distinctive effects in all the interactions of the radiation with matter. Thus the detection and measurement of the polarisation may be effected by observations on

(a) Photo-electric effect.
(b) Compton effect.
(c) Pair production.
(d) Nuclear photoeffect.

In general polarisation is measured by examining an azimuthal angular distribution. In the non-relativistic photo-electric effect for example the azimuthal angular distribution of the ejected photo-electrons is proportional to $\cos^2\varphi$ where φ is the angle between the azimuthal direction of the photo-electron and the electric vector of the γ-ray (fig. IX-2). For any method of measuring polarisation we may define a ratio of the type

$$R = (d\sigma)_{\varphi=0} / (d\sigma)_{\varphi=\pi/2}$$

where $(d\sigma)_{\varphi=0}$ is the cross section for the ejection of particles /

particles in the direction of the electric vector of a plane polarised γ-ray and $(d\sigma)_{\varphi=\pi/2}$ is the cross section for ejection of particles at right angles to this direction. This 'assymetry ratio' is a measure of the sensitivity of any method of polarisation measurement. For the non-relativistic photo-electric effect $R=\infty$.

We shall summarise the predictions of the theory for the various effects listed above by stating the form of the cross section and the assymetry ratio for each in turn.

(a) Photo-electric effect: (fig. IX-2).

$$d\sigma_{K\text{-ELECTRONS}} = [A(\varepsilon,\theta) + B(\varepsilon,\theta)\cos^2\varphi]\,d\theta\,d\varphi$$

$$R_{P.E.} = \frac{A+B}{B}$$

In this and future expressions ε is the γ-ray energy, θ the polar angle of ejection of a particle, and A and B are functions independent of φ. $R_{P.E.}$ is plotted as a function of γ-ray energy in figure IX-3.

(b) Compton effect: (fig. IX-4).

$$d\sigma_c = r_0^2/2 \; k^2/k_0^2 \left[k/k_0 + k_0/k - 2\sin^2\theta\cos^2\phi\right]$$

$$R_c = \left[k/k_0 + k_0/k - 2\sin^2\theta\right] / \left[k/k_0 + k_0/k\right]$$

where k_0 and k are the momenta of the incident and scattered photons, r_0 is the classical electron radius, θ is the usual polar angle, and ϕ is the angle which the electric vector of the incident γ-ray makes with the plane of the scattering. R_c is /

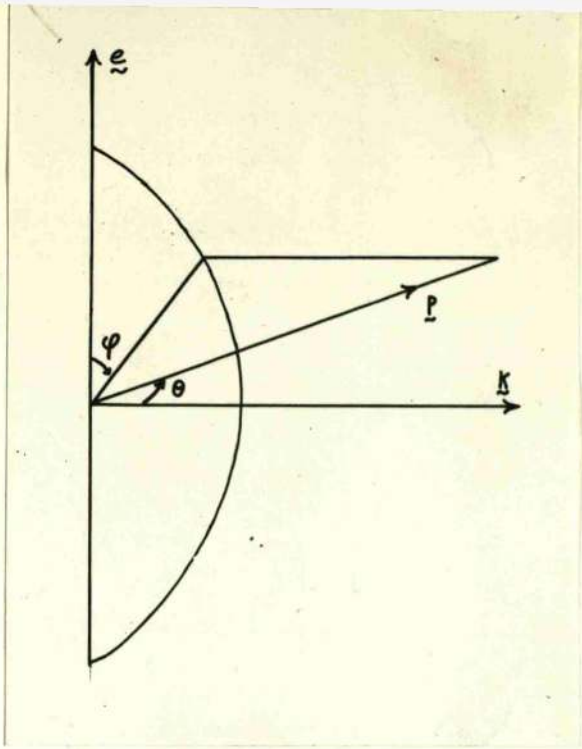

FIG. IX - 2.

Illustration of the angles involved for photo-electrons ejected by polarised γ - rays.

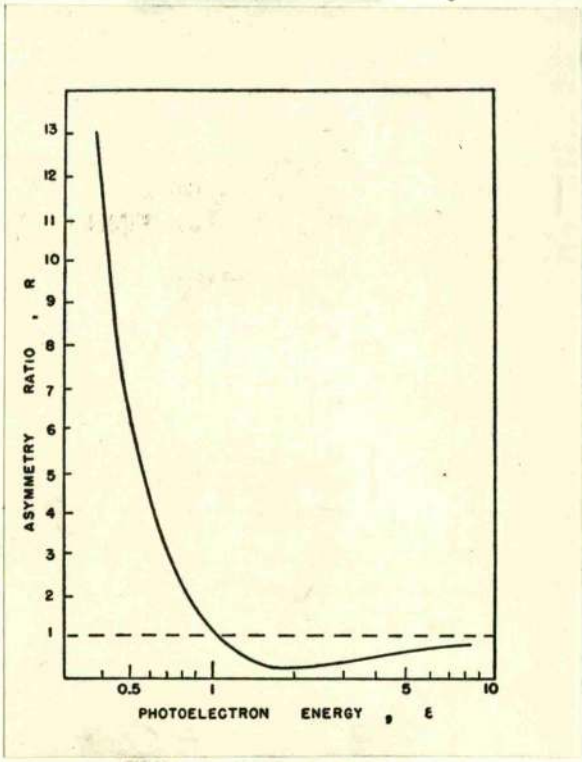

FIG. IX - 3.

Variation of the assymetry ratio R for photo-electrons ejected from the K shell by linearly polarised photons for $\theta = \pi/2$. The photo-electron energy is expressed in units of the electron rest mass.

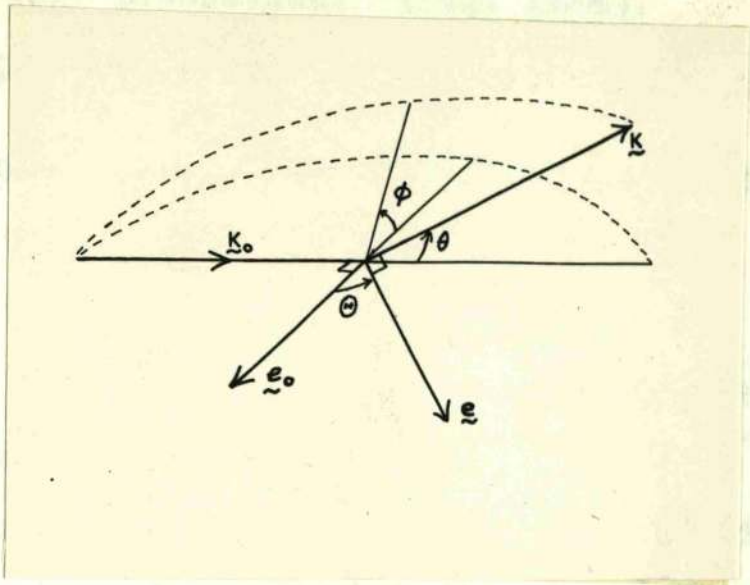

FIG. IX - 4.

Illustration of the angles involved for the Compton scattering of polarised γ -rays.

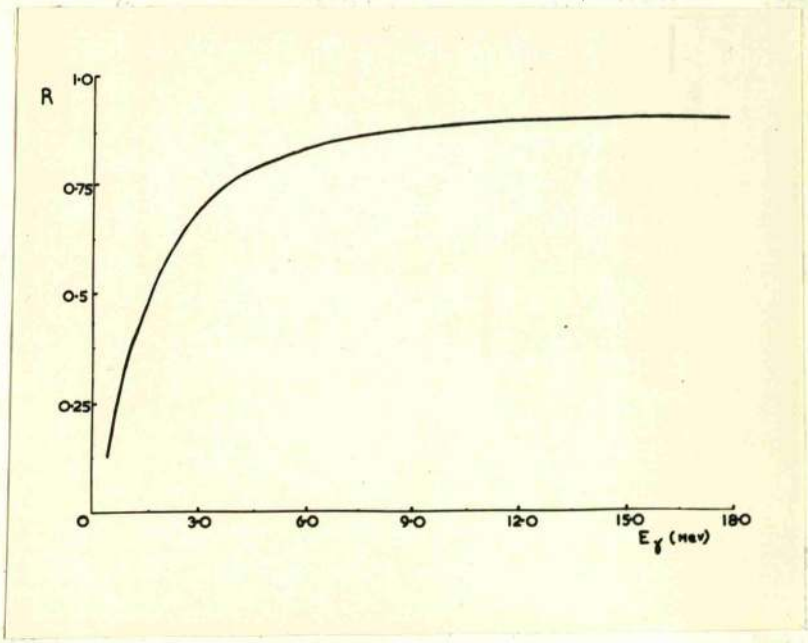

FIG. IX - 5.

Variation of the assymetry ratio R with γ -ray energy for the Compton effect. This curve applies for the most favourable polar angle .

is plotted against quantum energy in figure IX-5.

(c) Pair production: (fig. IX-6).

$$d\sigma_p = [A(\varepsilon,\theta) + B(\varepsilon,\theta)\cos^2\varphi]\, d\theta\, d\varphi$$

$$R_p = \frac{A+B}{B}$$

φ in this case is the angle between the direction of the electric vector of the γ-ray and the plane of the pair. The plane of the pair will not normally contain the direction of the incident γ-ray, and neglect of this consideration led Berlin and Madansky (1950) to the result $d\sigma_p = (A' + B'\cos 2\varphi)$ having maxima displaced by $\pi/2$ from the distribution quoted above which is due to May and Wick (1951) and May (1951).

(d) Nuclear photo-effect in deuterium: For the energy region 5 - 50 MeV the nuclear absorption is almost entirely by an electric dipole mechanism and the cross section may be written

$$\sigma_{P.D.} = f(\varepsilon,\theta)\cos^2\varphi\, d\varphi$$

Thus $R = \infty$ for this energy range.

The absolute values of the cross sections per atom are compared for all the effects in figure XI-7.

A consideration of figure XI-7 and of figures IX-3, and 5 leads to the following conclusions:

(i) For γ-ray energies $\lesssim$ 1 MeV (except near 0·5 MeV), the photoelectric effect is a good detector.

(ii) /

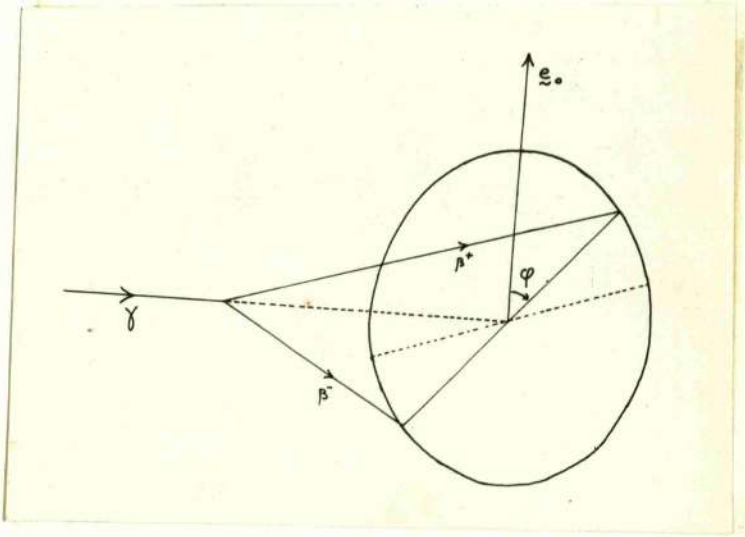

FIG. IX - 6.

Illustration of the angles involved for pair production by polarised γ-rays.

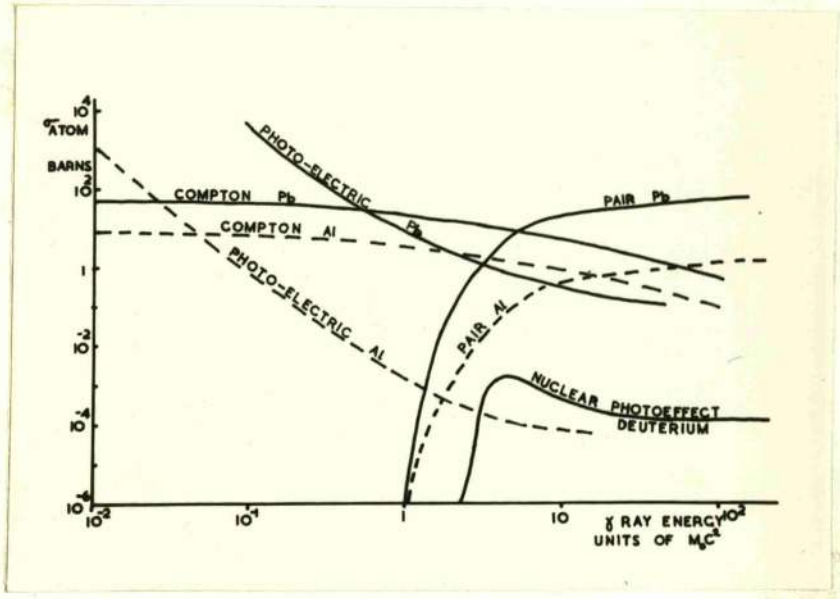

FIG. IX - 7.

Absolute values of the cross section per atom for the interaction of γ -rays with matter.

(ii) For energies 1 - 5 MeV. the Compton effect has a satisfactory value of R and a sufficiently large cross section.

(iii) At energies greater than 5 MeV. the nuclear photo-effect in deuterium competes favourably with the Compton effect as a detector of polarisation, and at energies greater than about 9 MeV. is undoubtedly to be preferred.

Apart from the factors considered in arriving at these conclusions, purely experimental difficulties may make it difficult to employ a particular effect as a polarisation detector and we have omitted pair production since such difficulties would appear to be very considerable for the use of this effect.

Measurements of polarisation have been made using both the photo-electric effect, (Kirkpatrick (1931) , 25 KeV. X-rays; MacMaster and Hereford (1954), 0·4 - 0·8 MeV. γ -rays), and the Compton effect, (Metzger and Deutsch, (1950), 1 - 2 MeV. γ -rays), as detectors of polarisation at low γ -ray energies. The experiments of Metzger and Deutsch and of other workers in this energy range were highly successful but French and Newton (1952) who attempted to use the Compton effect to study the polarisation of the 6·13 MeV. γ -ray from the reaction $F^{19}(p,\alpha\gamma)O^{16}$ state that they consider that the photo-disintegration of deuterium would be a better detection method at this energy.

At /

At the time when the present work was undertaken two experiments had been performed involving polarised γ-rays and deuterium photodisintegration. Wilkinson, (1952), had studied the distribution in azimuthal angle of photoprotons ejected from deuterium by the 5·5 MeV. γ-rays from the reaction $^2H(p,\gamma)^3He$. The polar angular distribution of these γ-rays is almost pure $\sin^2\theta$ which suggests that the reaction may proceed by a direct radiative transition. If there is little spin-orbit coupling then a transition involving only $\Delta m = 0$ would give a pure $\sin^2\theta$, plane polarised γ-ray. The azimuthal angular distribution of the photoprotons conformed closely to $\cos^2\varphi$ and this experiment may be taken as a confirmation of the theoretical predictions concerning the relationship between the polarisation and the azimuthal angular distribution of the photoprotons ejected from deuterium. Phillips, (1953), has used the photodisintegration of deuterium to study the polarisation of bremsstrahlung from a 20 MeV. betatron.

During the course of the present work results were published concerning the polarisation of γ-rays from the reaction $^{19}F(p,\alpha\gamma)^{16}O$, (Fagg and Hanna 1953), using a technique very similar to that employed by the author. Polarisation measurements of bremsstrahlung have also recently been /

been made using this technique by Tzara (1954) and by Muirhead and Mather (1954).

CHAPTER X

MEASUREMENT OF THE POLARISATION OF γ-RAYS FROM THE REACTIONS $^{27}Al(p,\gamma)^{28}Si$, $^{23}Na(p,\gamma)^{27}Al$ AND $^{26}Mg(p,\gamma)^{27}Al$.

(i) Introductory.

The intention of the present work was, in the case of the first two reactions studied, to check the parity assignments of the shell model to the ground states of ^{27}Al and ^{23}Na, the latter being of particular interest in view of the disagreement between the spin originally predicted by the shell model for this nucleus and its measured value. For the reaction $^{26}Mg(p,\gamma)^{27}Al$ the purpose of the measurements was to fix the parity of the first excited state in ^{27}Al. A secondary purpose of the work was the development of a technique of measurement for the polarisation of γ-rays having energies greater than 5 or 6 MeV, as a tool in nuclear spectroscopy.

The photodisintegration of the deuteron was chosen as a polarisation detector for reasons made clear in chapter IX. The theory of the polarisation dependence was regarded as reliable in view of the experimental results obtained by Wilkinson (1952, loc. cit.). The method used, exposure to the γ-rays of nuclear emulsions loaded with heavy water, was that employed by Wilkinson, and, concurrently with the present experiment, by Fagg and Hanna (1953).

(ii) /

(ii) Emulsions and Impregnation.

Ilford G5 nuclear emulsions usually 300μ but also 400μ in thickness were used throughout the series of exposures. Preliminary tests led to this choice of G5 rather than C2 emulsions since it was very desirable to obtain well defined tracks, and since the swelling of an emulsion with water causes attenuation of normally heavy tracks. Also, since long exposures were required, fading of the tracks was to be expected in a wet C2 emulsion but no evidence of fading was observed when using G5 plates. The density of background grains was not high when the plates were screened against soft X-rays.

The method of introducing the heavy water into the emulsion was to place a plate, cut to 1" x 1-5", in a perspex box, insert a U-shaped glass spacer to prevent the emulsion resting against the front of the box and then to add sufficient water to cover the plate.

Preliminary measurements were made to determine the variation of the rate of swelling of the emulsion with time. The thicknesses of two emulsions were measured by placing a cover glass on top of the emulsion and taking measurements with a micrometer screw gauge of the total thickness of emulsion, cover glass, and glass backing at nine points distributed in a regular fashion over the surface of the emulsion. Measurements of /

of the thickness of the cover glass at the same nine points were then made and finally the whole procedure was repeated after the processing of the emulsion. The thickness of the processed emulsion was measured using the microscope depth gauge. After the initial thickness measurements had been made one plate was placed in heavy water and one in ordinary water. Thickness measurements were made at increasing intervals for a total time of 170 hours and the complete set of measurements was used to obtain the curves shown in figure X-1, the temperature being 19°C. It is clear from this figure that swelling is virtually complete after about fifteen hours. At least this length of time was allowed to elapse between immersion and exposure of the emulsions. Less accurate measurements indicated that at temperatures below 19°C the swelling is less and saturation is is attained more quickly. At temperatures above 20°C the thickness measurements gave some evidence of distortion in the form of a sag in the emulsion of plates allowed to stand upright in water for long periods.

(iii) Temperature Control and shielding.

The perspex boxes containing the plates were sealed and placed in the container illustrated in figure X-2. The container was constructed in two halves in order to facilitate its removal when renewing the target in the H.T. set. The

cooling /

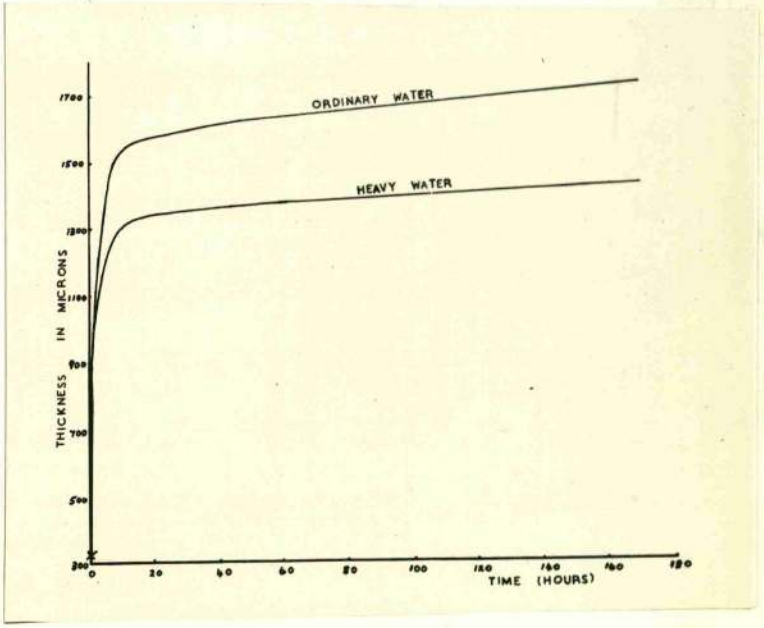

FIG. X - 1.

Swelling of nuclear emulsions in ordinary and heavy water as a function of time.

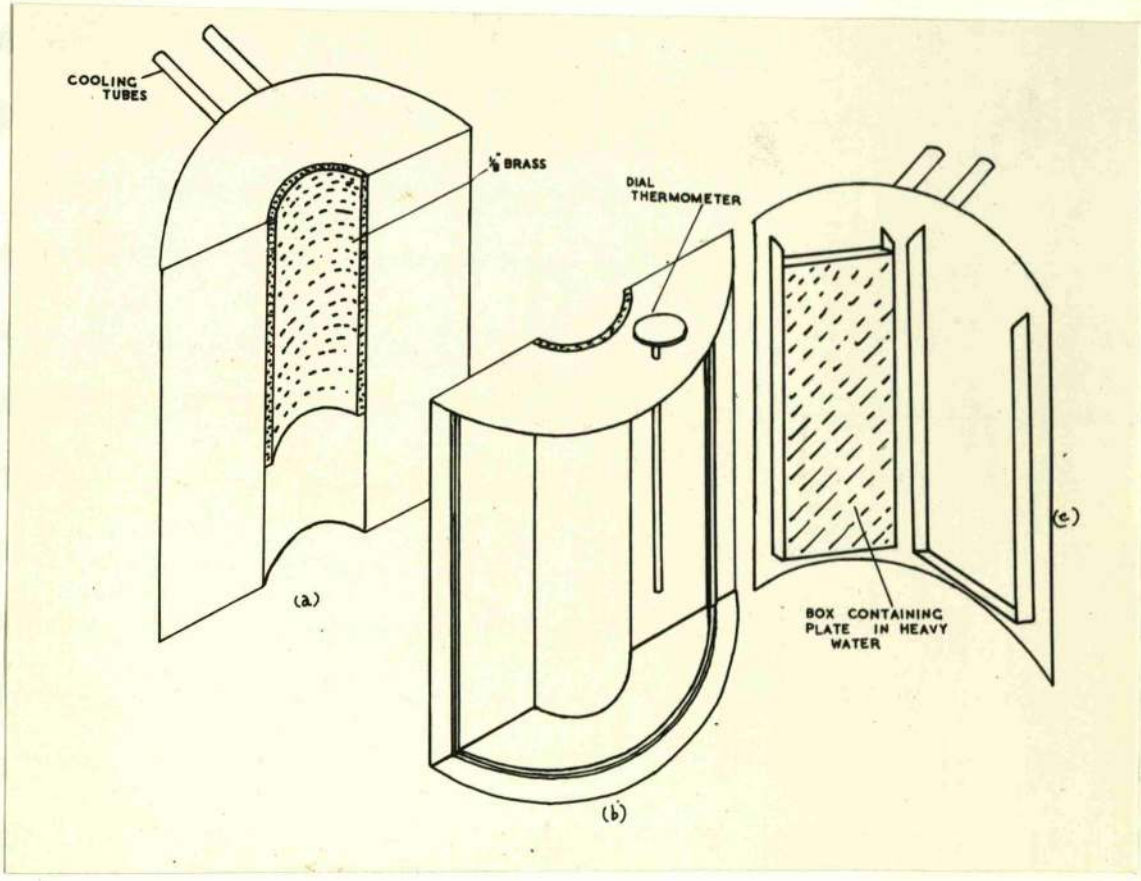

FIG. X - 2.

Plate container used in the polarisation experiments. (c) closes upon the back of (b) to form half the cylindrical box the opposite half of which is shown in (a).

cooling tubes on the outside of the box were added after the first exposures in order to maintain the emulsions at a constant temperature. Normal running temperatures were between 15°C and 17°C as read on the dial thermometer.

In the first exposures the emulsions showed a blackening above a line at the level of the target block. This was attributed to soft X-rays produced by protons in the target. A sheath of $\frac{1}{8}$" copper was inserted as shown in the figure and proved completely effective in removing this background.

Since the H.T. set is frequently used to accelerate deuterons, the accelerating tube and the resolving chamber tend to become contaminated with deuterium. This gives rise to a background of knock-on protons in the emulsions produced by neutrons from the reaction $^{2}H(d,n)^{3}He$. In order to detect such a background, in each group of four plates held by the container was included one impregnated with ordinary, instead of heavy, water. An emulsion impregnated with ordinary water is an efficient detector of neutrons since it contains about eight times as much hydrogen per square centimetre of surface area as does an emulsion impregnated with heavy water. In some of the first exposures the ordinary water emulsion showed tracks having a continuous range distribution with a maximum corresponding to a neutron energy of 3·3 MeV., (figure X-3), which is exactly equal /

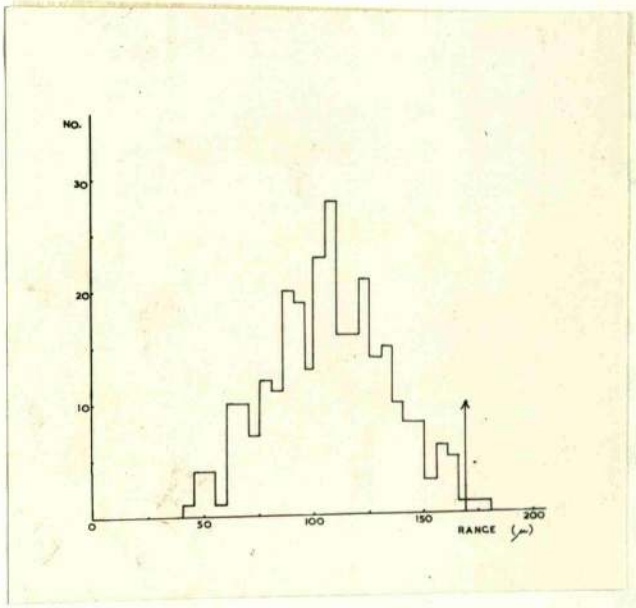

FIG. X - 3.

Range distribution of tracks found in a plate impregnated with ordinary water and exposed during an early experiment. The arrow marks the upper limit for the range of protons knocked on by neutrons from the reaction $^{2}H(d,n)^{3}He$.

equal to the maximum possible energy of neutrons from the reaction $^{2}H(d,n)^{3}He$. This background tends to obscure photo-protons arising from γ -rays having an energy of less than 8·8 MeV. In order to eliminate this background the following precautions were taken: (a) all accessible parts of the inside of the resolving chamber were cleaned with emery paper, (b) the H.T. set was used to accelerate protons for about eight hours prior to starting a run with target and emulsions in position, (c) a large cylindrical block of paraffin wax having a length of 11" was used to shield the emulsions from neutrons produced in the resolving chamber of the H.T. set. These precautions, particularly the wax shielding, proved completely effective in eliminating the neutron background as detected in the water soaked emulsion. The arrangement of emulsions and shielding is shown in figure X-4.

(iv) Target preparation and target heating.

Targets were made by condensing a suitable vapour upon a cleaned copper or brass backing. To produce targets of ^{27}Al, pure aluminium was condensed upon brass. For the targets of ^{23}Na, analar grade sodium chloride was normally used but in the last exposure it was replaced by sodium sulphate. The targets of sodium sulphate lasted better under bombardment and are less likely to contain fluorine as an impurity. For the reaction $^{26}Mg(p,\gamma)^{27}Al$ targets of the separated isotope were obtained from /

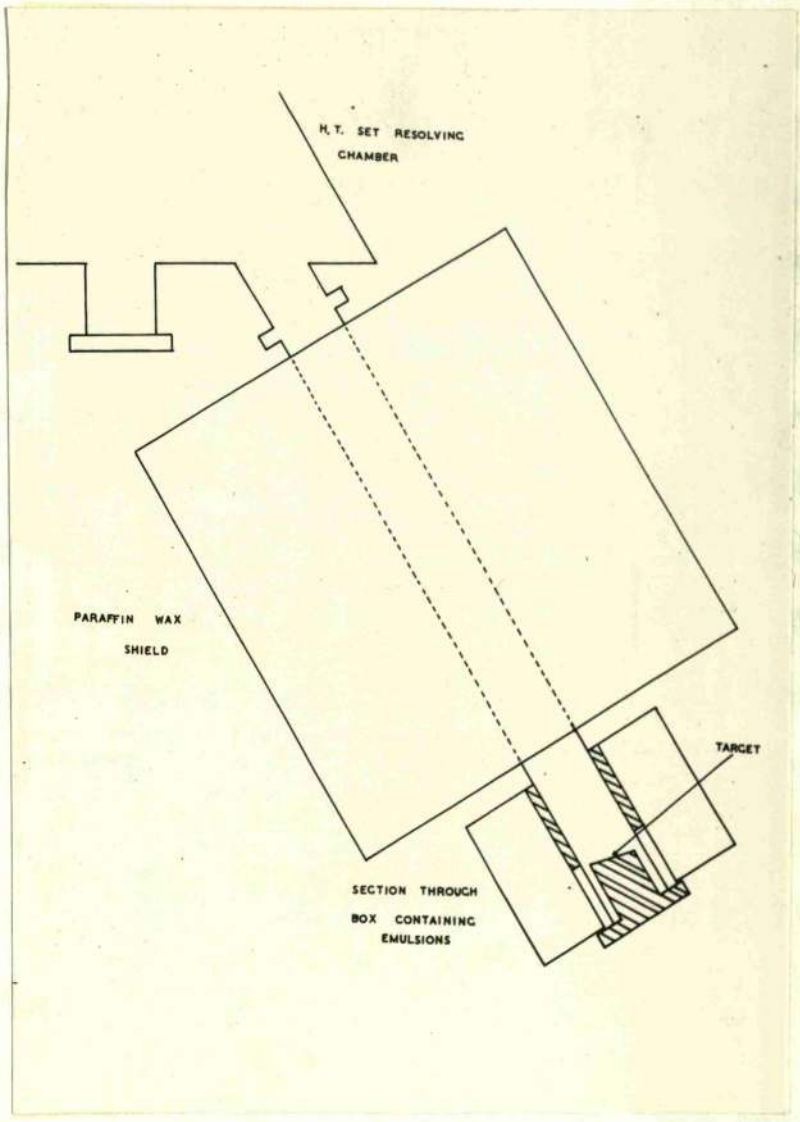

FIG. X - 4.

Arrangement of emulsions and shielding in the polarisation experiments.

from A.E.R.E. Harwell. All the targets were of such a thickness that only one resonance could be excited.

Deposition of carbon on the targets was experienced in most of the early exposures. Such contamination may render the target useless and also leads to a background of 8·03 MeV. γ-rays from the reaction $^{13}C(p,\gamma)^{14}N$ when the proton energy is $\gtrsim$ 550 KeV. For the exposures using targets of the separated isotope ^{26}Mg and for the later exposures with ^{23}Na the target was heated electrically to about 230°C, a temperature above the boiling point of the pump oil used in the H.T. set. The heated target is illustrated in figure X-5. A collar of stainless steel prevented overheating of the O-ring-glass seal at the base of the tube. The temperature of the target was determined by means of a thermocouple. It was customary not to open the valve linking the resolving chamber with the body of the H.T. set until the temperature of the target had attained the requisite value. The heating proved almost completely effective in preventing the deposition of carbon on the targets.

(v) Exposure to γ-rays.

Before putting the plate container into position a check was made on the target thickness by varying the proton accelerating voltage through the resonance to be studied and measuring /

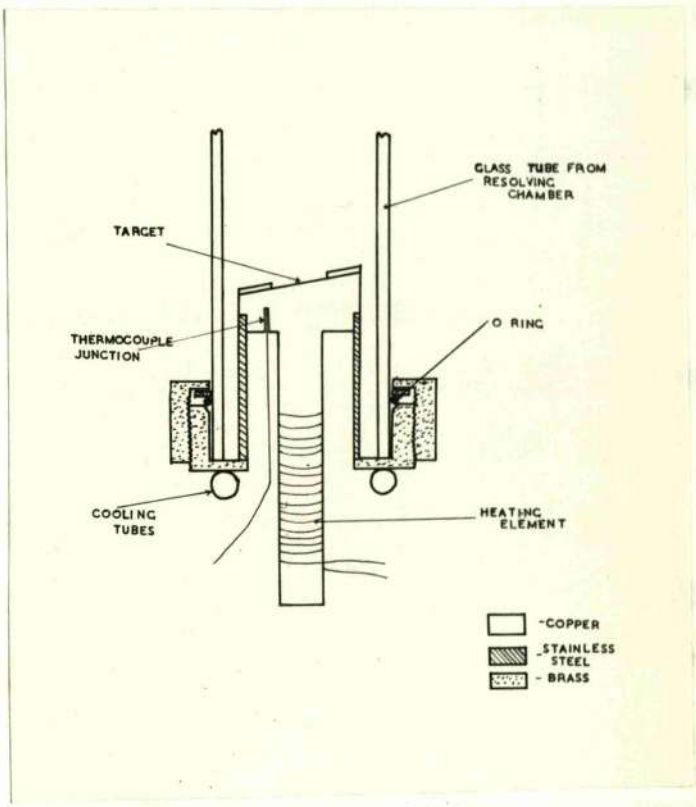

FIG. X - 5.

The heated target.

measuring the γ-ray flux by means of a scintillation counter. In this way it was ascertained that in no case was the target thickness such that it was possible to excite a lower resonance as well as the one intended. The scintillation counter was retained near the target throughout all the exposures so that it was easily possible to determine when the yield dropped and the target required replacement.

The resolved proton beam current was normally about 40μAmp. and exposures were made for times ranging from eleven to thirty hours. The results for γ-rays from the bombardment of ^{27}Al were obtained from one exposure of eleven hours, those for γ-rays from ^{23}Na from four exposures totalling about eighty hours and those for γ-rays from ^{26}Mg from one exposure of twenty hours.

(vi) Processing of the emulsions.

The G5 plates used in the experiment had been stored at a depth of 1400 feet below ground until immediately prior to use and had little cosmic ray background. In exposures of twenty or thirty hours however, even with the shielding used, it is difficult to avoid some background of developed grains. The purpose of the special form of development used for processing these plates was to suppress such a background while maintaining a sufficiently strong development of the proton tracks.

Three /

Three main types of development were tested with variations being tried within each type. The methods tested were (a) the conventional, temperature development using amidol, (Dainton et al. 1951); (b) Van der Grinten development using hydroquinone (see Yagoda 1948); (c) a modification of a method suggested by Bonnet, (1954). The amidol development (a) was used for many of the plates exposed and for 300 μ emulsions the procedure found most effective was as follows:

(1) Plates washed clear of D_2O in running water and temperature lowered to about 7°C - two hours.

(2) Temperature lowered to 4°C, plates in still water in refrigerator - one hour.

(3) Plates allowed to sit in developer consisting of 3 gm. amidol and 6·7 gm. of sodium sulphite in 930 c.c. of water. Temperature 4°C - one hour forty minutes.

(4) Plates on hotplate at 22°C - thirty minutes.

(5) Plates into 1% acetic acid (12° - 8°C) - thirty minutes.

During this time the surface of the emulsion was cleaned by wiping with chamois leather. The subsequent fixing, plasticising and drying of the emulsions followed the conventional techniques. This development gave very consistent results with well defined tracks but a moderate density of background grains.

The Van der Grinten development produced the desired result /

result of good tracks with almost no background grains but was found to be very unreliable, in some cases giving almost no development. Although numerous tests were carried out involving variations of the conditions of development, the source of the instability was not discovered. Faraggi, Bonnet and Cohen (1952), have also found the Van der Grinten developer unreliable and have modified its composition by substituting potassium carbonate for the potassium hydroxide in the original. Bonnet (1954) has further improved this developer by the addition of pyrogallol which appears to increase the speed of penetration of the developer into the emulsion. The formula proposed by Bonnet is as follows:-

Potassium carbonate	50 gm.	- A
Anhydrous sodium sulphite	10 gm.	
Potassium bromide	1 gm.	
Water	to 500 c.c.	
Hydroquinone	0.5 gm.	- B
Pyrogallol	0.6 gm.	
Water	to 500 c.c.	

Equal parts of A and B are used. This developer was used at temperatures of about 30°C by Bonnet for processing C2 emulsions. With a different procedure it was found to give satisfactory results with G5 emulsions under the conditions of the /

the present experiment. For 300μ emulsions the procedure was:

(1) Plates washed in running water at 7°C - two hours.

(2) Plates cooled in water to 1°C - two hours. Developer made up and cooled very rapidly to 1°C.

(3) Parts A and B of the developer mixed and plates placed in developer at 1°C - one hour thirty minutes.

(4) Plates put on hotplate at 25°C - forty five minutes, with the remaining steps as for the amidol development. It was found that this developer deteriorated rapidly particularly at room temperature.

(vii) Measurements and Analysis.

Thickness measurements using a cover glass and a micrometer screw gauge were made as described in section (ii) of this chapter, (a) before impregnation of the emulsion, (b) on removal of the emulsion from the water, and (c) after the processing of the emulsion. The final thickness of the processed emulsion was measured using the microscope depth gauge. From these measurements were obtained:

the shrinkage factor, $s = \frac{\text{dry unprocessed emulsion thickness}}{\text{dry processed emulsion thickness}}$

the overall shrinkage factor, $s' = \frac{\text{swollen emulsion thickness}}{\text{dry processed emulsion thickness.}}$

the swelling factor, $C = \frac{s'}{s}$ $C = \frac{\text{swollen emulsion thickness}}{\text{dry unprocessed emulsion thickness}}$

For /

For emulsions swollen to saturation C is a function of the temperature and acidity of the impregnating liquid. In the present experiments $C \sim 4$ for the emulsions impregnated with heavy water and ~ 5 for emulsions impregnated with ordinary water. The corresponding values of S' were 8·5 and 10·5. The variation of C and S' over the area of the plate was found to be about $\pm$ 4%, some of which variation is probably due to measurement errors.

Plates were fixed to the stage of Watson Bactil microscopes so that the long edge of the plate lay parallel to the x-movement. Thus the x-axis was parallel to the original direction of the protons striking the target in the H.T. set. On each plate an area of about 4·5 cm^2, centred near the level of the target and clear of the edges, was scanned using a x 20 objective and x 7 eyepieces. Single tracks which both started and ended in the emulsion and had a horizontal length greater than a certain minimum were noted and examined under a x 50 oil immersion objective and x 10 eyepieces. On each such track measurements were made of

(a) the horizontal projection of the length, using an eyepiece scale;

(b) the vertical projection of the length, using the microscope depth guage;

(c) the angle between the horizontal projection of the track and the direction of the x-movement.

The /

The measurements (a) and (b), together with the mean overall shrinkage factor s' for the emulsion, were used to obtain the true track length. Tracks having a dip angle of more than 45° in the unprocessed emulsion were discarded.

(viii) Experimental results.

The range distributions for the reactions studied are shown in figure X-6.

For the $^{27}Al(p,\gamma)^{28}Si$ reaction no tracks were measured having a horizontal projection of less than 80 μ and for this reaction the background observed on the plate impregnated with ordinary water was completely negligible. For the reaction $^{26}Mg(p,\gamma)^{27}Al$ no lower limit was imposed on the length of track to be measured and the distribution of tracks on the 'background' plate is shown in figure X-7(a). In figure X-7(b) is shown the distribution obtained from an emulsion impregnated with heavy water but not exposed to γ-rays. The two peaks which appear in (a) and (b), and also in data from emulsions exposed to γ-rays from other reactions when measurements are extended to this energy region, are attributed to the tracks of α-particles from thorium. The observed ranges, (see page xv), correspond precisely to those for the 6·04 MeV. α-particle from thorium A and the 8·78 MeV. α-particle from thorium C' both of which may appear as single tracks. The relative intensities of the two peaks are also in agreement with /

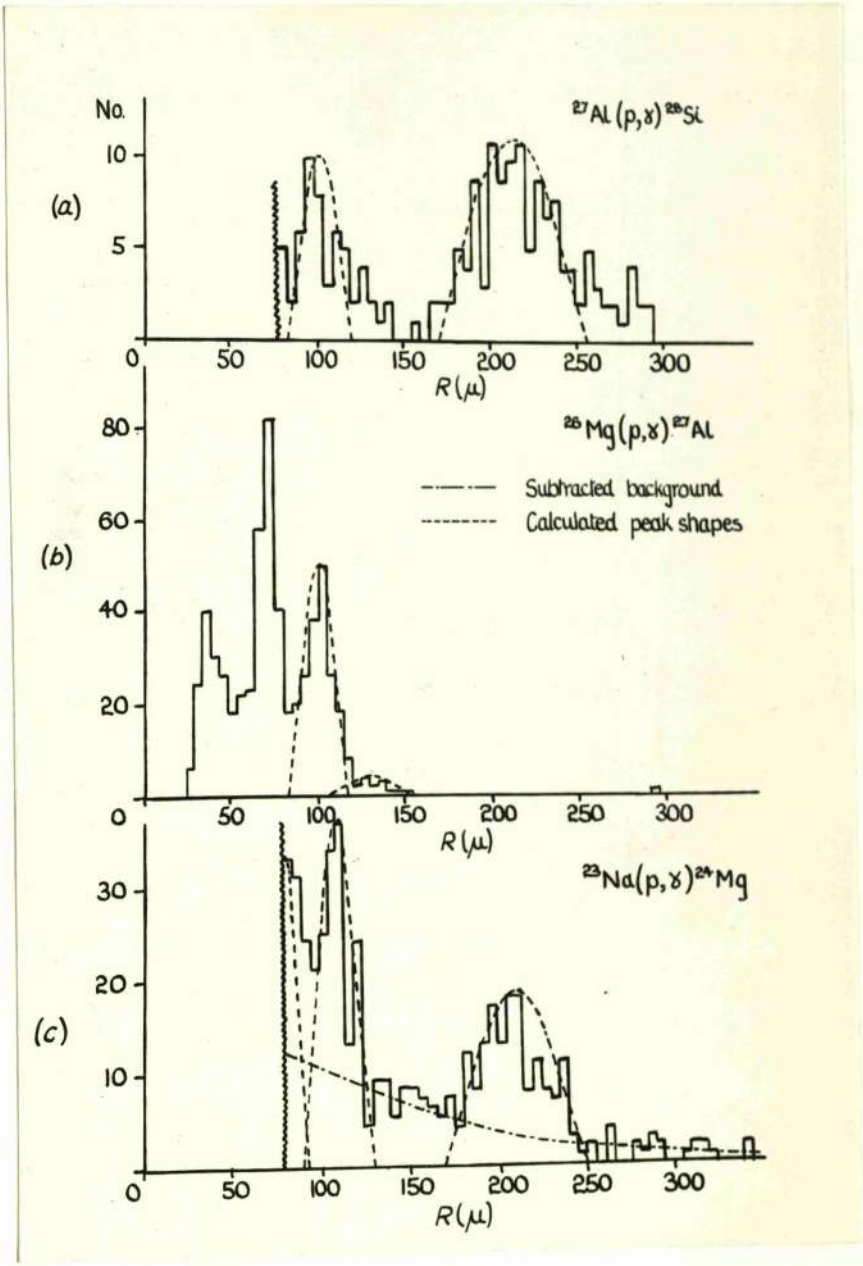

FIG. X - 6.

Range distributions of tracks found in emulsions exposed to γ-rays from the three reactions studied.

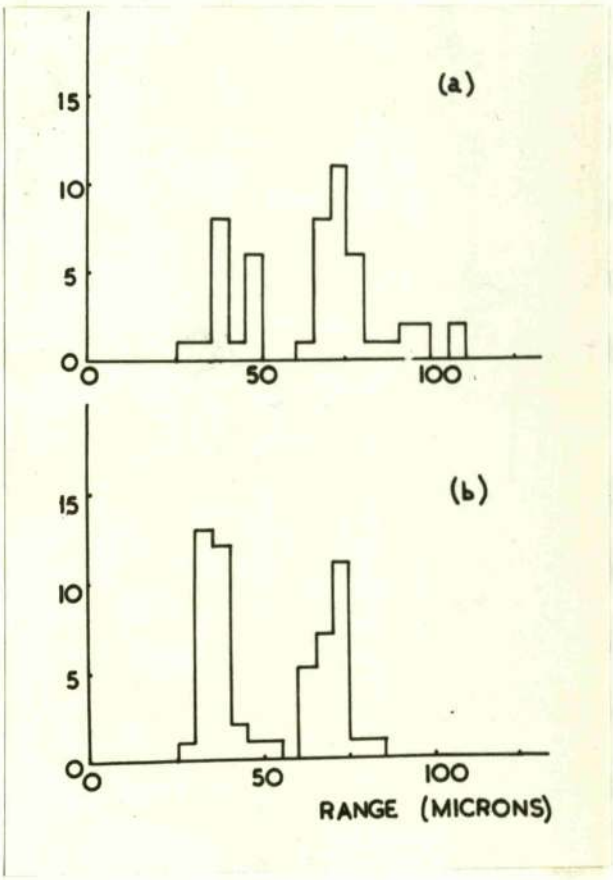

FIG. X - 7.

Range distributions of tracks on: (a) an emulsion impregnated with ordinary water and exposed to γ-rays from the reaction $^{26}Mg(p,\gamma)^{27}Al$, (b) an emulsion impregnated with heavy water and not exposed to γ-rays.

with approximate estimates based on this hypothesis.

The distribution for the reaction $^{23}Na(p,\gamma)^{24}Mg$ is the total of distributions drawn from four exposures. In the first two of these exposures the emulsion impregnated with ordinary water gave evidence of a large background of knock-on protons. The effect of this background is to mask any peaks corresponding to γ -rays of less than 8·8 MeV. Thus in figure X-6(c) the highest energy peak, (10·8 MeV. γ -ray), represents tracks from four exposures whereas the lower energy peaks represent tracks from only the two later exposures free from background and are normalised to the remainder of the spectrum. An additional unexplained spurious background appears to be present in the distribution associated with this reaction.

The energies of the γ -rays to be expected from each reaction were accurately known from scintillation counter measurements. Gibson et al. (1952) have given a range-energy relation for protons in wet emulsions for a limited range of energies and swellings. A range-energy curve close to their's, but extrapolated over a greater range of values, was found to fit all the peaks of energy known from the counter measurements. Details of this range-energy relation are given in appendix B.

The resolution of the peaks in the range distributions is influenced by the following effects:-

(a) /

(a) Observational and microscope errors in track measurement, including the uncertainty in fixing the end points of the track - maximum spread about 15μ .

(b) Changes in the swelling of the emulsion due to temperature variations during the exposure. During the exposure to γ -rays from the bombardment of ^{27}Al the temperature varied by as much as seven centigrade degrees. The improved resolution of the peaks when the temperature was held constant to within one degree, as in the exposure to γ -rays from the bombardment of ^{26}Mg and the later exposures to γ -rays from the $^{23}Na(p,\gamma)^{24}Mg$ reaction, is clear from figure X-6.

(c) The dependence of the energy of the photoproton on the angle it makes with the incident γ -ray. This effect accounts for most of the spread in peaks due to γ -rays with an energy of 7·5 MeV. or greater. The expected shapes of the photoproton peaks calculated taking only this effect into account, are shown by broken lines superimposed upon the distributions in figure X-6.

Angular distributions were obtained for each of the peaks in the range spectra. It is possible that these distributions may be slightly distorted due to certain features of the geometry of the experimental arrangement.

(a) /

(a) The angle measured for each photoproton track was the angle in the plane of the emulsion between the track and the direction of the proton beam in the H.T. set. This is only the true azimuthal angle when the γ-ray is incident at exactly 90° to the plane of the emulsion. Thus the measured angle is, in general less than the true angle. A correction for this effect was applied to the angular distributions for γ-rays from the reaction $^{26}Mg(p,\gamma)^{27}Al$. Instead of using fixed limits of 30° and 60° for the boundaries of the angular intervals employed for counting, these limits were varied with the position of the track on the plate so that the true limits remained constant at 30° and 60°. The required variation was calculated from simple geometrical considerations and the correction resulted in a transference of 7% of tracks originally in the interval 60° - 90° to the interval 30° - 60° and of 6% of tracks in this interval to the 0° - 30° interval, the actual numbers involved being 3 and 4 tracks respectively. The effect of the correction is to steepen the distribution slightly and a similar slight steepening should take place for the other distributions if this correction were applied.

(b) /

(b) The area scanned on each plate was not symmetrical about the x and the y axes, (figure X-8). A maximum limit is imposed on the dip angle and since the polar angular distribution of the photoprotons with respect to the γ-ray is approximately proportional to $\sin^3\theta$ it is likely that the assymetry in the area might lead to a small spurious assymetry in the azimuthal angle distribution. A test of the magnitude of such an effect was made by examining the azimuthal angular distribution of tracks in the symmetrical area A, (figure X-8) and in the whole area. No difference was detected and no correction was applied for this effect.

The relative heights of the peaks in the range distributions have not been corrected either for the effects of imposing a lower limit on the horizontal projection of the track length or for the variation of the photodisintegration cross section with energy, since it was not an object of the experiment to examine the intensities of the γ-rays.

The angular distributions of the photoproton tracks from each of the peaks are shown in table XI-1 and also in figures XI - 1, 2, 3. The distribution of the continuous background, as assessed from regions between the peaks, has been subtracted in the distribution shown for the $^{23}Na(p,\gamma)^{24}Mg$ reaction.

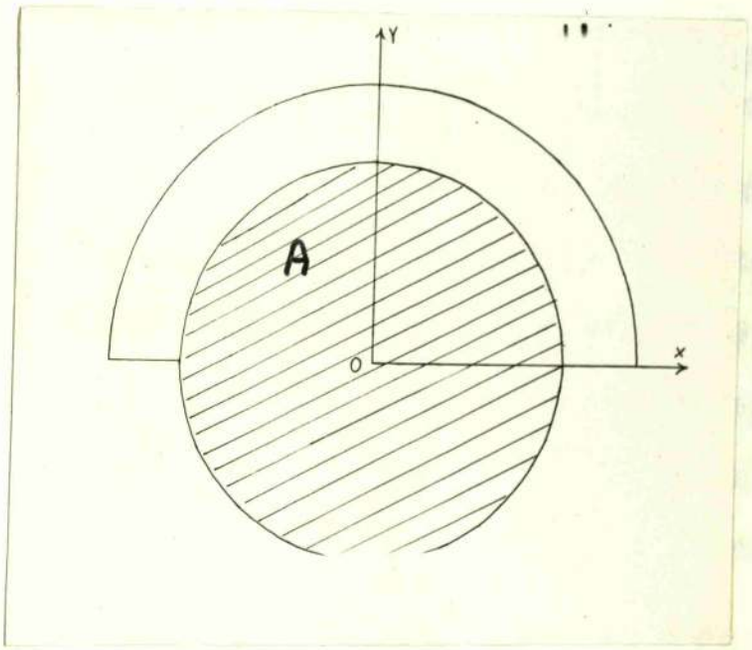

FIG. X - 8.

Shape of area scanned.

CHAPTER XI

DISCUSSION OF THE RESULTS OF THE PRESENT EXPERIMENT.

(i) Assignments of parity to the ground states of ^{23}Na and ^{27}Al and to the first excited state of ^{27}Al.

It has been shown in chapter IX that, for dipole radiation emitted in a (p,γ) reaction and having a polar angular distribution

$$1 + a_2 \cos^2\theta$$

with respect to the incident proton beam, then the ratio of the intensity of radiation plane polarised in the plane of incident proton and emitted γ-ray to that plane polarised at right angles to this plane is

$$R = \frac{1 + a_2 \cos 2\theta}{1 + a_2} = \frac{1 - a_2}{1 + a_2} \text{ for } \theta = \pi/2,$$

for electric dipole, and the inverse quantity for magnetic dipole radiation. Thus if the polar angular distribution of the radiation is known the polarisation distribution may be predicted as having one of two complementary forms.

The azimuthal angular distribution of the photoprotons ejected from deuterium by a γ-ray of polarisation described by the ratio R is given by

$$1 + (R - 1)\cos^2\varphi$$

In the present experiment a finite spread in the angle θ (70° /

TABLE XI - 1.

Measured and calculated azimutal angular distributions of photoprotons ejected from deuterium by γ-rays from the reactions $^{27}Al(p,\gamma)^{28}Si$, $^{26}Mg(p,\gamma)^{27}Al$ and $^{23}Na(p,\gamma)^{24}Mg$. The errors shown are standard deviations.

Reaction	γ-Ray Energy (Mev.)	Measured angular distribution			Calculated angular distribution assuming electric radiation.			Calculated angular distribution assuming magnetic radiation			Assignment
		0-30°	30°-60°	60°-90°	0-30°	30°-60°	60°-90°	0-30°	30°-60°	60°-90°	
$^{27}Al(p,\gamma)^{28}Si$	10·4	49±7	35±6	26±5	51·8	36·7	21·4	21·4	36·7	51·8	Electric
"	7·5	18±4	21±5	16±4	14·8	18·2	22	22	18·2	14·8	Undetermined
$^{26}Mg(p,\gamma)^{27}Al$	8·6	5±2	5±2	4±2	5	4·7	4·3	4·3	4·7	5	"
"	7·6	88±9	64±8	38±6	94	63	32	31	62	92	Electric
$^{23}Na(p,\gamma)^{24}Mg$	10·8	70±11	36±9	20±6	50	42	34	34	42	50	Electric
"	8·1	19±7	20±5	21±5	23	20	17	17	20	23	Undetermined
"	7·2	12±5	10±4	11±4	12	11	10	10	11	12	"

$(70^\circ - 90^\circ - 121^\circ)$ was used and the value taken for R was

$$\bar{R} = \frac{\int_{\theta_1}^{90^\circ}(1+a_2\cos 2\theta) + \int_{90}^{\theta_2}(1+a_2\cos 2\theta)}{(1+a_2)(\theta_2-\theta_1)}$$

Since all values of θ are not equally probable $\bar{R}$ is strictly a more complicated function depending on the geometrical conditions. The error introduced by using the expression given has been estimated in particular cases and found to be negligible. The number of photoprotons emitted into an angular interval $\varphi_1 - \varphi'$ is

$$N_{\varphi-\varphi'} = \int_{\varphi}^{\varphi'} [1-(\bar{R}-1)\cos^2\varphi]\, d\varphi$$
$$= \tfrac{1}{2}(\varphi'-\varphi)(1+\bar{R}) + \tfrac{1}{4}(\bar{R}-1)\sin 2(\varphi'-\varphi)$$

Using this result the azimuthal angular distributions of the photoprotons were calculated from the polar angular distributions of the corresponding γ-rays measured by Rutherglen et al. (1954) for the reaction $^{27}Al(p,\gamma)^{28}Si$, Grant et al. (1955) for the reaction $^{23}Na(p,\gamma)^{24}Mg$ and Rutherglen, Deuchars and Wallace (private communication) for the reaction $^{26}Mg(p,\gamma)^{27}Al$. These calculated values are shown in table XI-1 for the alternatives of electric and magnetic radiation, together with the measured distributions. The measured distributions can be accounted for by these calculations in all cases except for the 10.8 MeV. γ-ray from the /

the reaction $^{23}Na(p,\gamma)^{24}Mg$, and, where an assignment of the nature of the radiation has been possible, the distributions are shown graphically in figures XI - 1, 2, 3.

For all three of the reactions the γ-rays which have been studied are anisotropic. Since the proton resonance energy is in no case sufficiently high to make it likely that d-wave particles are responsible for the reaction, we assume that all the reactions are due to p-wave protons. The polar angular distributions of Rutherglen et al. (1954), Grant et al. (1955) and Rutherglen, Deuchars and Wallace (private communication), indicate a dipole transition, and the present measurements electric rather than magnetic radiation, in each case. Thus each reaction involves a double change of parity and therefore the parities of the ground state of the initial nucleus and of the final excited state of the product nucleus will be the same.

We now consider each of the reactions in detail:

(a) $^{27}Al(p,\gamma)^{28}Si$; 652 KeV. resonance: The 10·5 MeV. γ-ray from the reaction arises from a dipole transition between the 12·23 MeV. and 1·8 MeV. levels in ^{28}Si (Rutherglen et al. 1954), figure XI-4. At the 404 KeV. resonance for this reaction Rutherglen et al. have shown that there is no d-particle emission to the ground state of ^{24}Mg which has spin zero with even parity. Since anisotropic γ-rays are emitted at /

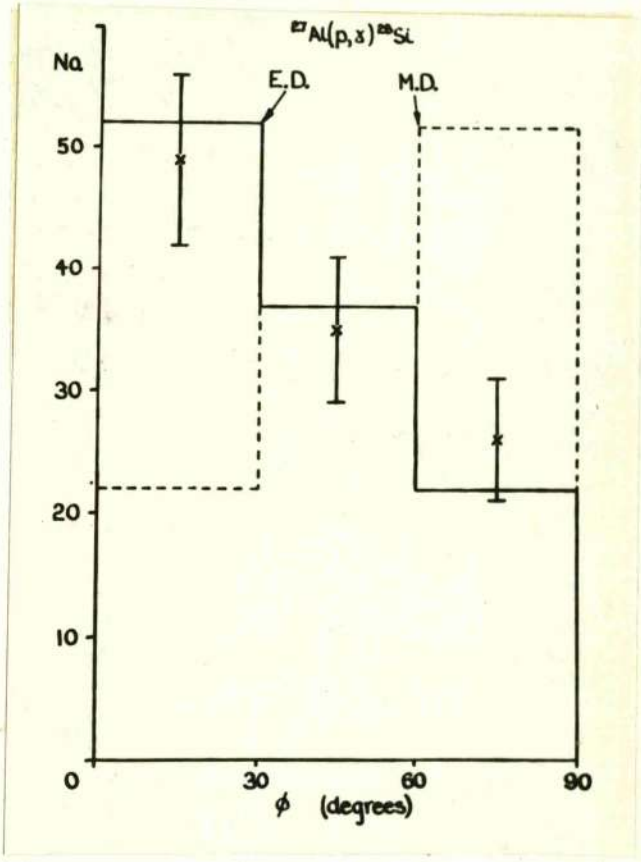

FIG. XI - 1.

Azimuthal angular distribution of photoprotons ejected by the 10·4 Mev γ -ray from the reaction $^{27}Al(p,\gamma)^{28}Si$. The errors indicated in this and the following figures are standard deviations. The continuous and broken lines represent the calculated distributions assuming electric dipole and magnetic dipole radiations respectively.

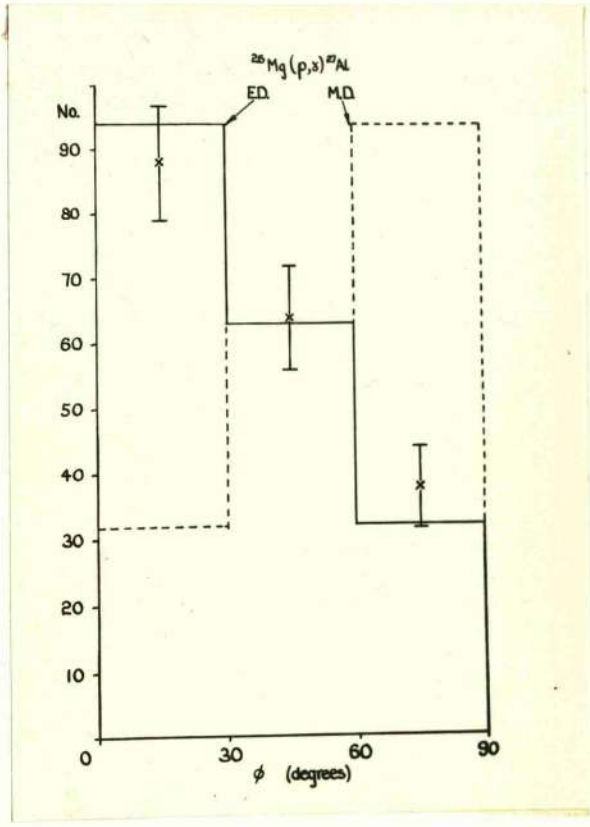

FIG. XI - 2.

Azimuthal angular distribution of photoprotons ejected by the 7.6 Mev γ -ray from the reaction $^{26}Mg(p,\gamma)^{27}Al$.

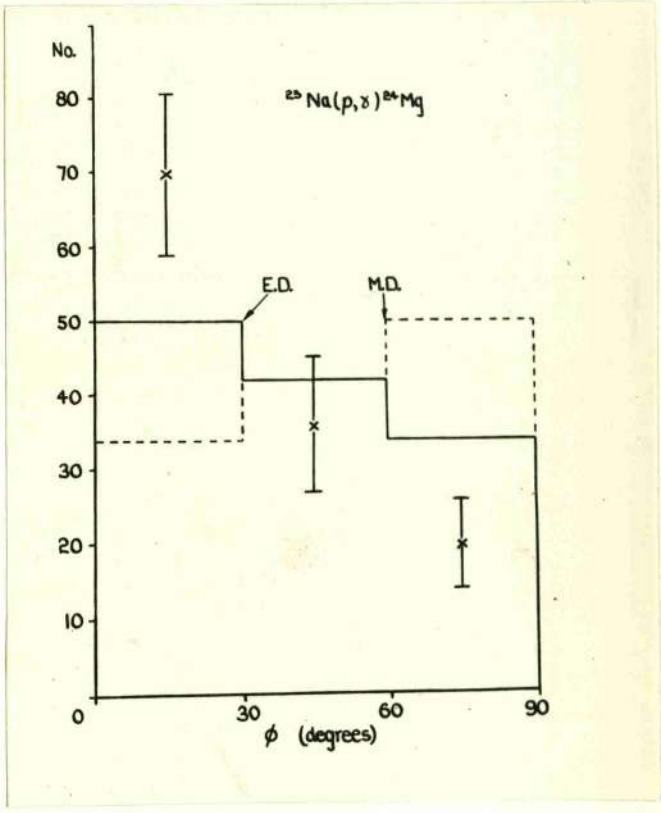

FIG. XI - 3.

Azimuthal angular distribution of photoprotons ejected by the 10·8 Mev γ -ray from the reaction $^{23}Na\,(p,\gamma)\,^{24}Mg$.

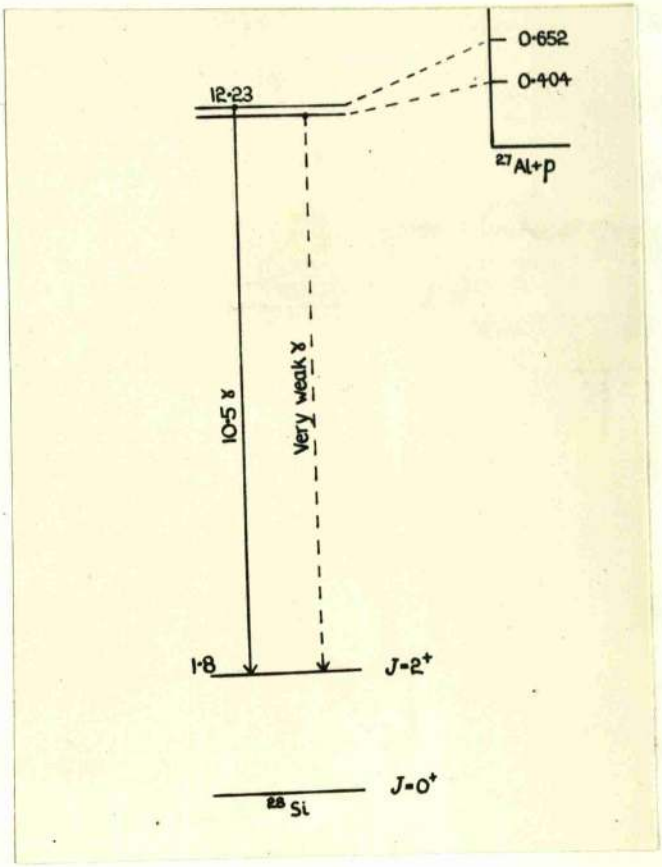

FIG. XI - 4.

Level diagram for the reaction $^{27}Al(p,\gamma)^{28}Si$.

at this resonance it must, therefore, have spin and parity 2(-), 4(-) or 1(+), 3(+) according as the ground state parity of ^{27}Al is even or odd. No γ-ray transition to the ground state of ^{28}Si is observed and so $J = 4(-)$ or $3(+)$ is assigned to the excited state formed at this resonance. Since only a very weak transition is observed to the 1·8 MeV. excited level in ^{28}Si this level is unlikely to have J greater than 2 with even parity. $J = 1$ is improbable since in the β-decay of ^{28}Al the transition to the ground state of ^{28}Si is found to be highly forbidden compared with the less energetic transition to the 1·8 MeV. level indicating $J \geqslant 2$ for this level. In addition no low-lying dipole level has been observed in an even-even nucleus and such a dipole level is also believed to be unlikely on theoretical grounds (Touschek 1950). An assignment of $J = 2$ (+) to the 1·8 MeV. level is consistent with all the data on γ-ray intensities.

Since the present measurements indicate an electric rather than a magnetic transition we assign odd parity to the 12·23 MeV. level in ^{28}Si and, assuming p-wave protons, we thus have even parity for the ground state of ^{27}Al. This assignment is in agreement with the prediction of the shell model for Z = 13 as discussed in chapter IX.

(b) /

(b) $^{26}Mg(p,\gamma)^{27}Al$; 339 KeV. resonance: Since ^{26}Mg is an even-even nucleus, we may assume that it has even parity in its ground state. The 7·6 MeV. γ-ray results principally from a dipole transition between the 8·5 MeV. level and the 0·84 MeV. level, the first excited state, in ^{27}Al (Rutherglen et al. private communication). Thus by the arguments presented above we assign even parity to the 0·84 MeV. level in ^{27}Al. This result is in agreement with the indications from other sources (Daniel et al. 1953).

(c) $^{23}Na(p,\gamma)^{24}Mg$; 593 KeV. resonance: The 10·8 MeV. γ-ray in this reaction arises from a dipole transition between the 12·27 MeV. and the 1·38 MeV. levels in ^{24}Mg, (Grant et al. 1955), and the 1·38 MeV. level is known to have spin and parity 2(+) (cf. Endt and Kluyver 1954). We may therefore assign even parity to the ground state of ^{23}Na. This assignment is again in agreement with the predictions of the shell model.

It has not been found possible to explain the discrepancy between the measured angular distribution for the photoprotons produced by the 10·8 MeV. γ-ray from the bombardment of ^{23}Na and the distribution as calculated from the polar angular distribution of the γ-ray. The discrepancy may arise, in part, from the very low γ-ray yield in this reaction and the consequent increase in the importance of background effects./

effects.

(ii) Further applications of the method of polarisation measurement.

An attempt was made to measure the polarisation of the 20 MeV. γ -ray from the reaction $^3H(p,\gamma)^4He$ which has a polar angular distribution $1 + 10 \sin^2\theta$ and may thus be expected to be very nearly plane polarised. A target of tritium in zirconium was exposed to the resolved proton beam in the H.T. set for about twenty hours with beam currents $\sim 50\mu A$. Emulsions exposed dry, impregnated with ordinary and with heavy water, all showed a high density of proton tracks. An analysis was made of tracks on the emulsion exposed dry assuming that the tracks were due to protons knocked-on by neutrons coming from the target and accepting only tracks the direction of which was ascertainable and which made an angle of more than 50° with the incident neutrons, (that is, having comparatively small dips in the emulsion). The neutron spectrum obtained in this way is shown in figure XI-5. The probable errors in this distribution are large, (about $\pm$ 2 MeV. at the higher energies), since the experiment was not designed to measure neutron energies, but the distribution seems to be mainly accounted for if one postulates the reactions $^3H(\alpha,n)^4He$ giving neutrons of about 14 MeV. and $^3H(T,2n)^4He$ giving neutrons of about 5·6 MeV. An approximate calculation shows that if 2% of the deuterium present /

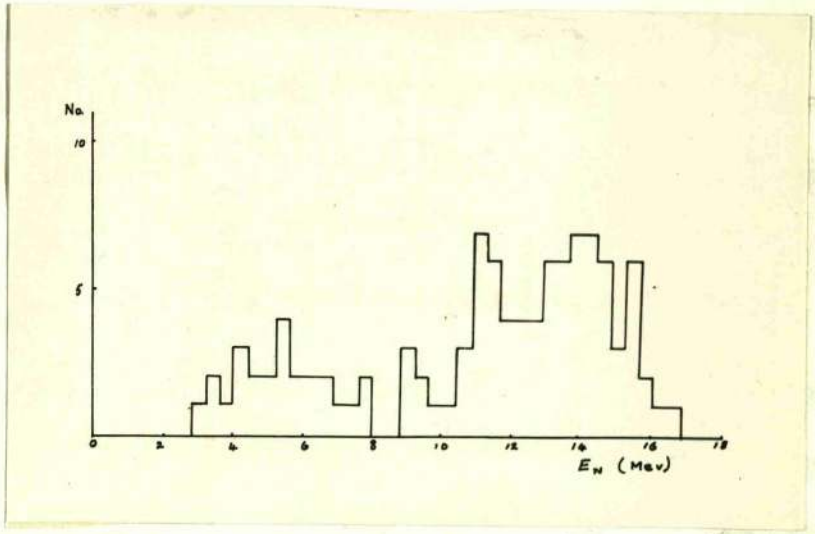

FIG. XI - 5.

Energy distribution of neutrons as deduced from plates exposed in an attempt to measure the polarisation of the γ -rays from the reaction $^3H(p,\gamma)^4He$.

present in the natural hydrogen of the ion source passes round the resolving magnet and strikes the target all the 14 MeV. neutrons can be accounted for. Recoiling tritons can give rise to the $^{3}H(T,2n)^{4}He$ reaction.

The considerable background of knock-on tracks due to 14 MeV. neutrons made it impossible to distinguish the photo-disintegration protons without a prohibitive amount of labour. It is however intended to attempt to eliminate the deuterons in the beam by a thin coating of aluminium absorber on the tritium target. This technique will only be possible when rather higher accelerating energies are achieved with the H.T. set.

It is believed that a source of plane polarised γ - radiation of moderately high energy ($\gtrsim$ 15 MeV.) would be of considerable use in studying the photodisintegration of nuclei especially in so far as direct processes may be concerned and it was to this purpose that the measurements on the γ-rays from the $^{3}H(p,\gamma)He^{4}$ reaction were attempted. Also for this purpose and for studies of meson production it would seem desirable to obtain a polarised beam of bremsstrahlung of high energy. A preliminary study of this problem reveals very considerable difficulties in obtaining a polarised beam of even moderate intensity for high energies.

APPENDIX 1.

THE ANNIHILATION OF POSITRONS AT 10 Mev.

In the course of the experiment on the single scattering of positrons and electrons a number of examples were observed of tracks which appeared to stop abruptly in the emulsion. Such an apparent disappearance may be due to a very steep deflection of the track, to an insensitive region in the emulsion, or to a true annihilation. A particularly careful search through the depth of the emulsion and throughout the area surrounding each event of this kind, was made independently by the author and by Dr. H. Muirhead. In this way all but four of the apparent electron annihilations were identified as steep scatters or gaps in the track. Two of the remaining events were in areas of a plate where the density of tracks and background grains was high and it seems possible that a scattered track could have been missed. Eighteen positron annihilations remained after careful examination, all on plates having a low density of tracks and background grains.

Dirac, (1930), has given expressions for the annihilation cross sections for one- and two-quantum annihilation. Dirac's formula predicts 21 two-quantum and one single-quantum annihilations for the conditions of the present /

present experiment. Allowing for two spurious events among the positron annihilations the number of events found is 16.

APPENDIX 2.

IDENTIFICATION OF EVENTS OF THE TYPE

$$P + P \longrightarrow \pi^{+} + p + n$$

The measured grain densities of the primary track and of the tracks of the secondary proton and the meson may be written

$$G_0 \pm \Delta G_0,\ G_p \pm \Delta G_p,\ G_\pi \pm \Delta G_\pi$$

where ΔG_0, ΔG_p and ΔG_π are the standard deviations of the grain densities G_0, G_p, and G_π. Since the energy of the primary particle is known it was convenient to express the grain densities of the secondary tracks in terms of that of the primary. Thus we obtain

$$\frac{G_p - \Delta G_p}{G_0 + \Delta G_0} = G_{p1}, \qquad \frac{G_p}{G_0} = G_{p2}, \qquad \frac{G_p + \Delta G_p}{G_0 - \Delta G_0} = G_{p3}$$

and three similar quantities for the π meson. These quantities may be written in terms of the momenta of the particles

$$P_1, P_2, P_3 \quad \text{and} \quad p_1, p_2, p_3,$$

where capitals represent the momentum of the proton and the small letters that of the meson. The correctness of the calculated calibration of grain density and momentum used was checked by means of evaluating the energies of secondary tracks in elastic proton-proton collisions from the angle of

scattering/

scattering, and comparing this value with that derived from measurements of grain density.

In the early stages of the work the balance of momentum was made in two orthogonal planes in the laboratory frame of reference. For the majority of the events examined, however, the balance was made in the centre of momentum system and this second technique is described. The centre of momentum method, although less direct, derives the quantities of interest in the centre of momentum system as a by-product of the acceptance calculation whereas in the earlier method these quantities had to be calculated separately for acceptable events.

Using the values of P and p obtained as described above and the measured angles α_p and α_π between the primary and the secondary proton and π meson we may obtain the momenta and angles of the secondary particles in the centre of momentum system, (c - system). Thus we have the quantities

$$\left.\begin{array}{ll} P_1^*, P_2^*, P_3^* & P_1^*, P_2^*, P_3^* \\ \alpha_{p1}^*, \alpha_{p2}^*, \alpha_{p3}^* & \alpha_{\pi 1}^*, \alpha_{\pi 2}^*, \alpha_{\pi 3}^* \end{array}\right\} \quad (1)$$

These transformations to the c - system and the subsequent transformations back to the laboratory frame were made by means of a number of specially constructed nomograms which gave the solutions /

solutions P and p of the equations

$$W^* = \frac{W_L - \beta_c P \cos\alpha}{(1-\beta_c^2)^{1/2}} \qquad p^* = (W^{*2} - M^2)^{1/2}$$

$$\sin\alpha^* = \frac{P}{p^*}\sin\alpha$$

where the starred quantities refer to the c - system, W is the total energy of the particle and M its mass, while β_c is the velocity of the c - system with respect to the laboratory frame.

Using the quantities (1) above we may obtain the momentum of the neutron and its angle with the primary direction in the c - system by means of a triangle of momenta. In the most general case nine different combinations of the proton and meson quantities are possible, leading to nine corresponding momenta and angles for the neutron. Possible simplifications of the general case are described later. The triangle of momenta calculation was made using a simple mechanical device and the several angular calculations required were made by means of the Sigsbee diagram.

The c - system neutron quantities obtained by balancing momenta were used to obtain the corresponding neutron kinetic energies $E'_{N1} \cdots\cdots E'_{N9}$ in the laboratory frame.

A second set of neutron energies in the laboratory frame is derived from the principle of conservation of energy. If E is the energy available in the laboratory frame, (E = energy of the /

the primary proton minus the rest mass of the meson), then $E - E_P - E_\pi = E_N$ where E_P and E_π are the kinetic energies of the proton and the meson corresponding to the momenta P_P and P_π. In this way a set of neutron energies $E_{N1} \ldots\ldots E_{N9}$ is obtained.

We now consider a three dimensional co-ordinate system having axes E_P, E_π, and E_N, (figure 2 - 1). The points corresponding to $E_{N1} \ldots\ldots E_{N9}$ lie on three parallel coplanar lines ABC, DOE and FGH each of which corresponds to a constant value of E_π with varying E_P. Thus the point O corresponds to the measured values of E_P and E_π while the other points correspond to combinations of measured values and measured values plus or minus the errors. The points corresponding to energies $E'_{N1} \ldots\ldots E'_{N9}$ obtained by balancing momenta, lie on a surface on which the three curves RST, UVW, and XYZ correspond to the three parallel lines obtained by balancing energy. If the curves and straight lines intersect at L, M and N respectively, (figure 2 - 1), then the line L M N represents the intersection of the plane defined by the conservation of energy and the surface defined by the conservation of momentum. Thus points on L M N give energies for the particles for which energy and momentum are conserved with the angles of the particles as measured.

In figure (2 - 2), have been drawn curves joining points for /

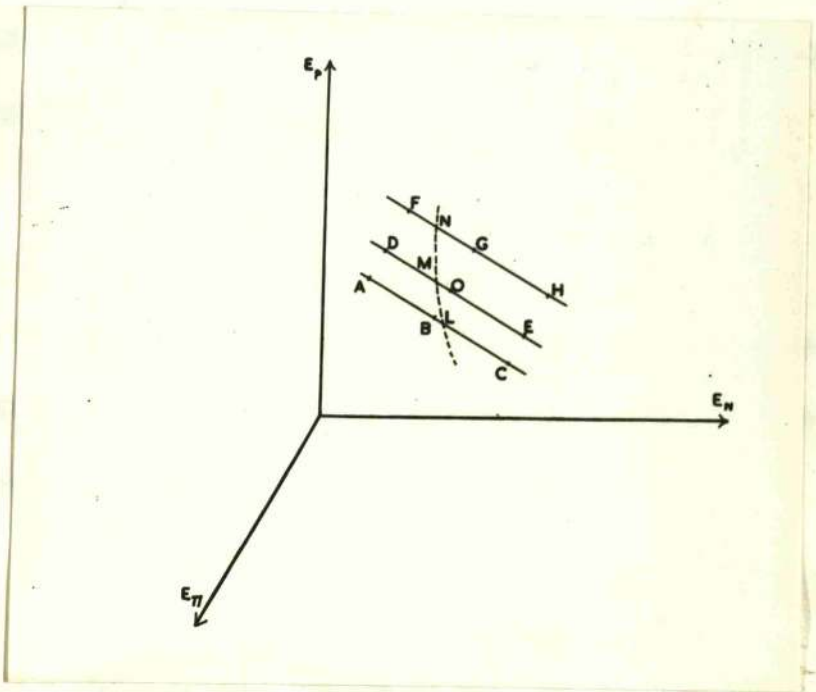

FIG. 2 - 1.

Illustration of momentum and energy balancing techniques.

for which the probability that the measured values of the energies of the particles have a given error is constant, the probability decreasing as we move outwards from O. It is clear that, unless the line of intersection L M N is highly curved compared with a contour of probability, L M N will always cross its contour of maximum probability on one or other of the axes DOE or BOG. This assumption is found to be completely justified in practice. Suppose now that L M N cuts the axis D O E at a point of higher probability than the point at which it cuts the axis B O G. Then the ratio $^{OM}/_{OD}$, (figure 2 - 2), is a measure of the maximum probability that the event in question can balance energy and momentum. Movement along the axis D O E represents variation of the proton energy keeping that of the meson fixed. Thus we may write

$$\frac{OM}{OD} = \frac{|E_{p2} - E_p|}{|E_{p2} - E_{p3}|}$$

where E_p is the energy of the proton corresponding to the balance point M. Instead of using this ratio as a criterion of acceptance we in fact use the ratio

$$R = \frac{|G_{p2} - G|}{|G_{p2} - G_{p3}|}$$

R is the ratio of the difference between the measured grain density of the proton and the grain density which the proton must have /

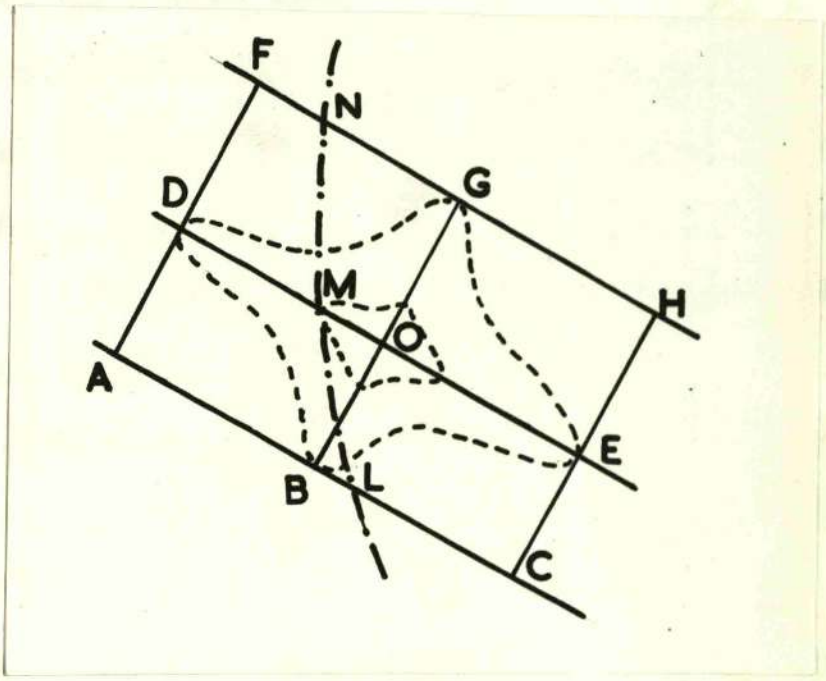

FIG. 2 - 2.

Probability contours and line of intersection LMN of the momentum and energy balance surfaces.

have in order to balance energy and momentum, and the 'maximum error' in the grain density of the proton. For the present calculation the maximum error is always close to 1·5 times the standard deviation. Thus the distribution of R for true events should be of the form

$$W(R) \propto e^{-1.12 R^2}$$

An exactly similar treatment applies if the line of intersection L M N cuts the π meson variation axis at a point of higher probability than that for the proton.

In practice several modifications were made to the analysis as described above:

(a) In no case were nine points calculated for the neutron energy. With seven points it was possible to draw two of the lines on each of the surfaces through three points each, and to estimate the form of the third line from the first two and the seventh point.

(b) In many cases the maximum error in the momentum of either the proton or the meson is small compared with the error in the momentum of the other particle. In such a situation the three lines fall very close together and may be satisfactorily replaced by a single line. Thus only the central value of the momentum of the particle having the smaller /

smaller error is taken and combined with the three possible values for the other particle and only three points are plotted instead of nine.

(c) In order to avoid the practical complications of plotting points in a three dimensional co-ordinate system the graphical work was always performed using a projection of the lines on either the $E_p - E_N$ or the $E_\pi - E_N$ plane. Since the result obtained is in the form of a ratio no alteration in the magnitude of the result is caused by using this projection.

APPENDIX 3.

RANGE-ENERGY RELATION FOR PROTONS IN AN EMULSION IMPREGNATED WITH HEAVY WATER.

Several authors have reported measurements and calculations bearing on the range-energy relation for protons in nuclear emulsions containing different amounts of ordinary and heavy water. These results do not show complete agreement. The present experiment involved the measurement of the ranges of photoprotons ejected from deuterium, in an emulsion impregnated with heavy water, by γ-rays of accurately known energy.

Measurements were made of the range of photoprotons ejected from deuterium by γ-rays of 10·8 Mev, 8·09 Mev, and 7·01 Mev from the reaction $^{23}Na(p,\gamma)^{24}Mg$ and of 7·6 Mev from the reaction $^{26}Mg(p,\gamma)^{27}Al$. The protons ejected at 90° to the incident γ-ray, therefore have energies of 4·3 Mev, 2·93 Mev, 2·39 Mev and 2·7 Mev. The γ-ray energies are based on scintillation counter measurements, (Flack, Rutherglen and Grant, 1954; Rutherglen, Deuchars and Wallace, private communication), and are thought to be accurate to within 1%. The ranges corresponding to the centre of peaks in the range energy spectrum have a probable error $\sim \pm$ 2 or 3μ.

The amount of water in the emulsion is specified by the 'swelling /

'swelling factor' C, where C is the ratio of the thickness of the swollen emulsion to the thickness of the original dry emulsion. It is assumed that the volume of water and emulsion add without any overall change in density. C was determined by a series of measurements made at specified points on the emulsion using a cover plate and a micrometer screw gauge. The values obtained for C have a probable error ~ ± 4%.

The results are presented in Table 3 - 1 in which the calculated values of Gibson et al., (1952), and of Krohn and Schrader, (1952), are shown for comparison. Those obtained from the present work have been

TABLE 3 - 1.

Energy (Mev)	RANGE IN MICRONS								
	C = 2·8			C = 3·3			C = 3·8		
	Present work	Gibson et al.	Krohn and Schrader	Present work	Gibson et al.	Krohn and Schrader	Present work	Gibson et al.	Krohn and Schrader
2.0	60	57·5	54	60	58	56	64	59	57
3·0	115	112	105	116	115	109	125	117	112
4·0	185	-	172	190	-	179	197	-	185
5·0	263	-	254	269	-	265	284	-	277

extrapolated /

extrapolated from 4·3 Mev to 5 Mev and from 2·39 Mev to 2 Mev for convenience of presentation.

Gibson et al. (1952) have also measured the range of 2·0 Mev and 2·4 Mev protons in an emulsion having C = 3·94 and find close agreement with their own calculated curve. Hough, (1950), has measured the range of 2·0 Mev and 2·4 Mev protons in an emulsion having C = 3·85 and obtains values in precise agreement with the present work. Goldhaber, (1951), has measured the range of protons of the same energies with a swelling factor C = 1·7 and obtains values in rough agreement with an extrapolation of the present work although a detailed comparison is not possible since the present measurements only extend down to C = 2·8. Waffler and Younis, (1949) have measured ranges at a number of proton energies, but obtain values considerably larger than those of other workers.

REFERENCES.

The references are divided into four sections according to the part of the thesis with which they are concerned.

A. Single Scattering of Electrons and Positrons.

Acheson, K. L., 1951, Phys. Rev., 82, 488.

Barber, A., and Champion, F. C., 1938, Proc. Roy. Soc., A168, 159.

Bartlett, J. E., and Watson, R. E., 1939, Proc. Am. Acad. Arts and Sciences, 74, 53.

Bartlett, J. E., and Welton, T. A., 1941, Phys. Rev., 59, 281.

Bayard, R. T., and Yntema, J. L., 1954, Phys. Rev., 93, 1412.

Curr, R. M., 1955, Proc. Phys. Soc. A66, 156.

Dainton, A. D., Gattiker, A. R., and Lock, W. O., 1951, Phil. Mag. 42, 396.

Dirac, P. A. M., 1928, Proc. Roy. Soc., A117, 610.
1930, Proc. Camb. Phil. Soc., 26, 361.

Elton, L. R. B., 1950, Proc. Phys. Soc., A63, 1115.

Elton, L. R. B., and Parker, K., 1953, Proc. Phys. Soc. A66, 428.

Feshbach, H., 1951, Phys. Rev., 84, 1206.
1952, Phys. Rev., 88, 295.

Fowler, W. A., and Oppenheimer, J., 1938, Phys. Rev., 54, 320.

Hofstadter, R., Fechter, H. R., and McIntyre, J. A., 1953, Phys. Rev., 92, 978.

Hofstadter, R., Hahn, B., Knudsen, A. W., and McIntyre, J. A., 1954, Phys. Rev., 95, 512.

Howatson, A. F., and Atkinson, J. R., 1951, Phil. Mag., 42, 1136.

Lipkin,/

Lipkin, H. J., 1952, Phys. Rev., 85, 517.

Lyman, E. M., Hanson, A. O., and Scott, N. B., 1951, Phys. Rev., 84, 626.

Massey, H. S. W., 1942, Proc. Roy. Soc. A181, 14.

McKinley, W. A., and Feshbach, H., 1948, Phys. Rev., 74, 1759.

Mohr, C. B. O., and Tassie, L. J., 1954, Proc. Phys. Soc., A67, 711.

Mott, N. F., 1929, Proc. Roy. Soc., A124, 425.
1932, Proc. Roy. Soc., A135, 429.

Parzen, G., and Wainwright, T., 1954, Phys. Rev. 96, 188.

Pidd, R. W., Hammer, C. L., and Raka, E. C., 1953, Phys. Rev., 92, 436.

Rose, M. E., 1949, Phys. Rev. 73, 279.

Schiff, L. I., 1953, Phys. Rev., 92, 988.

Schwinger, J., 1949, Phys. Rev., 75, 898.

Skobelzyn, D., and Stepanowa, E., 1936, Nature, 137, 456.

Smith, J. H., 1954, Phys. Rev., 95, 271.

Van de Graaf, R. J., Buechner, W. W., and Feshbach, H., 1946, Phys. Rev., 69, 452.

Vigneron, L., 1949, J. Phys. et Rad., 10, 305.

Wentzel, G., 1922, Ann. der Phys., 69, 335.

Yadav, H. N., 1952, Proc. Phys. Soc., A65, 673.

Yennie, D. R., Ravenhall, D. G., Wilson, R. N., 1954, Phys. Rev., 95, 500.

B./

B. Multiple Scattering of Electrons and Positrons.

Babha, H. J., 1936, Proc. Roy. Soc., A154, 195.

Bethe, H. A., 1953, Phys. Rev., 89, 1256.

Bethe, H. A., and Heitler, W., 1934, Proc. Roy. Soc., 146, 83.

Bosley, W., and Muirhead, H., 1952, Phil. Mag., 43, 63.

Corson, D. R., 1951, Phys. Rev., 84, 605.

Cusack, N., and Stott, P., 1955, Phil. Mag., 46, 632.

Davies, H., and Bethe, H. A., 1952, Phys. Rev., 87, 156.

Fano, U., 1954, Phys. Rev., 93, 117.

Fisher, P. C., 1953, Phys. Rev., 92, 420.

Fowler, P. H., 1950, Phil. Mag., 41, 169.

Gottstein, K., Menon, M. G. K., Mulvey, J. H., O'Ceallaigh, C., Rochat, O., 1951, Phil. Mag., 42, 708.

Goudsmit, S., and Saunderson, J. L., 1940, Phys. Rev., 57, 552.

Groetzinger, G., Humphrey, W., and Ribe, F. L., 1952, Phys. Rev., 85, 78.

Hisdal, E., 1952, Phil. Mag., 43, 790.

Heymann, F. F., and Williams, W. F., 1956, Phil. Mag., 1, 212.

MacDiarmid, I. B., 1951, Phys. Rev., 84, 851.

Maximon, L. C., and Bethe, H. A., 1952, Phys. Rev., 87, 156.

Mohr, C. B. O., and Tassie, L. J., 1954, Aust. J. Phys., 7, 217.

Molière, G., 1947, Z. f. Naturforschung, 2A, 133.
1948, Z. f. Naturforschung, 3A, 78.

Møller, C., 1931, Z. f. Phys., 70, 786.
1932, Ann. der Phys., 14, 568.

Rohrlich, /

Rohrlich, F., and Carlson, B. C., 1954, Phys. Rev., 93, 38.

Rossi, B., and Griesen, K., 1941, Rev. Mod. Phys., 13, 262.

Snyder, H. S., and Scott, W. T., 1949, Phys. Rev., 76, 220.

Voyvodic, L., and Pickup, E., 1952, Phys. Rev., 85, 91.

Williams, E. J., 1939, Proc. Phys. Soc., A169, 531.

C. Proton-Proton Scattering.

Aitken, A., Mahmoud, H., Henley, E. M., Ruderman, M. A., Watson, K. M., 1954, Phys. Rev., 93, 1349.

Bogachev, N. P., and Vzorov, I. K., 1954, Doklady Acad. Nauk., S.S.S.R., 99, 931.

Case, K. M., and Pais, A., 1950, Phys. Rev., 80, 203.

Cester, R., Hoang, T. F., Kernan, A., 1955, Phys. Rev., 100, 940.

Chamberlain, O., Donaldson, R., Segré, E., Tripp, R., Wiegand, C., Ypsilantis, T., 1954, Phys. Rev., 95, 850.

Christian, R. S., and Noyes, H. P., 1950, Phys. Rev. 79, 85.

Cork, B., and Wenzel, W. A., 1955, B. Am. Phys. Soc., 30, 5.

Duke, P. J., Lock, W. O., March, P. V., Munir, B. A., 1955, J. Sci. Inst., 32, 365.

Fermi, E., 1950, Prog. Th. Phys., 5, 570.
1951, Phys. Rev., 81, 683.
1953, Phys. Rev., 92, 452.
(Erratum, Phys. Rev., 93, 1434).

Fernbach, S., Serber, R., and Taylor, T. B., 1949, Phys. Rev., 75, 1352.

Fischer, D., and Baldwin, J., 1955, Phys. Rev., 100, 1445.

Fried, B. D., 1954, Phys. Rev., 95, 851.

Garren, A., 1953, Phys. Rev., 92, 213 and 1587.

Gell-Mann, M., and Watson, K. M., 1954, Ann. Revs. Nuc. Phys., 4, 245.

Goldhaber, /

Goldhaber, G., 1952, Phys. Rev., 87, 220.
1953, Phys. Rev., 89, 1187.

Heisenberg, W., 1949, Nature, 164, 65.
1949, Zeits. f. Phys., 126, 569.

Jastrow, R., 1951, Phys. Rev., 81, 165.

Kao, S. K., and Clark, A. F., 1954, Phys. Rev., 95, 662(A).

Kovacs, J. S., 1956, Phys. Rev., 101, 397.

Landau, L. D., 1953, Ivz. Akad. Nauk. S.S.S.R. (Ser. Fiz.) 17, No. 1, 51.

Mescheryakov, M. G. 1954, Doklady Akad. Nauk. S.S.S.R., 99, 955.

Moon, P. B., Riddiford, L., and Symonds, J. L., Proc. Roy. Soc., A230, 204.

Morris, T. W., Garrison, J. D., Fowler, E. C., Fowler, W. B., Shutt, R. D., Thorndike, A. M., and Whittemore, W. L., 1955, B. Am. Phys. Soc., 30, 28(A), and private communication.

Peaslee, D. C., 1954, Phys. Rev., 94, 1084.
1954, Phys. Rev., 95, 1580.

Rosenfeld, A. H., 1954, Phys. Rev., 96, 139.

Serber, R., and Rarita, W., 1955, Phys. Rev. 99, 629(A).

Shapiro, A. M., Leavitt, C. P., and Chen, F. F., 1954, Phys. Rev., 95, 663(A).

Smith, L. W., McReynolds, A. W., and Snow, G., 1955, Phys. Rev., 97, 1186.

Sutton, R. B., Fields, T. H., Fox. J. G., Kane, J. A., Mott, W. E., and Stallwood, R. A., 1955, Phys. Rev., 97, 783.

Thaler, R. M., and Bengston, J., 1954, Phys. Rev., 94, 679.

Wright, R. W., Saphir, G., Powell, W. M., Maenchen, G., Fowler, W. B., 1955, Phys. Rev., 100, 1802.

Yuan, /

Yuan, L. C. L., and Lindenbaum, S. J., 1954, Phys. Rev., 93, 1431, and Report of the 5th Rochester Conference, 1955.

D. Polarisation of γ -Rays.

Berlin, T. H., and Madansky, L., 1950, Phys. Rev., 78, 623.

Blatt, J. M., and Weisskopf, V. F., 1952, Theoretical Nuclear Physics, chapter XII, (New York: John Wiley).

Bonnet, A., 1954, J. Phys. Radium, 15, 587.

Dainton, A. D., Gattiker, A. R., Lock, W. O., 1951, Phil. Mag., 42, 396.

Daniel, H., Koester, L., and Mayer-Kuckuk, T., 1953, Z. Naturf., 8a, 447.

Edmonds, A. R., and Flowers, B. H., 1952, Proc. Roy. Soc. A214, 515.

Endt, P. M., and Kluyver, J. C., 1954, Rev. Mod. Phys., 26, 103.

Fagg, L. W., and Hanna, S. S., 1953, Phys. Rev., 92, 372.

Faraggi, H., Bonnet, A., and Cohen, J., 1952, J. Phys. Radium, 13, 105.

Flack, F. C., Rutherglen, J. G., and Grant, P. J., 1954, Proc. Phys. Soc., A67, 973.

French, A. P., and Newton, J. O., 1952, Phys. Rev., 85, 1041.

Gibson, W. M., Grotdal, T., Orlin, J. J., and Trumpy, B., 1952, Phil. Mag., 43, 457.

Goldhaber, G., 1951, Phys. Rev., 81, 930.

Grant, P. J., Rutherglen, J. G., Flack, F. C., and Hutchinson, G. W., 1955, Proc. Phys. Soc., A68, 369.

Hamilton, D. R., 1948, Phys. Rev., 74, 782.

Hough, P. V. C., 1950, Phys. Rev., 80, 1069.

Kirkpatrick, P., 1931, Phys. Rev., 38, 1938.

Krohn, /

Krohn, V. E., and Schrader, E. F., 1952, Phys. Rev., 86, 393.

MacMaster, W. H., and Hereford, F. L., Phys. Rev., 95, 723.

May, M. M., 1951, Phys. Rev., 84, 265.

May, M. M., and Wick, G. C., 1951, Phys. Rev., 81, 628.

Metzger, F., and Deutsch, M., Phys. Rev., 78, 551.

Muirhead, E. G., and Mather, K. B., 1954, Aust. J. Phys., 7, 527.

Phillips, K., 1953, Metropolitan Vickers Research Report.

Pryce, M. H. L., 1954, Rep. Prog. Phys. XVII, 1.

Rutherglen, J. G., Grant, P. J., Flack, F. C., and Douchars, W. M., 1954, Proc. Phys. Soc., A67, 101.

Rutherglen, J. G., Douchars, W. M., and Wallace, K., (private communication).

Talmi, I., 1951, Phys. Rev., 82, 101.
1952, Helv. Phys. Acta, 24, 623.

Touschek, B. F., 1950, Phil. Mag., 41, 849.

Tzara, C., 1954, C. R. Acad. Sci., Paris, 239, 44.

Waffler, H., and Younis, S., 1951, Helv. Phys. Acta, 24, 483.

Wilkinson, D. H., 1952, Phil. Mag., 43, 659.

Yagoda, H., 1949, Radioactive Measurements with Nuclear Emulsions, (New York: John Wiley).

Yang, C. N., 1948, Phys. Rev., 74, 764.